

# Measurement of the Pion Charge-Exchange Differential Cross Section on Argon with the ProtoDUNE-SP Detector

Imperial HEP Seminars

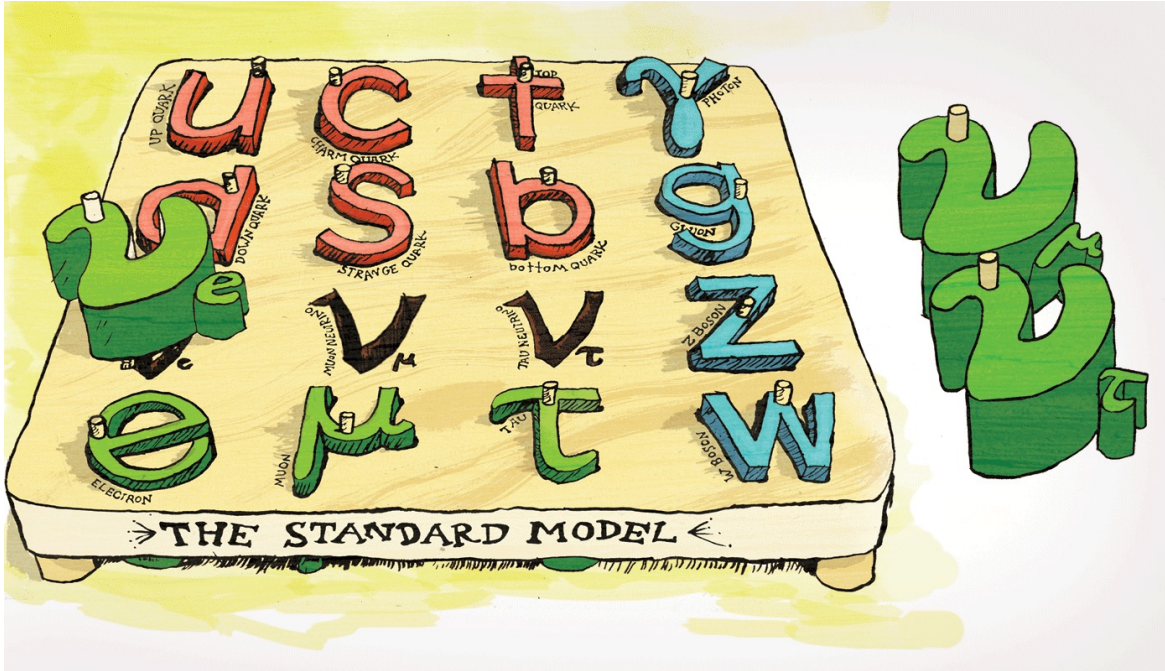
Kang Yang (杨康) University of Oxford (\*)

31<sup>st</sup> Jan 2024

\* Now at Imperial College London



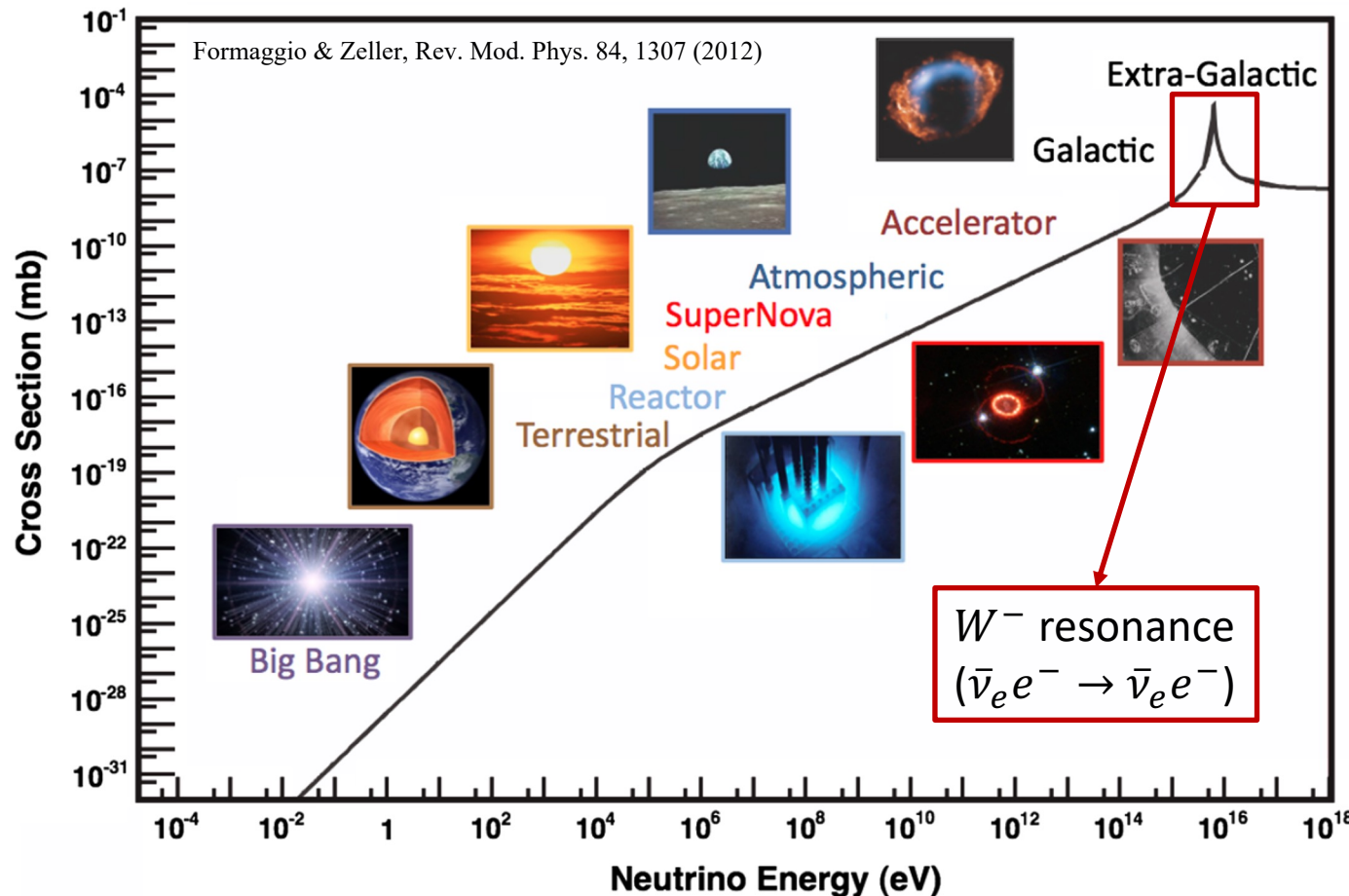
# Neutrinos in Standard Model



[@Symmetry magazine](#)

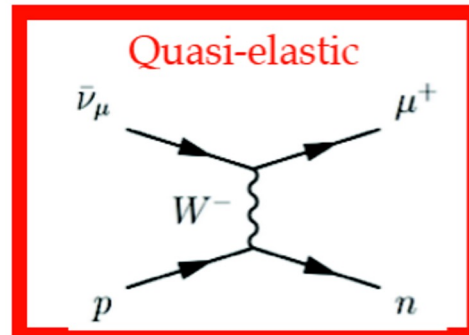
- The Standard Model contains two types of matter particles:
  - ❖ **Hadrons** (composed of quarks)
  - ❖ **Leptons** (elementary particles)
- Neutrinos are leptons **without electrical charge**.
  - ❖ Feel only the weak force.
  - ❖ Very difficult to detect.
  - ❖ Extremely low mass

# Neutrino Sources

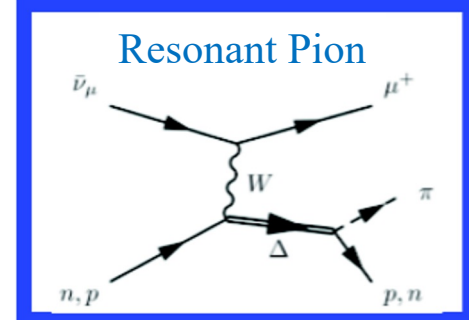


- **Artificial neutrino sources**
  - ❖ Reactor neutrinos
  - ❖ Accelerator neutrinos
- **Astrophysical neutrino sources**
  - ❖ Solar neutrinos
  - ❖ Atmospheric neutrinos
  - ❖ Supernova neutrinos
  - ❖ Neutrinos from astrophysical accelerators

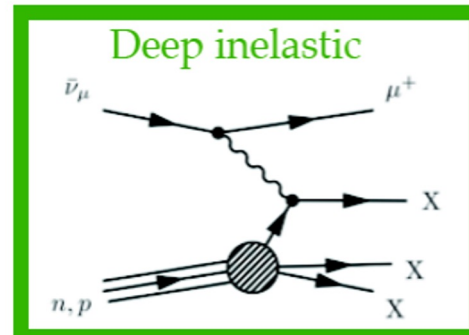
# Neutrino Interactions



QE

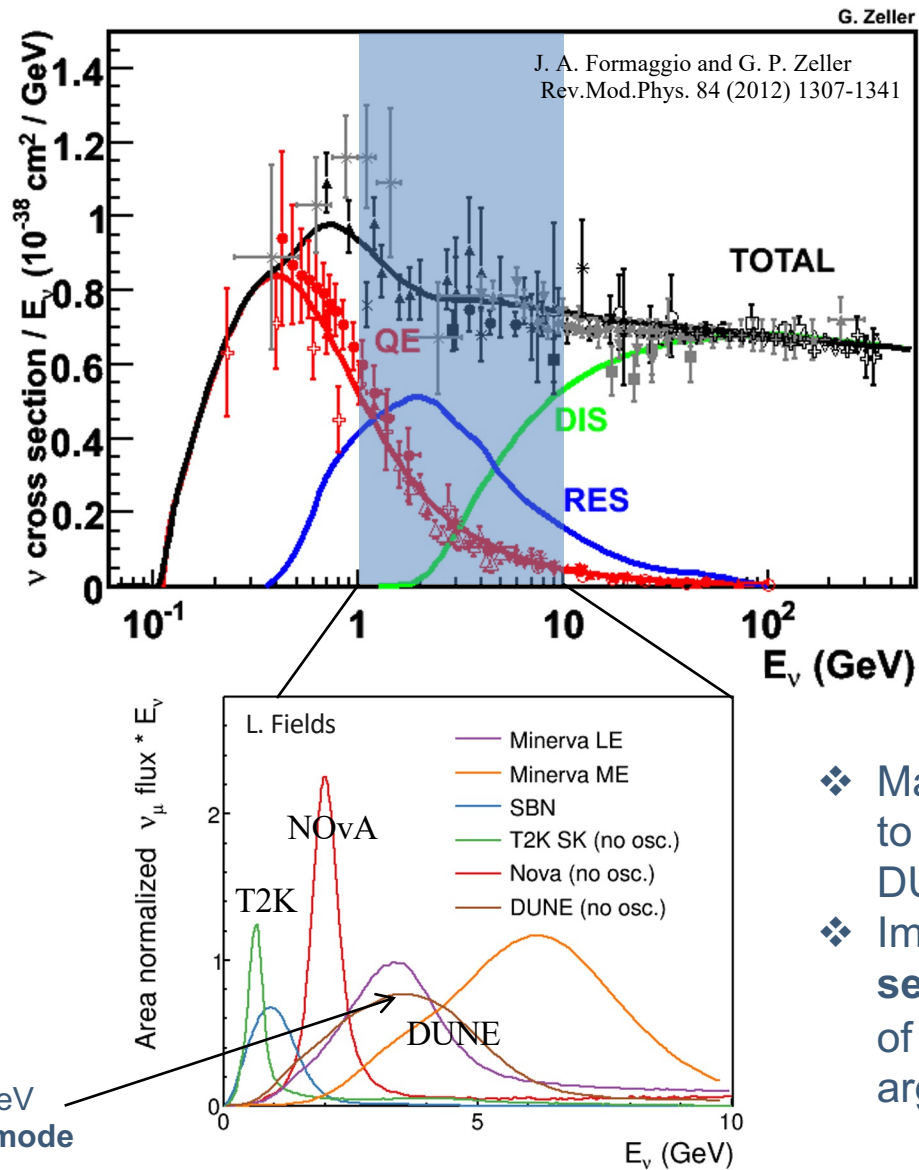


RES



DIS

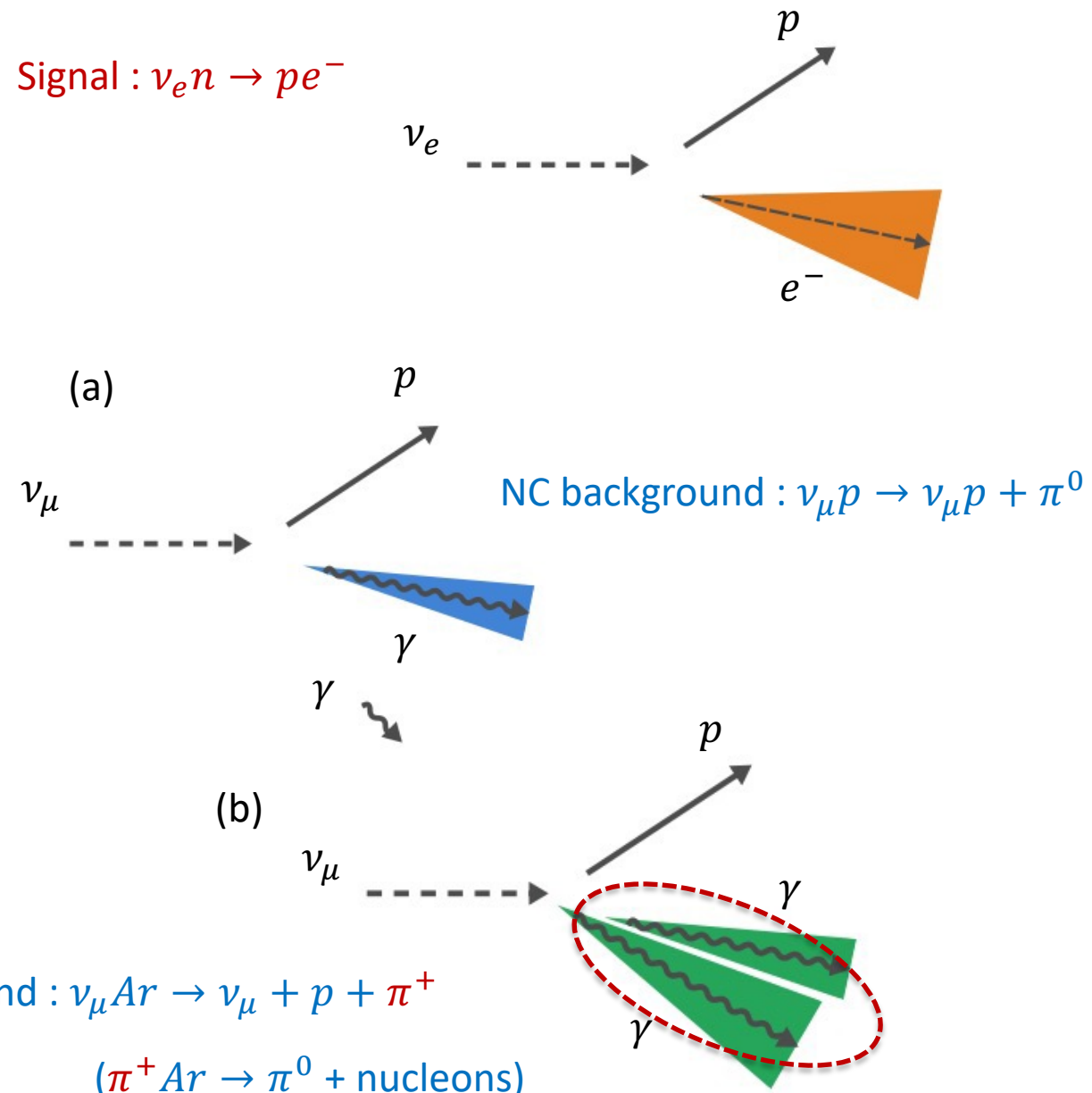
DUNE  $\langle E_\nu \rangle \sim 3$  GeV  
dominated by RES mode



- ❖ Many **pions** are expected to be produced with the DUNE neutrino flux.
- ❖ Important to measure the **secondary interactions** of final state pions with argon.

# Motivations

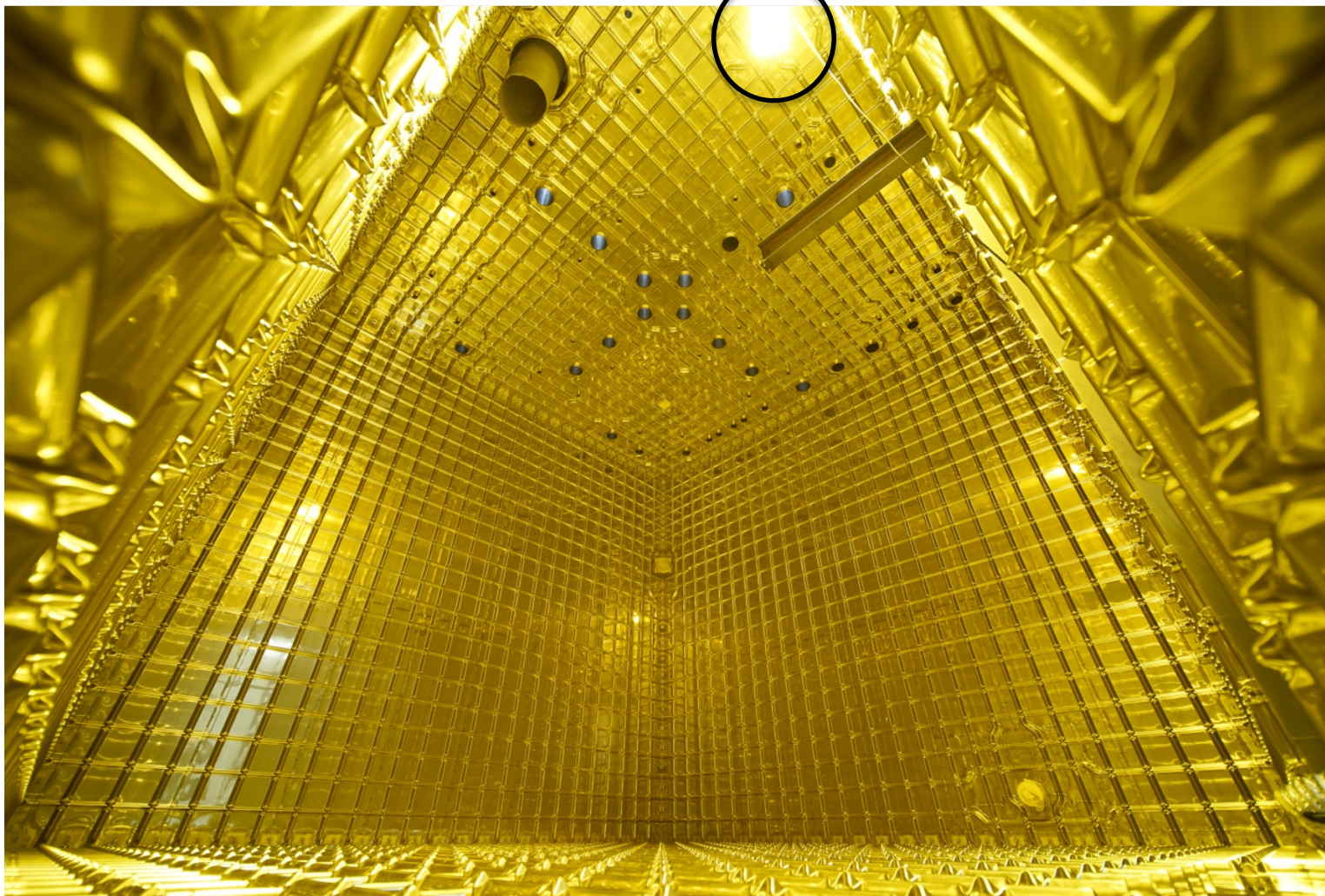
- The  $\pi^0$  reconstruction is driven by two key motivations in DUNE:
  - $\pi^0$  forms a major background to the  $\nu_e$  appearance signal
  - $\pi^0$  decay signature can be used as calibration source for EM shower.
- DUNE  $\nu$  flux is dominated by RES mode.
- The production of  $\pi^0$  can occur when a final state  $\pi^+$  undergoes **charge exchange** within the detector.



# ProtoDUNE-SP

# ProtoDUNE in Pictures

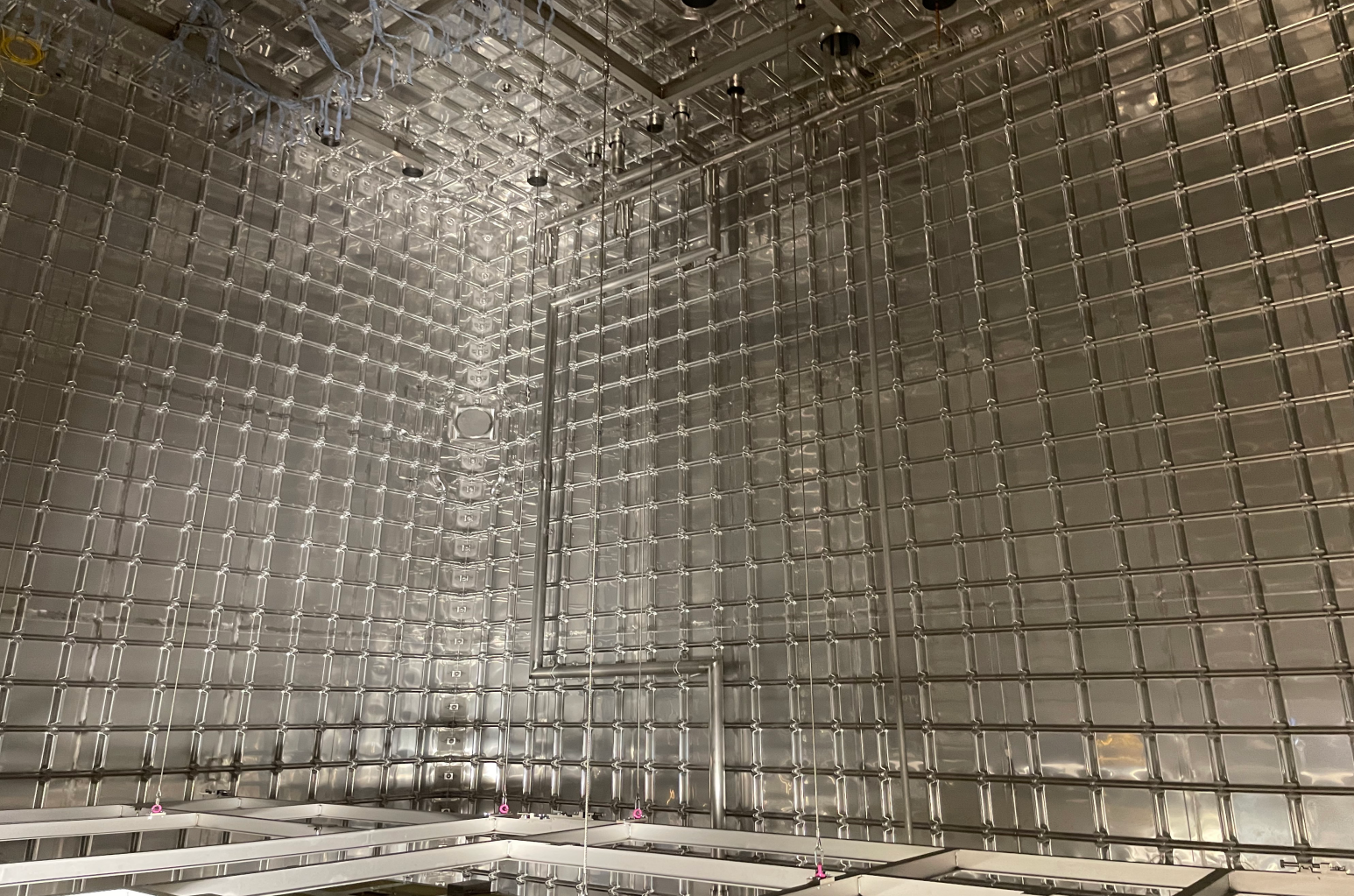
Credit: M Brice/CERN-201710-248-1



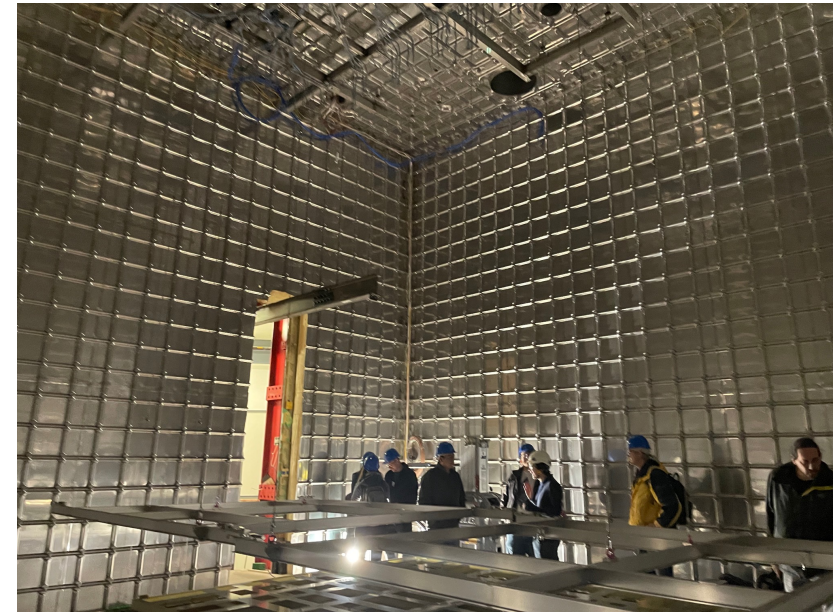
- Often appear in photographs as giant **gold-colored** cubes
  - ❖ It's a trick of the light!
  - ❖ **Yellow light** reflects off the stainless-steel surfaces.
  - ❖ To protect certain properties of the photon detection system.

# ProtoDUNE in Reality

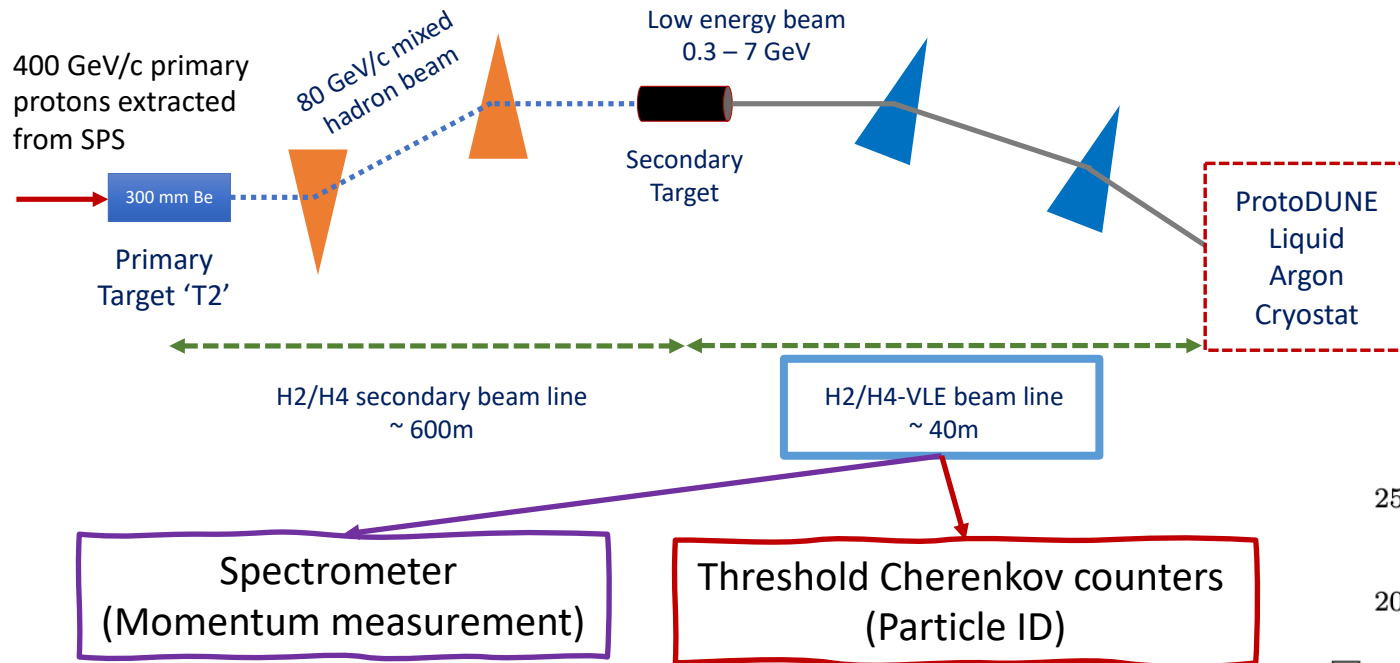
Credit: Myself ☺ 25 Jan. 2023



- Light off ☹
  - ❖ It's a huge detector
  - ❖ DUNE is even bigger

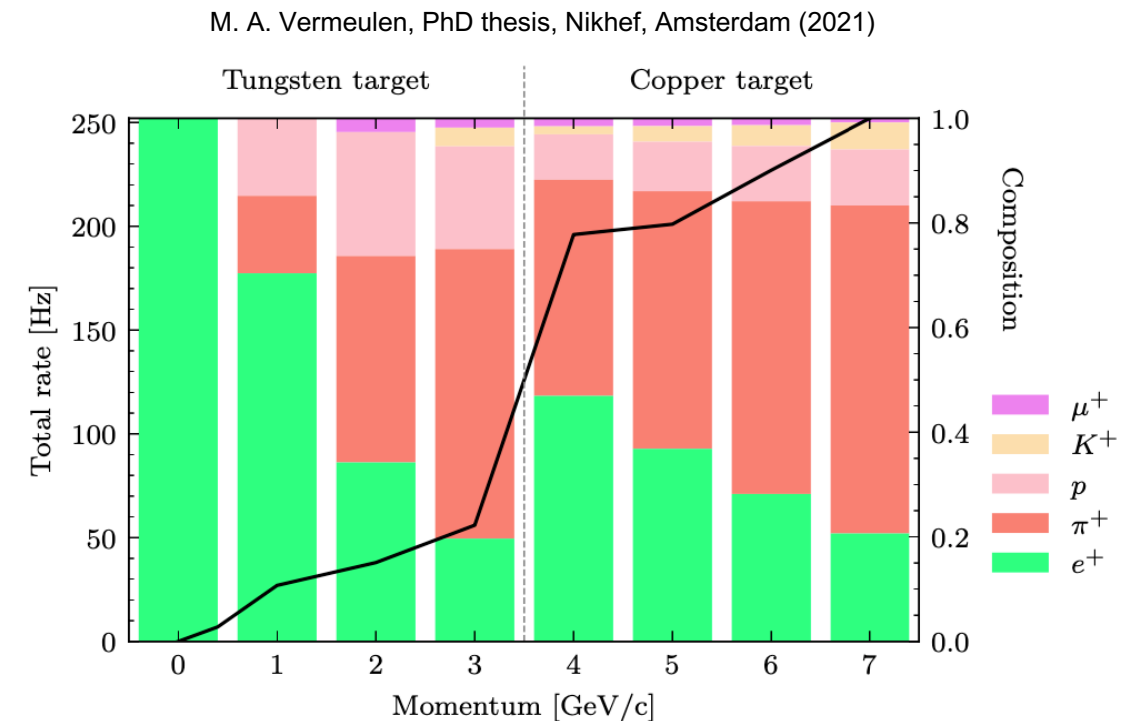


# ProtoDUNE Test Beam



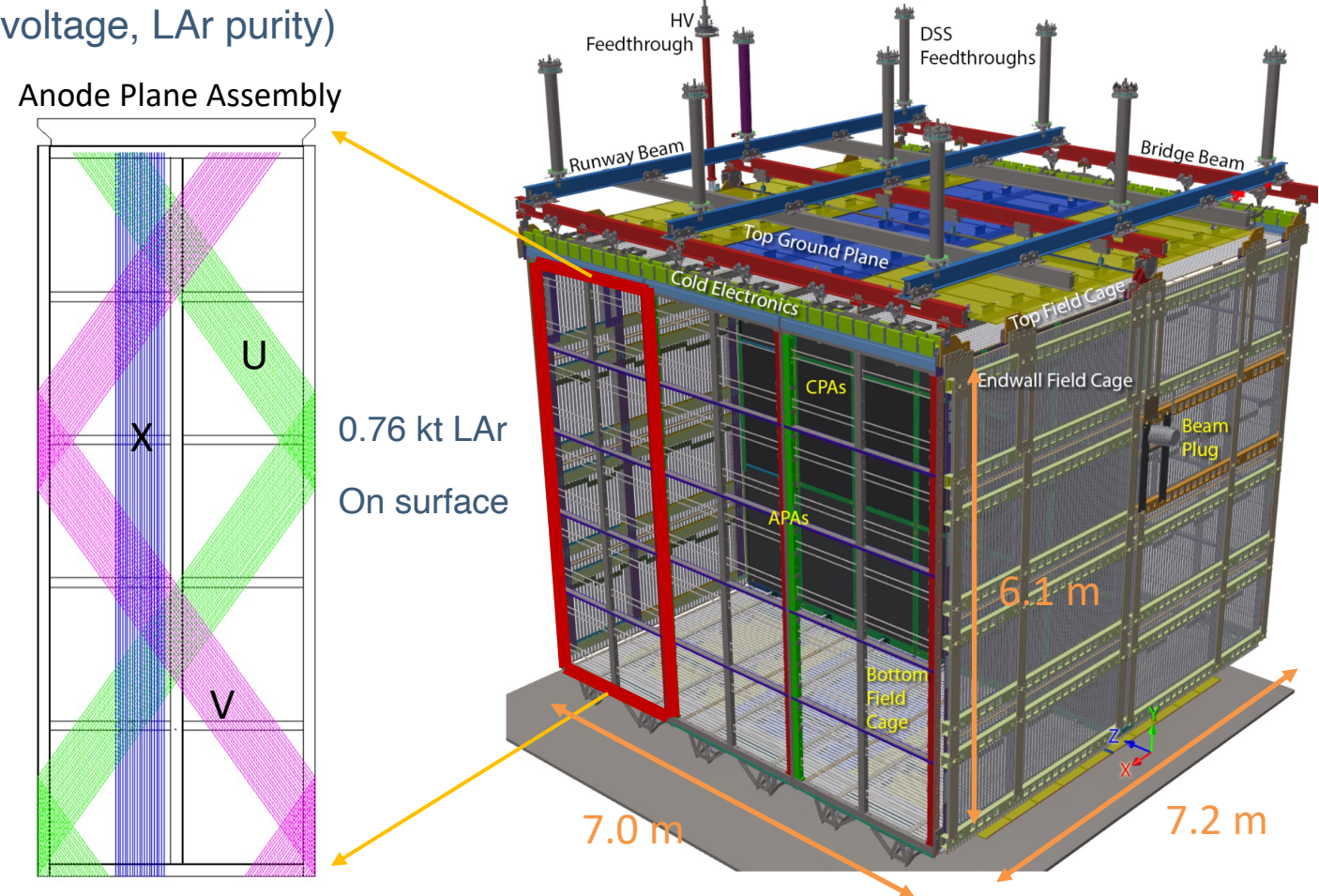
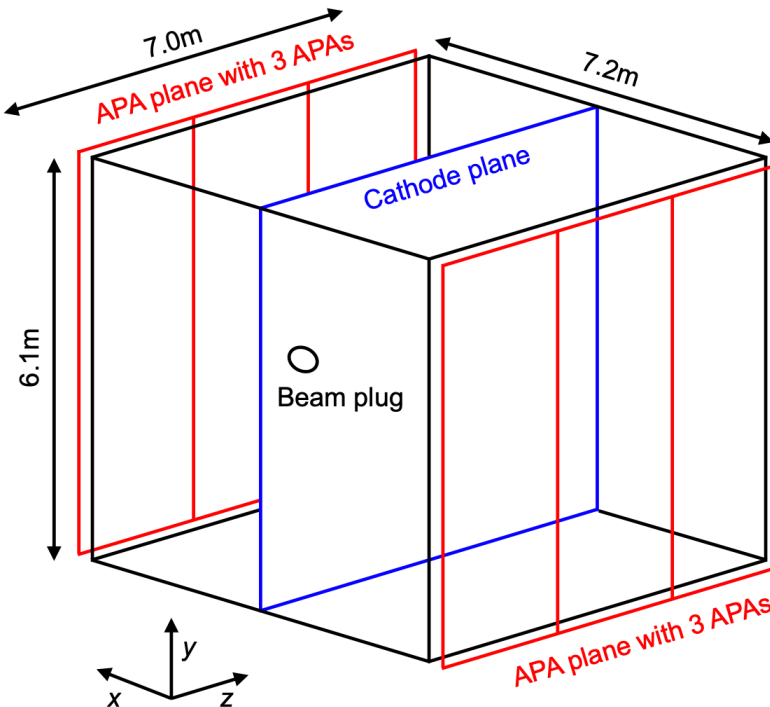
- At the lower end of the momentum range, the beam predominantly consists of **electrons and positrons**.
- As the momentum increases, **pions** become the dominant particle in the higher momentum beams.

- Between 10 October and 12 November 2018, ProtoDUNE was exposed to a **charged particle beam** sourced from the Super Proton Synchrotron (SPS) at CERN.



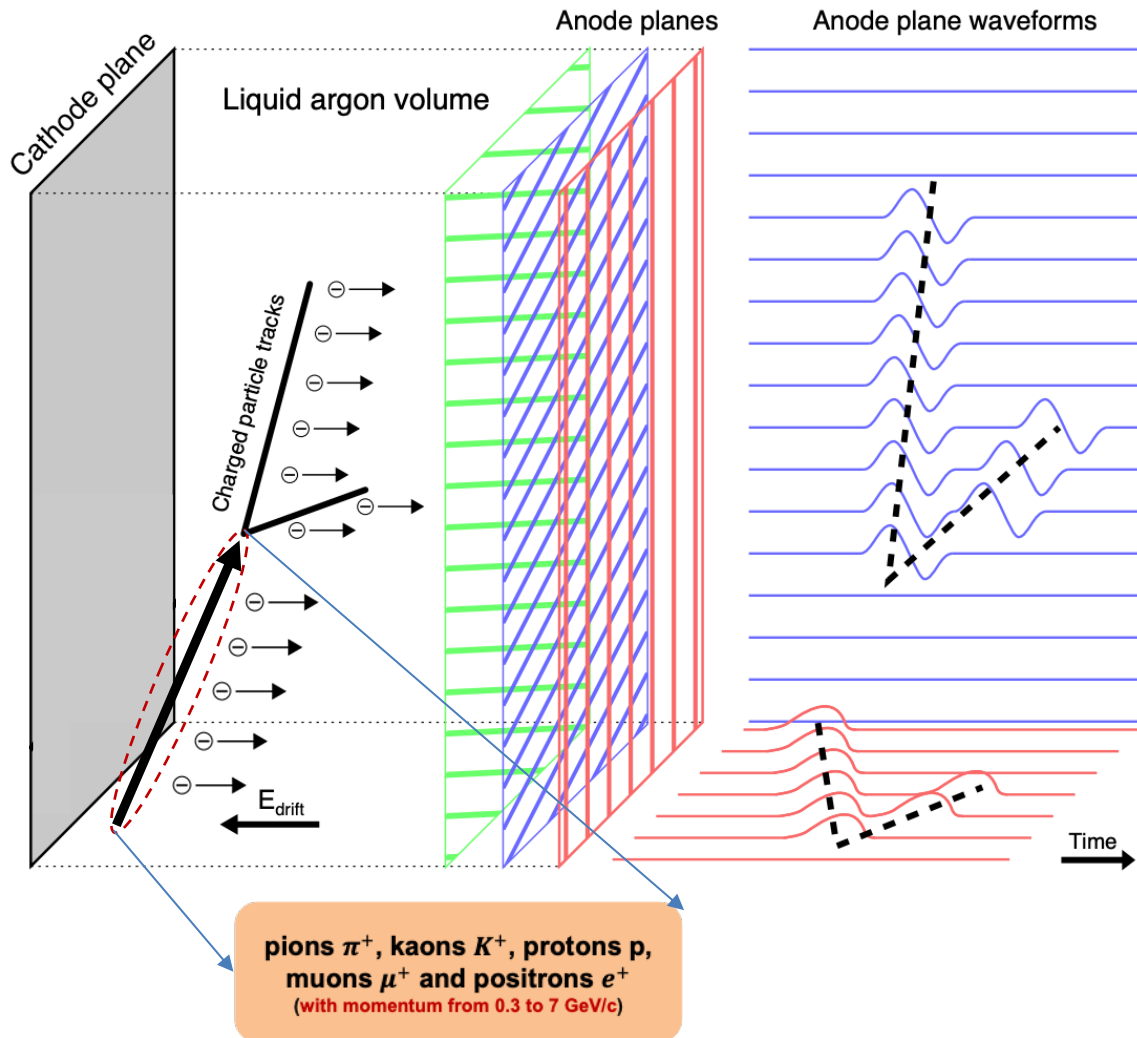
# ProtoDUNE Single Phase

- The ProtoDUNE single-phase apparatus is a large-scale prototype of the far detector module of DUNE,  
@ CERN Neutrino Platform.
- Several goals:
  - Cryostat design validation (electronics, high voltage, LAr purity)
  - Data acquisition and storage
  - Detector performance characterisation
  - Event reconstruction and analysis



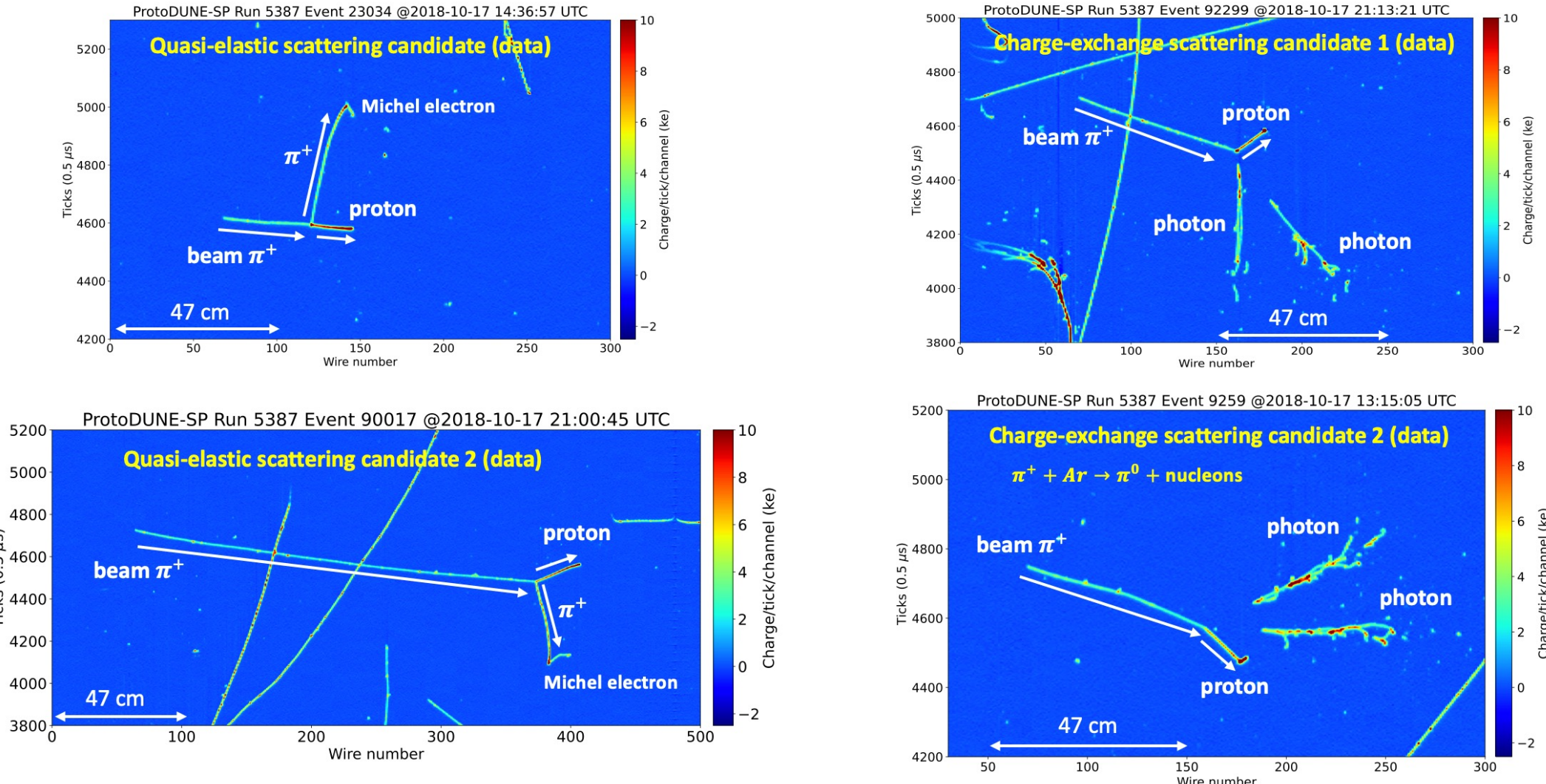
# LArTPC Working Principle

M. A. Vermeulen, PhD thesis, Nikhef, Amsterdam (2021)



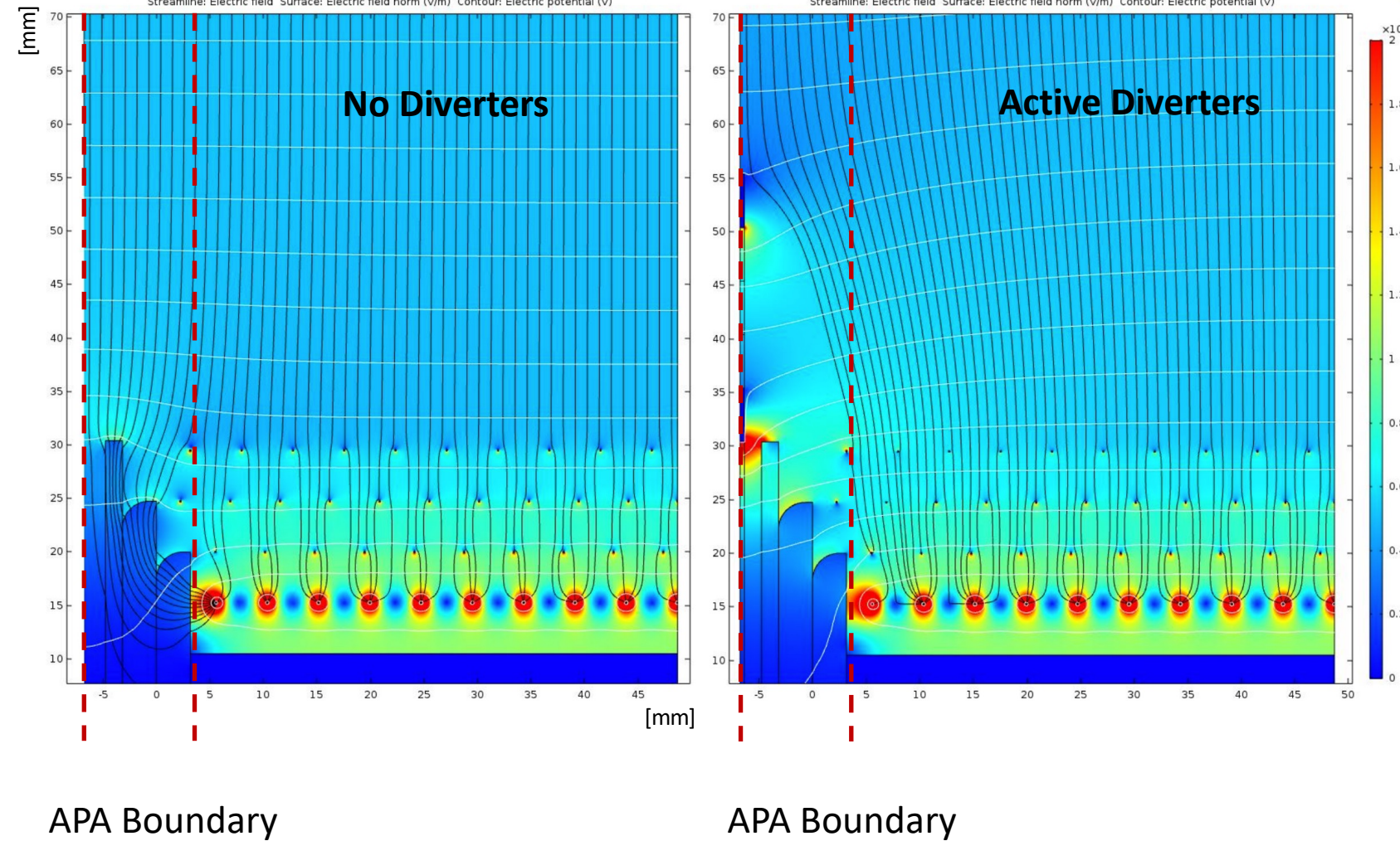
- Free ionised electrons drift towards the anode planes against  $E$  field.
  - ❖ y-z position can be identified.
- Scintillation light from the de-excitation of the Argon excimers.
  - ❖ x position can be determined.
- Maximum drift time is 2.25 millisecond with a transverse diffusion of 2 mm perpendicular to their travel direction.

# ProtoDUNE Data Event Display (1GeV/c)



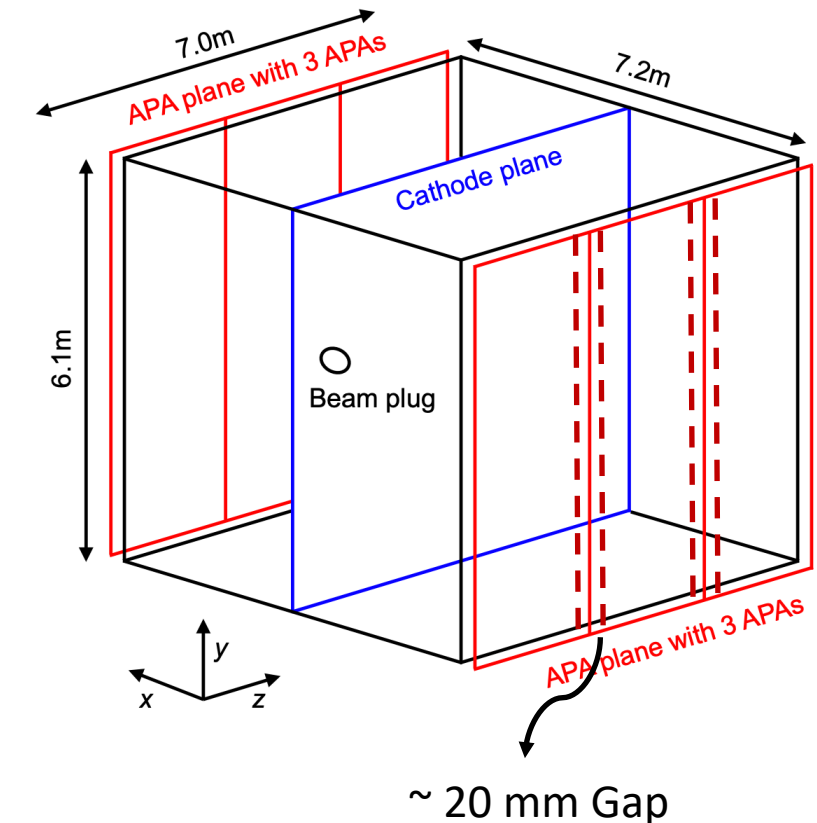
Reconstruction by Pandora Software Development Kit [arXiv:2206.14521](https://arxiv.org/abs/2206.14521)

# Electron Divertor



APA Boundary

APA Boundary



7.0m  
APA plane with 3 APAs

7.2m

Cathode plane

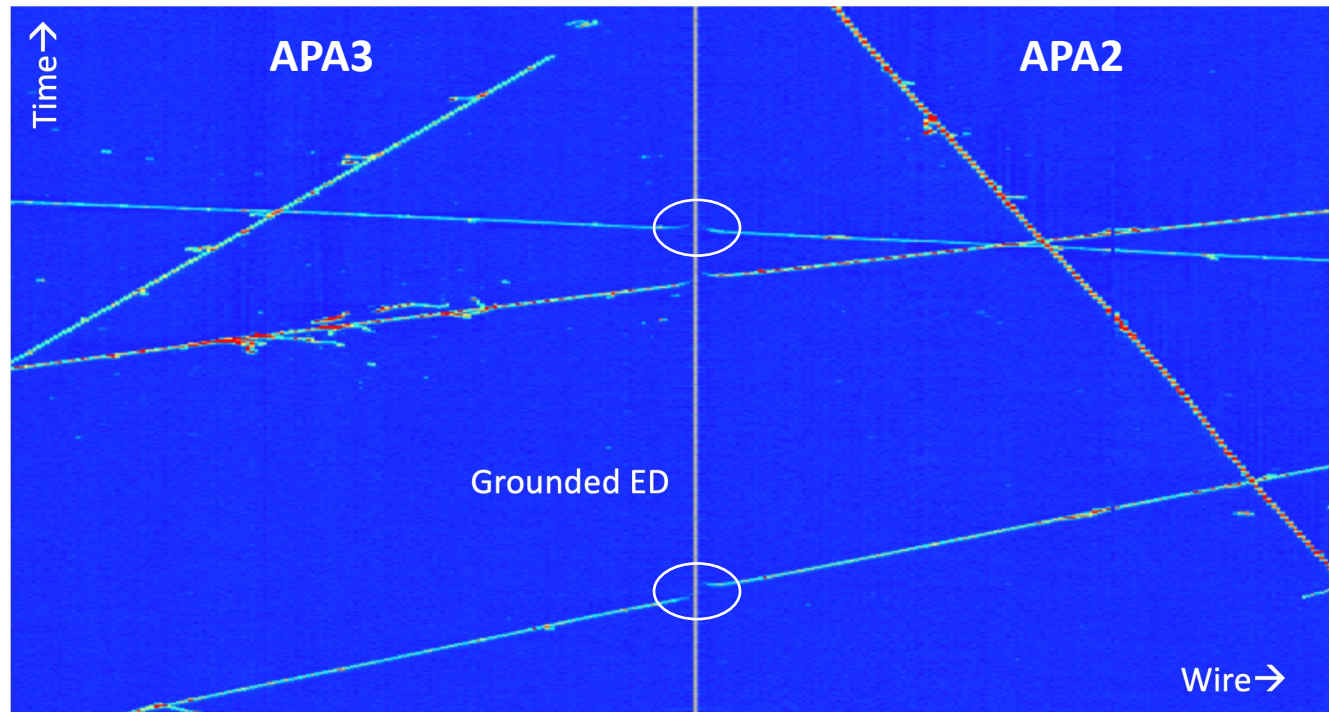
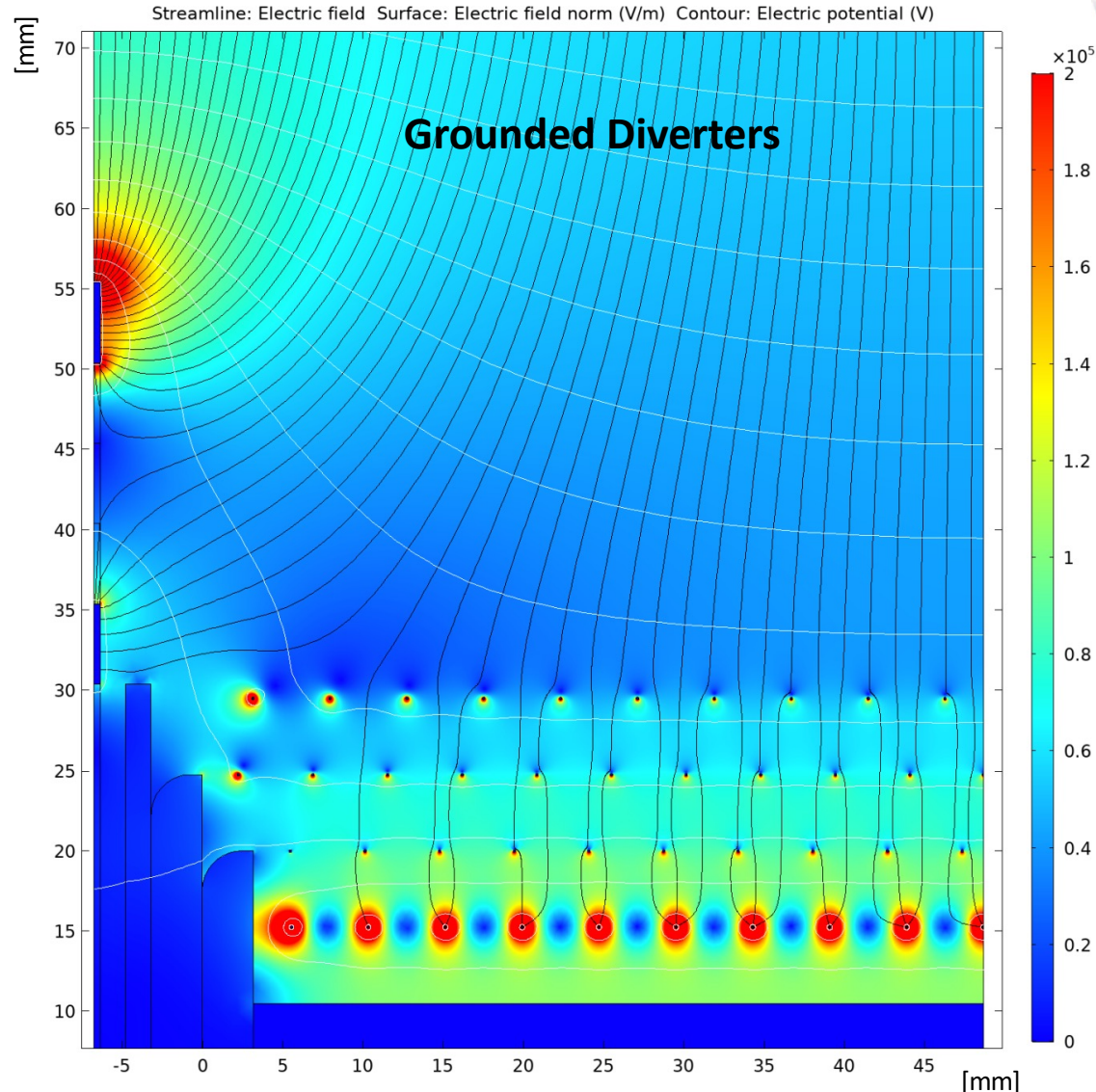
Beam plug

APA plane with 3 APAs

~ 20 mm Gap

- ❖ Diverters' power supplies turned off during beam run.
- ❖ Later discovered that this meant **grounding** them (!)

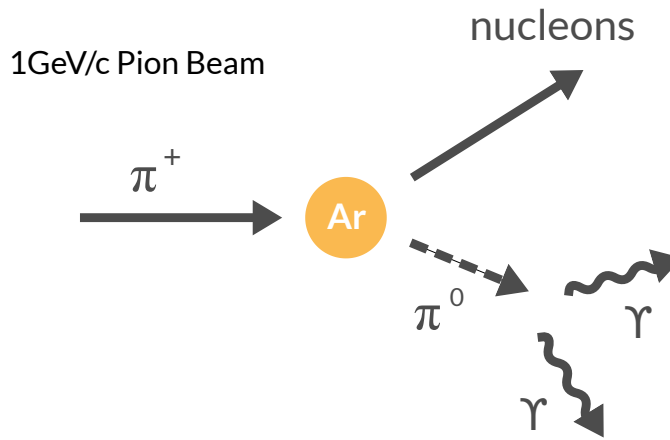
# Electron Divertor



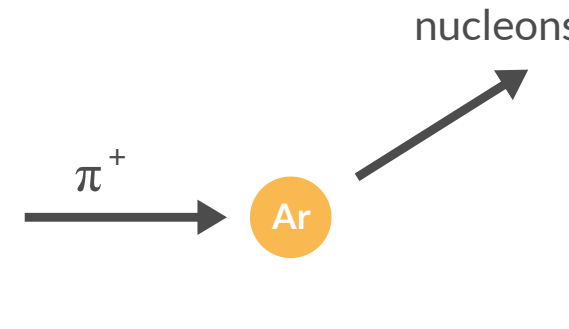
- ❖ Instead of pushing charge away from the gap, grounded divertor draws drifting charge towards it.
- ❖ Charge loss and spatial distortions present
- ❖ Broken tracks (!)

# Pion Charge Exchange Cross-section

# Signal & Background Definition

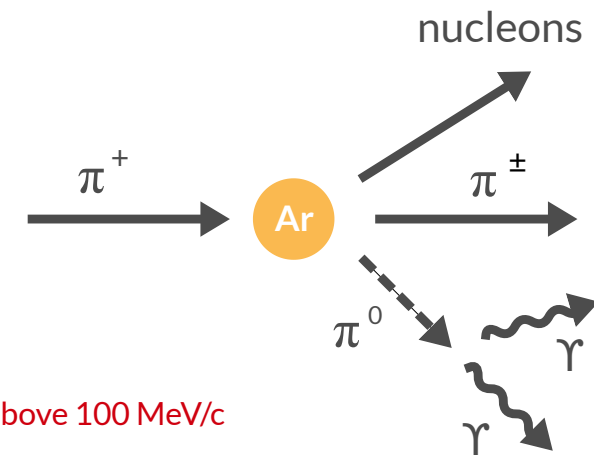


Pion Charge Exchange (Signal)

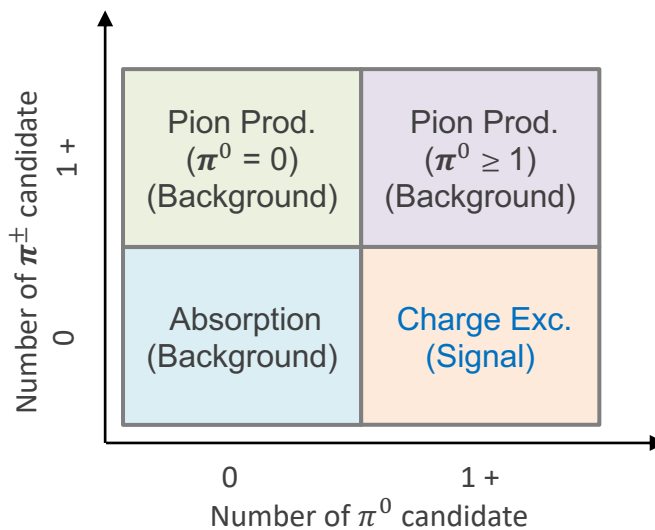


\* The visible daughter charged pions have momentum above 100 MeV/c

Pion Absorption (Background)

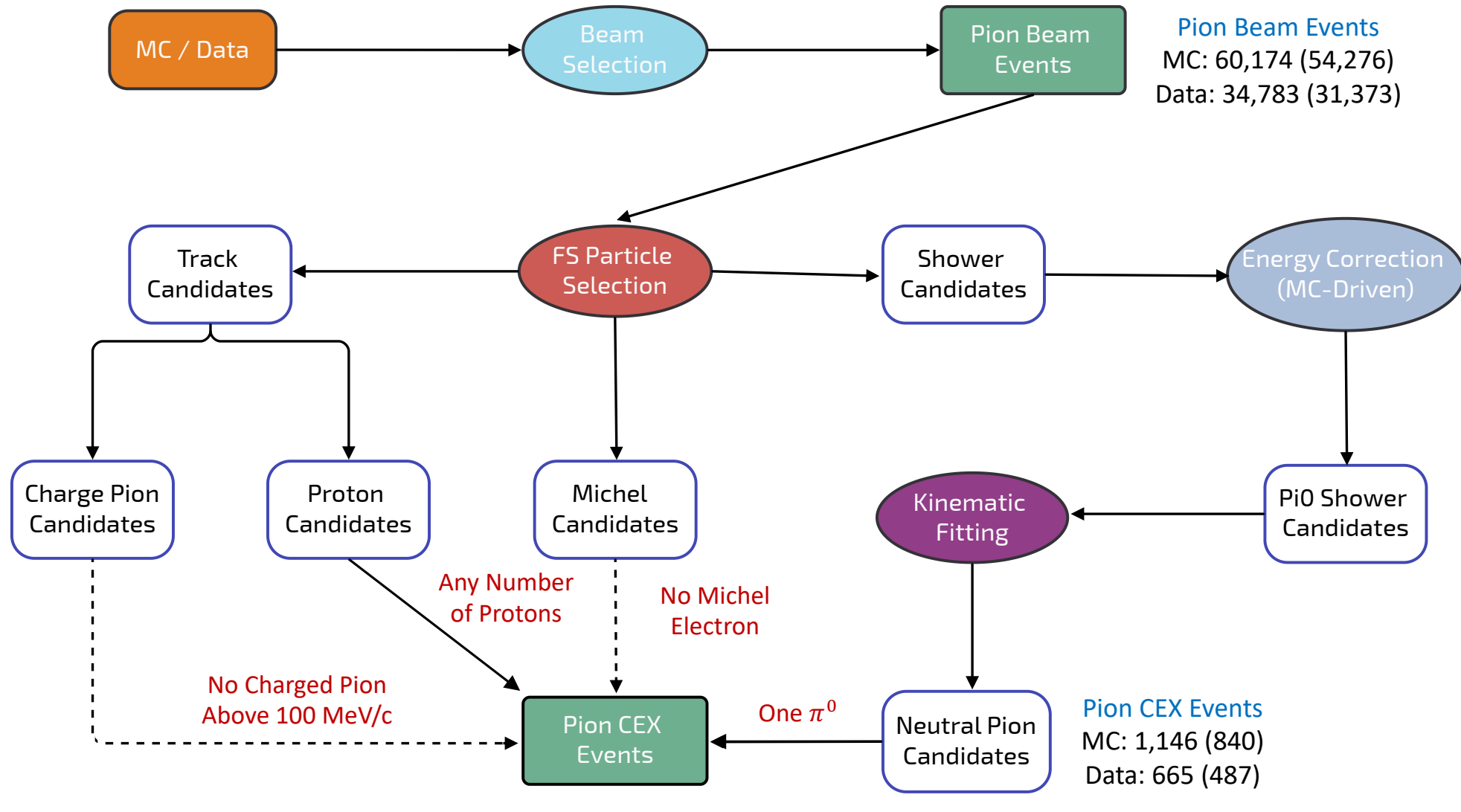


Pion Production (Background)

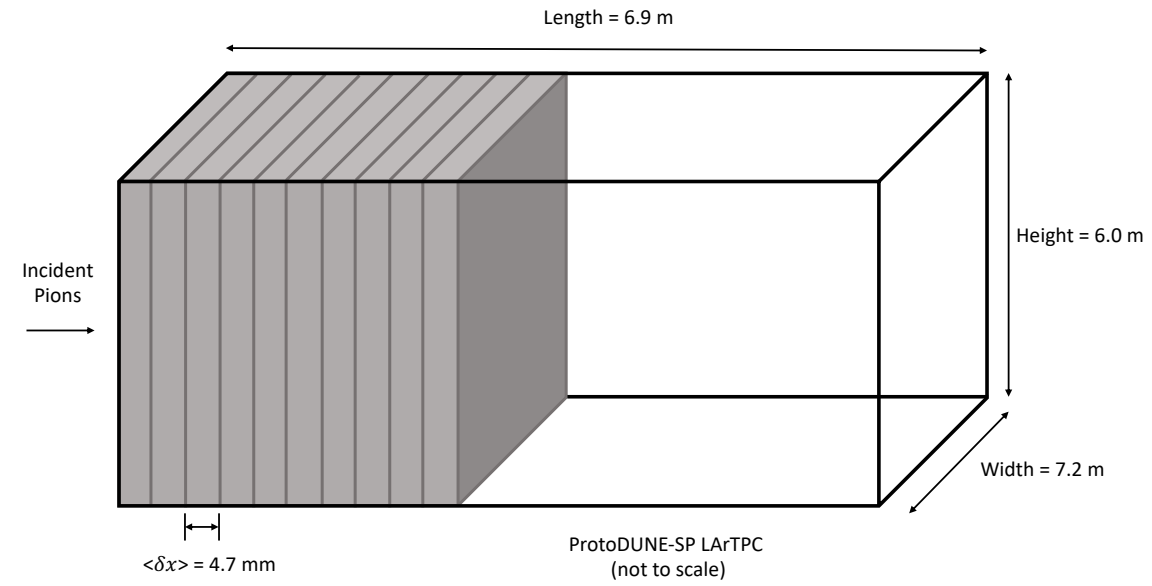
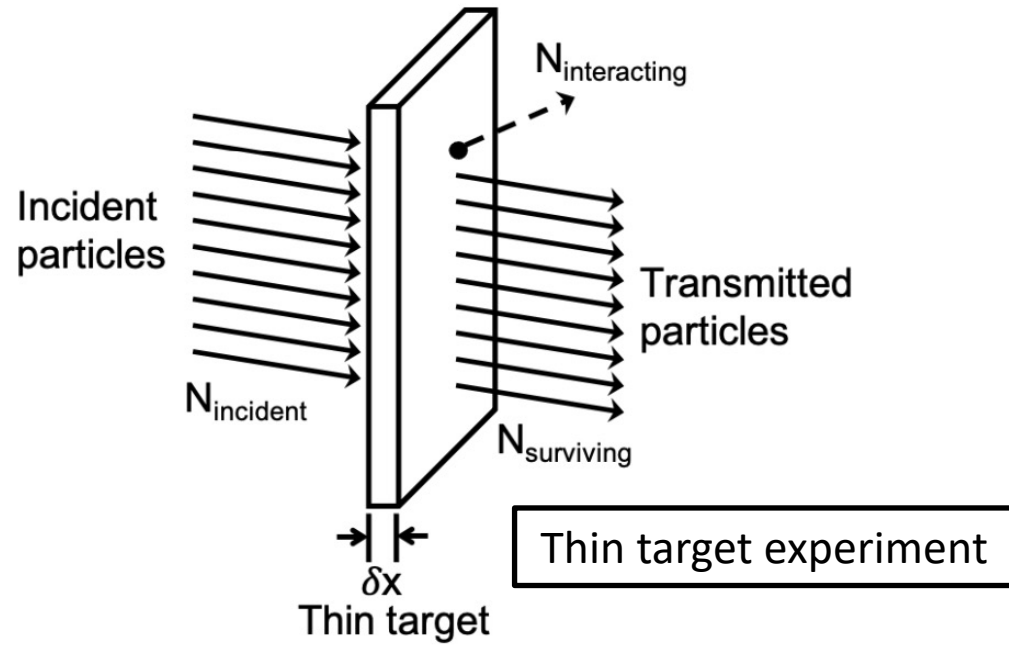


- Analysis strategy:
  - **Total charge exchange cross-section** as a function of beam  $\pi^+$  kinetic energy.
  - **Differential charge exchange cross-section** with daughter  $\pi^0$  kinematics at a particular beam energy.

# Event Selection

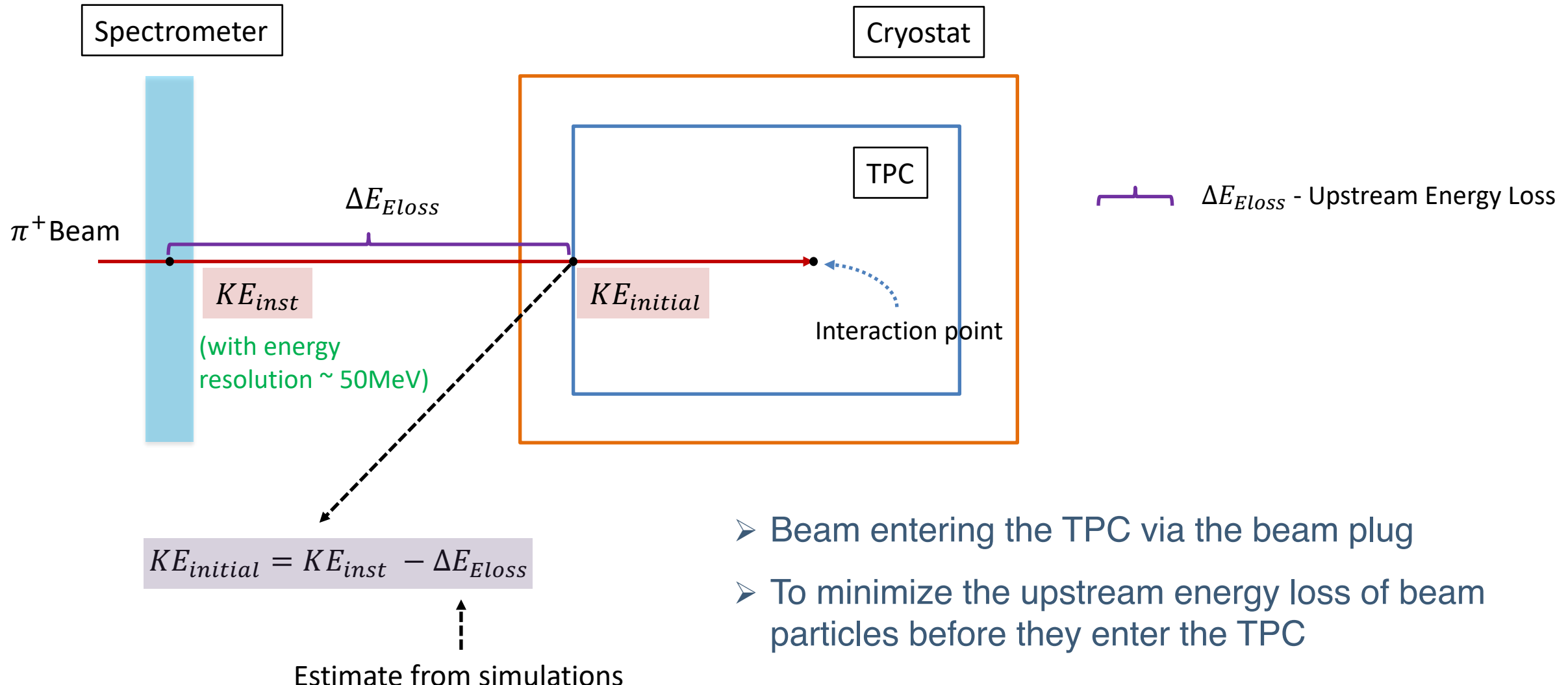


# Thin-Slice Method

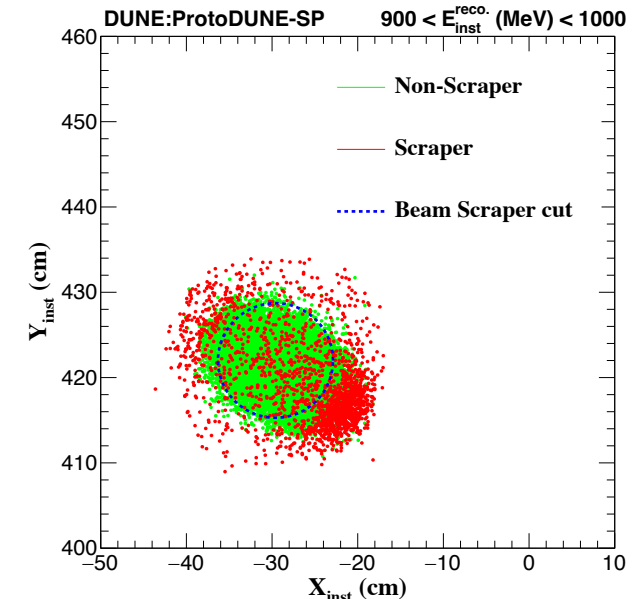
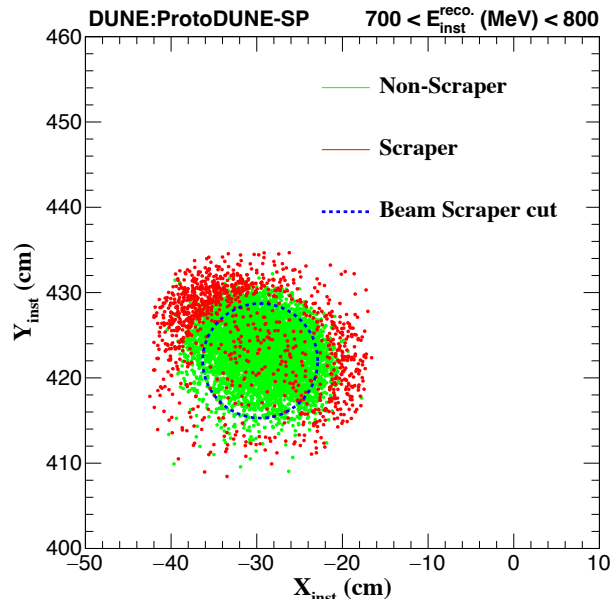
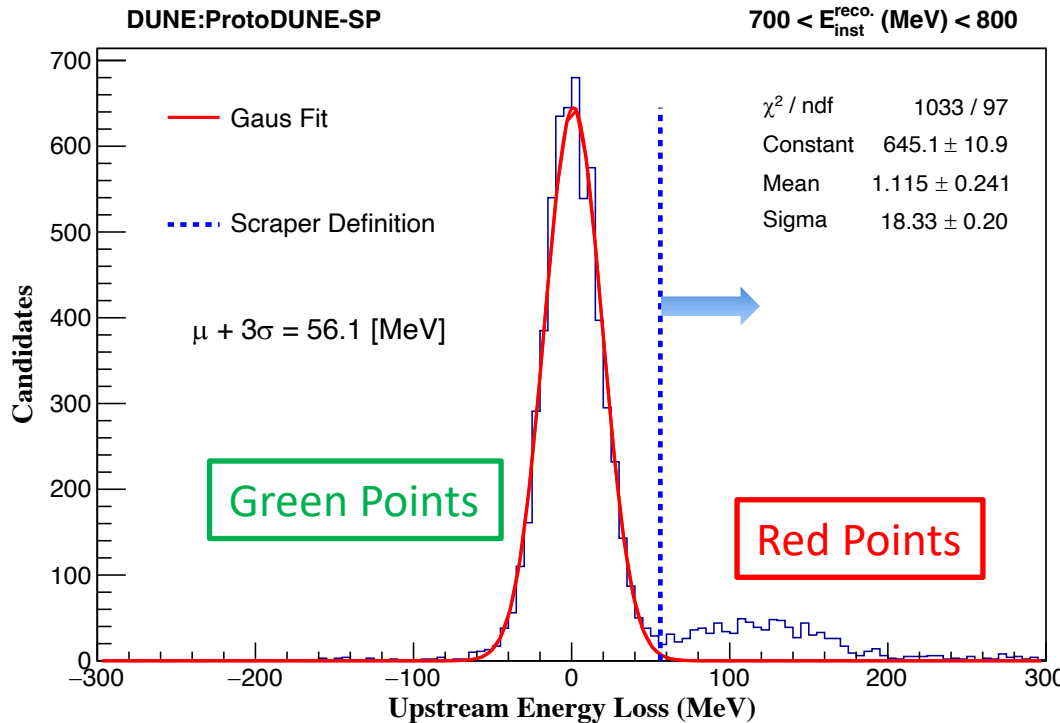


- Interaction probability  $\frac{N_{\text{int}}}{N_{\text{inc}}} = P_{\text{Int}} = 1 - e^{-\sigma_{\text{Tot}} n \delta X}$ ,  $n = \frac{\rho N_A}{m_{\text{Ar}}}$  is the density of the target.
- The interaction length of pions in liquid argon is of the order of  $\sim 50 \text{ cm}$ .
- Treat the argon volume as a sequence of many adjacent thin targets.

# Measure the Initial Energy



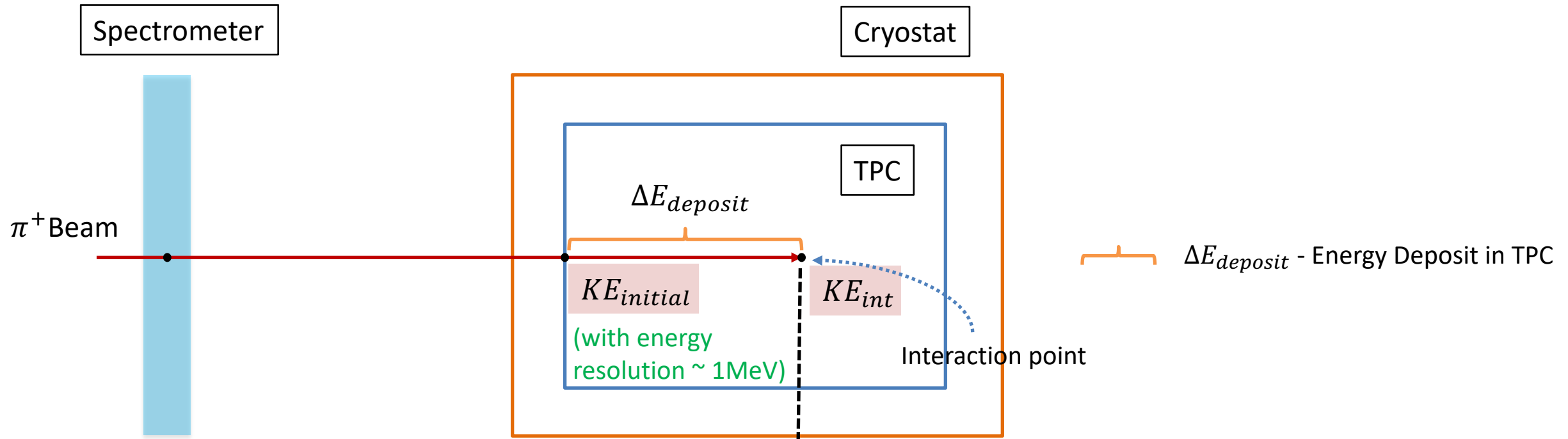
# Beam Scraper



- Beam scraper events
  - ❖  $\Delta E_{Eloss}$  is  $3\sigma$  away from the fitted mean value

- Scraper events **do not** enter TPC through the beam plug:
  - ❖ More  $\Delta E_{Eloss}$  upstream energy loss
- The circular shape of the beam plug is visible.

# Measure the Interacting Energy

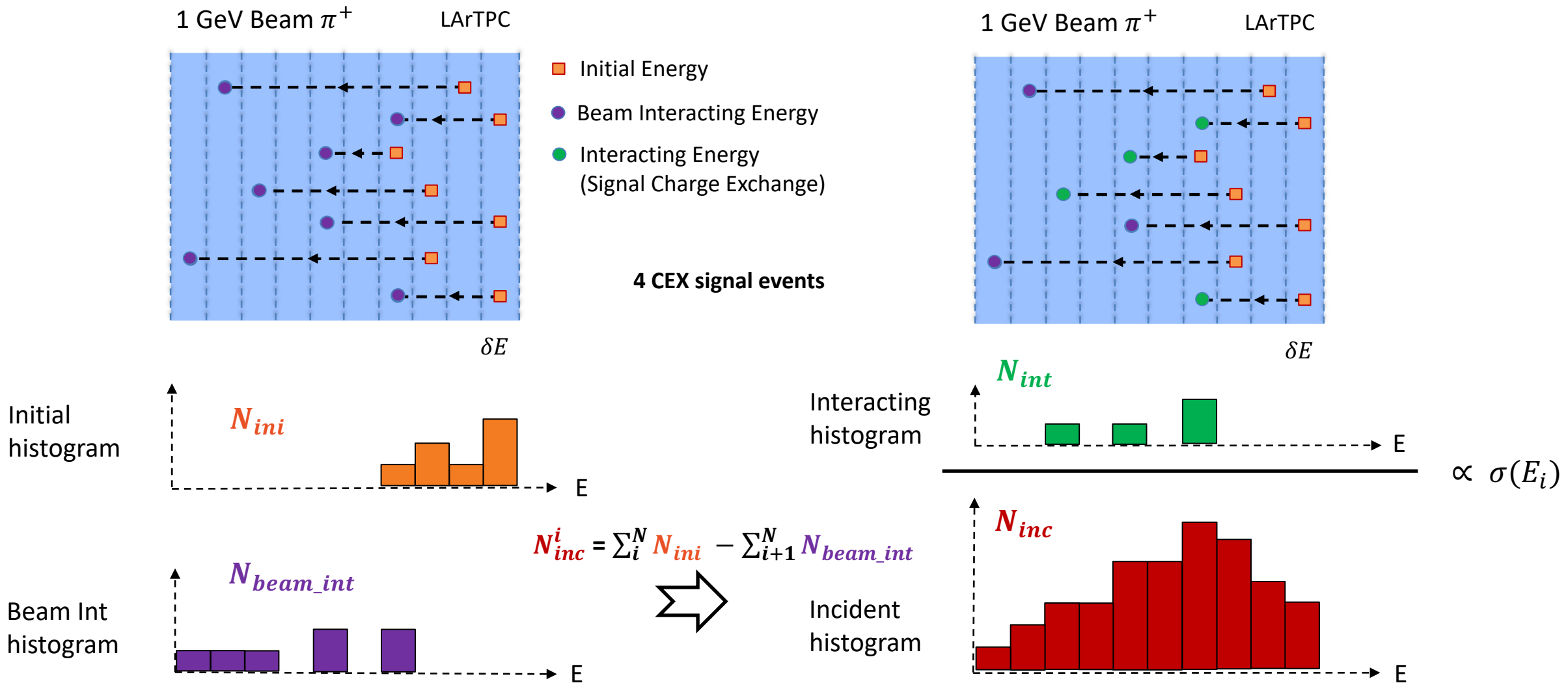


- Get energy at interaction point from:
  - ❖ Initial energy
  - ❖ Energy deposit in the detector

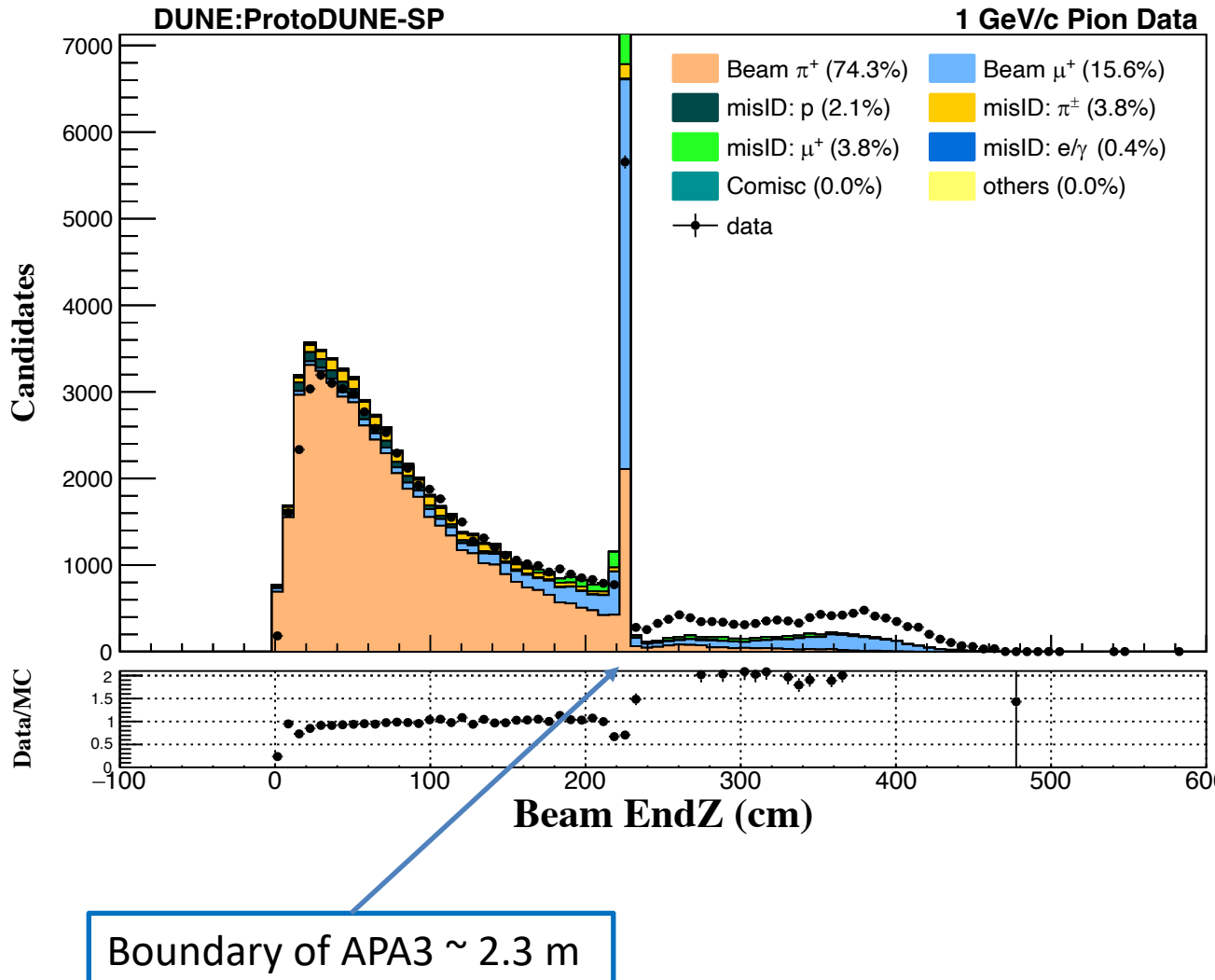
$$KE_{int} = KE_{initial} - \Delta E_{deposit}$$

- 1.  $\int \frac{dE}{dx} dx$  ----- Range based
- 2.  $\sum \Delta E_{calo}$  ----- Calorimetry Based

# How to Compute Incident & Interacting Flux

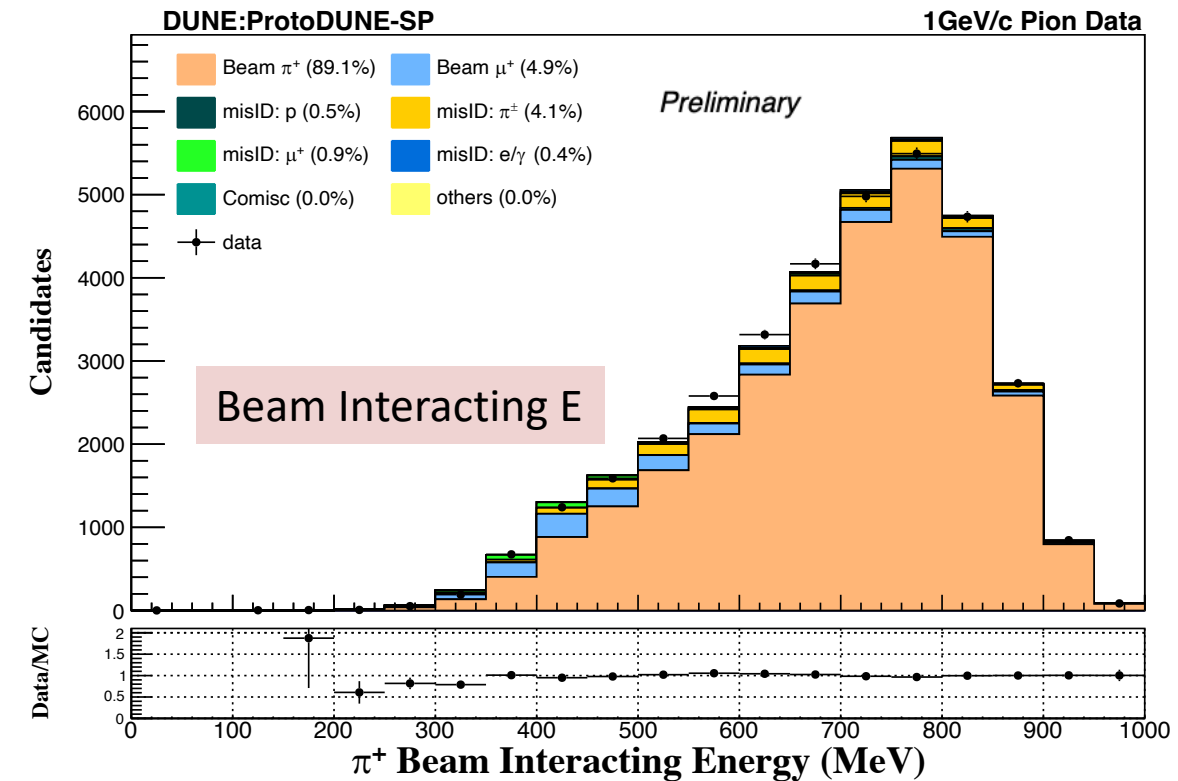
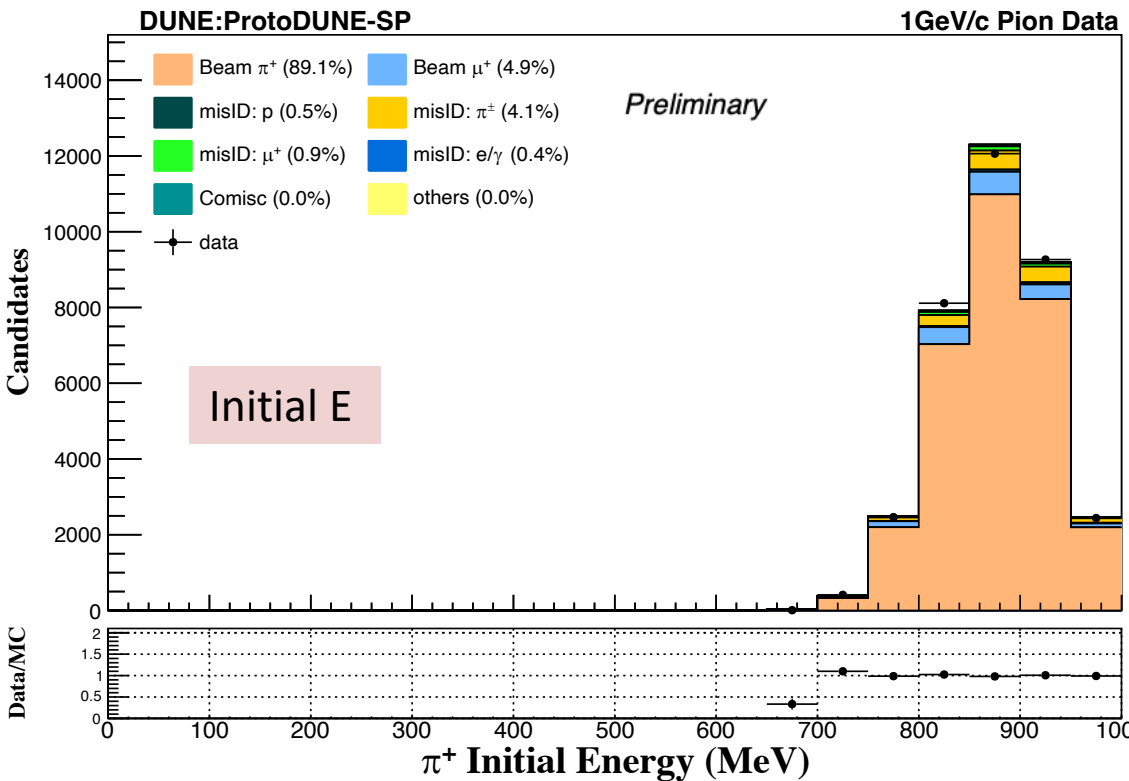


# Electron Diverter (Grounded)



- Beam end Z position of all beam events
- Grounded electron diverter:
  - Single track reconstructed as two
  - Not well simulated
- Tracks to prematurely "break" when they cross one APA boundary
- Limits the lowest beam energy range in the following cross-section measurement.

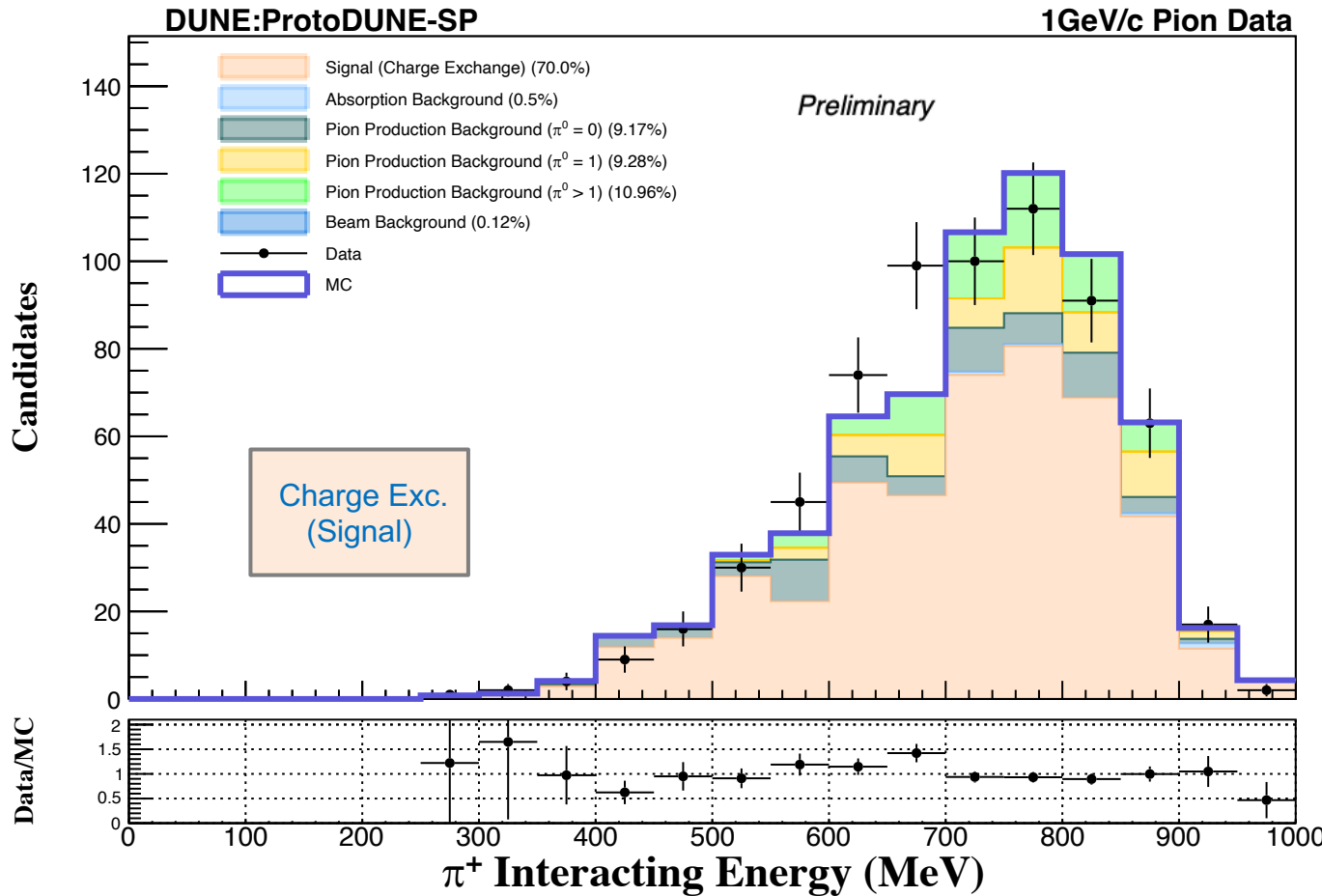
# Initial & Beam Interacting Energy



- The leading background is the beam muon (4.9%) followed by the misidentified secondary pions (4.1%).
- The beam pion sample purity after all cuts is 89.1%.

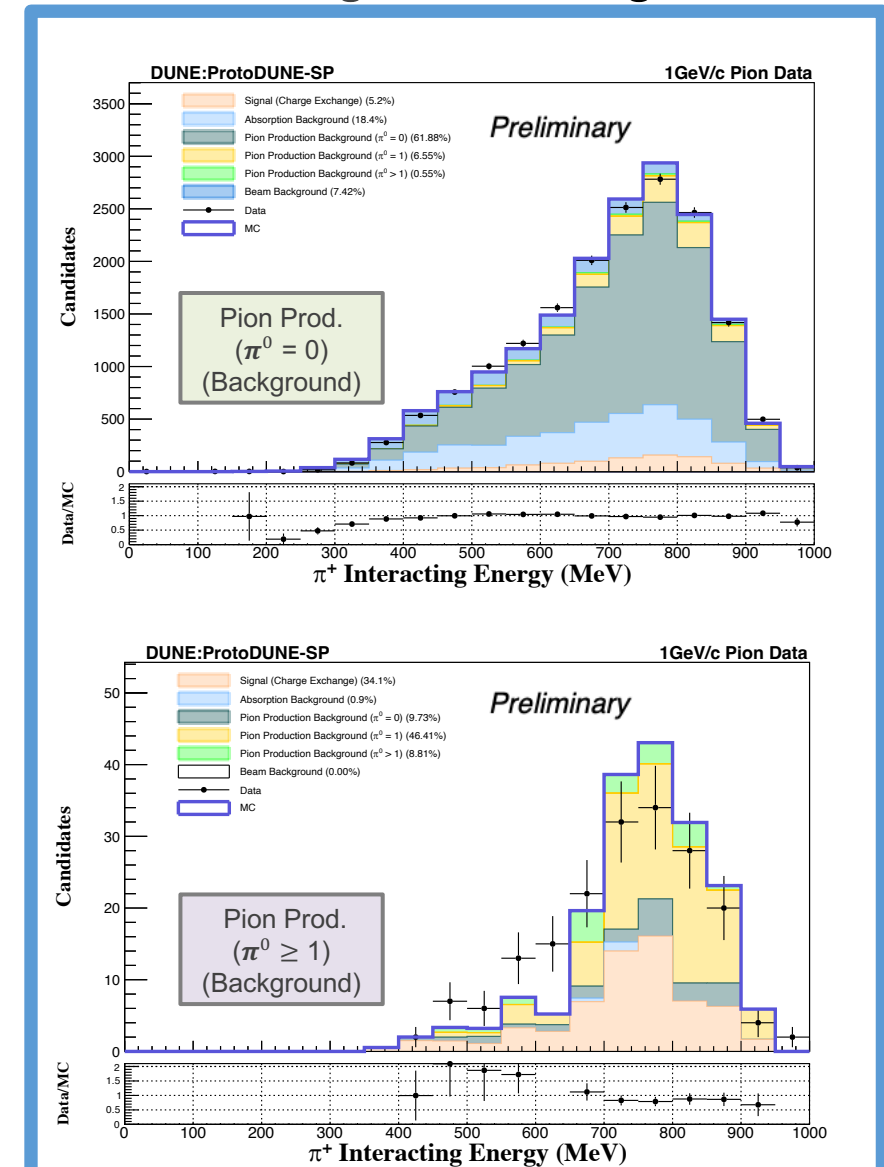
$$N_{inc}^i = \sum_i^N N_{ini} - \sum_{i+1}^N N_{beam\_int}$$

# Sideband Bck. Tuning

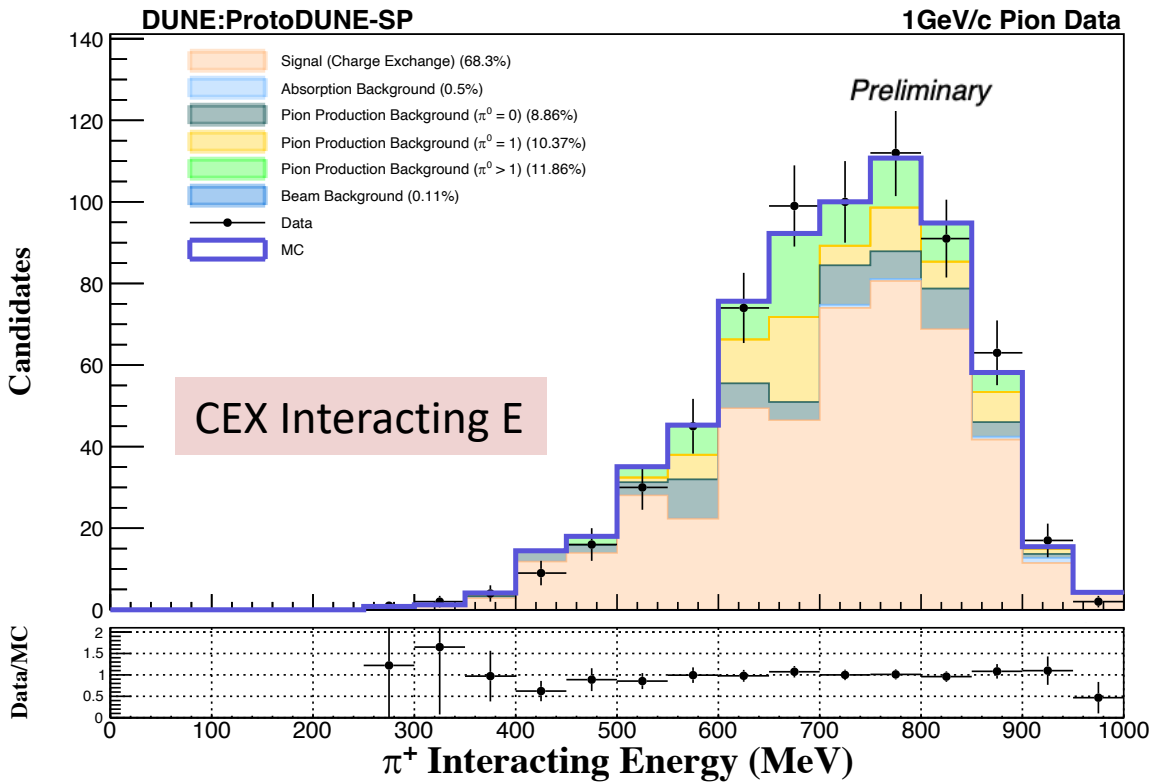
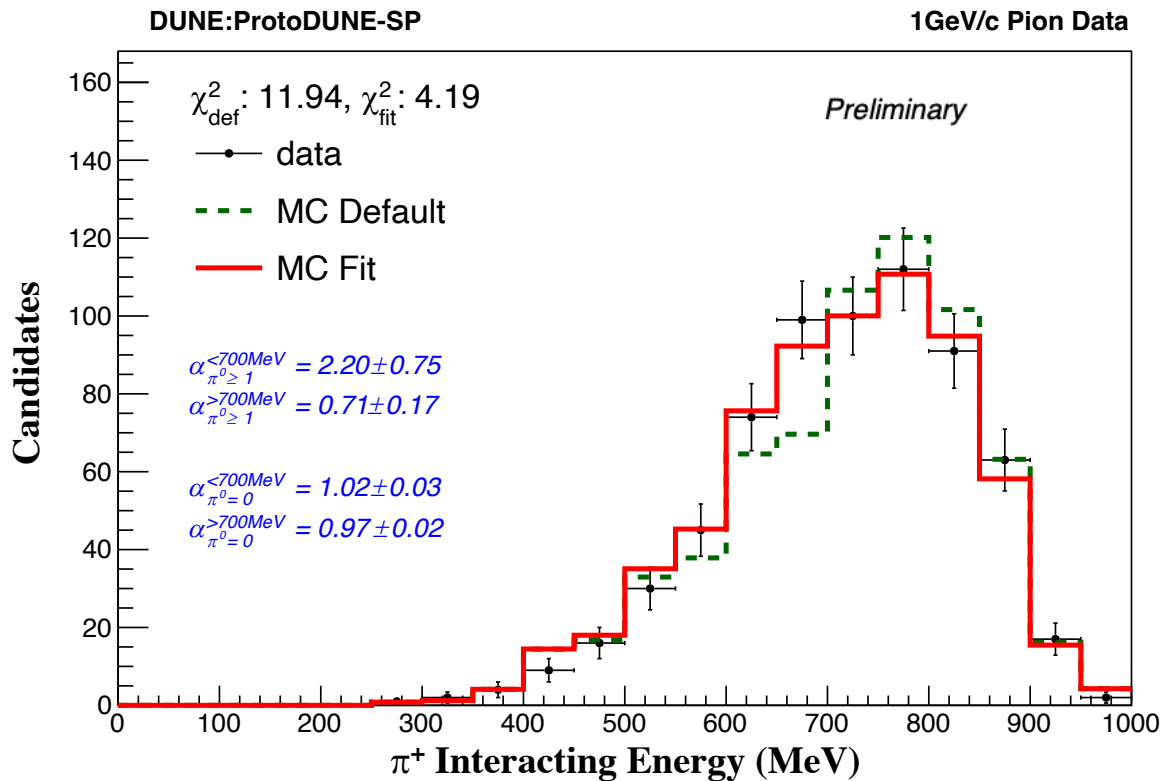


- Keep the signal part unchanged, simultaneously vary the  $\pi^0 = 0$  and  $\pi^0 \geq 1$  pion production backgrounds to minimise the  $\chi^2$  between data and MC.

Fit Background scaling factors



# CEX Interacting Energy

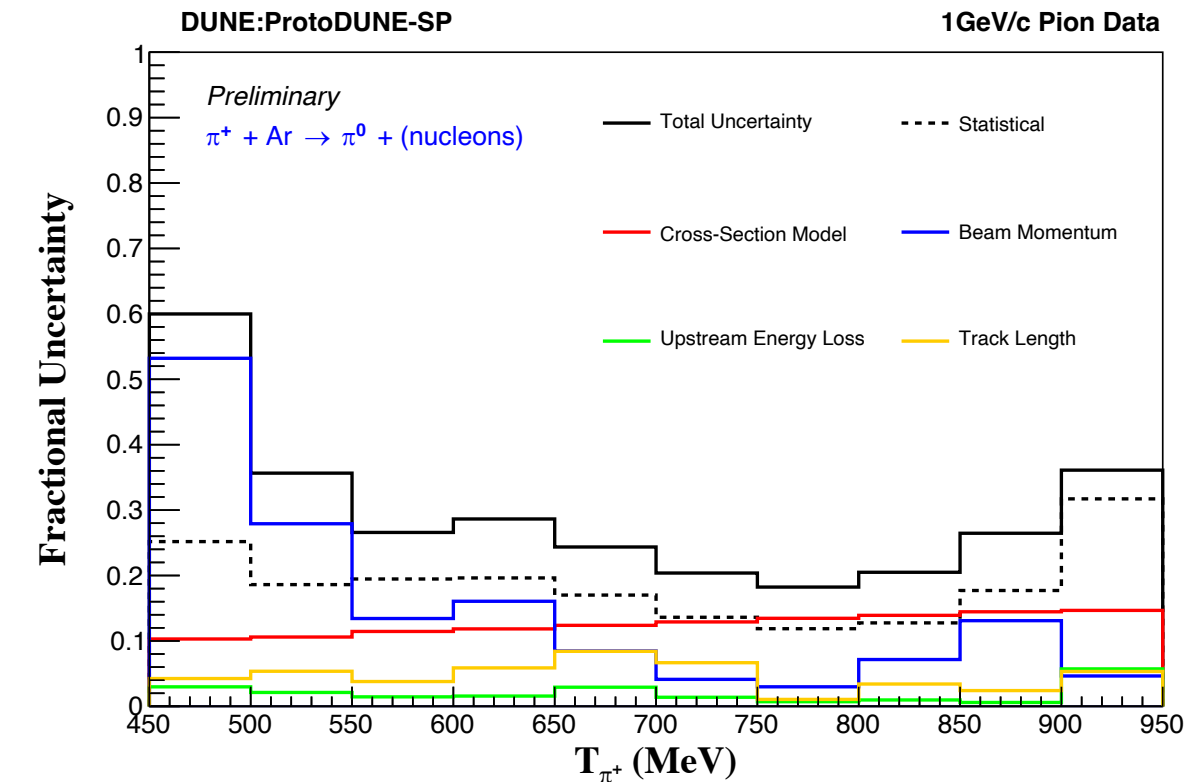
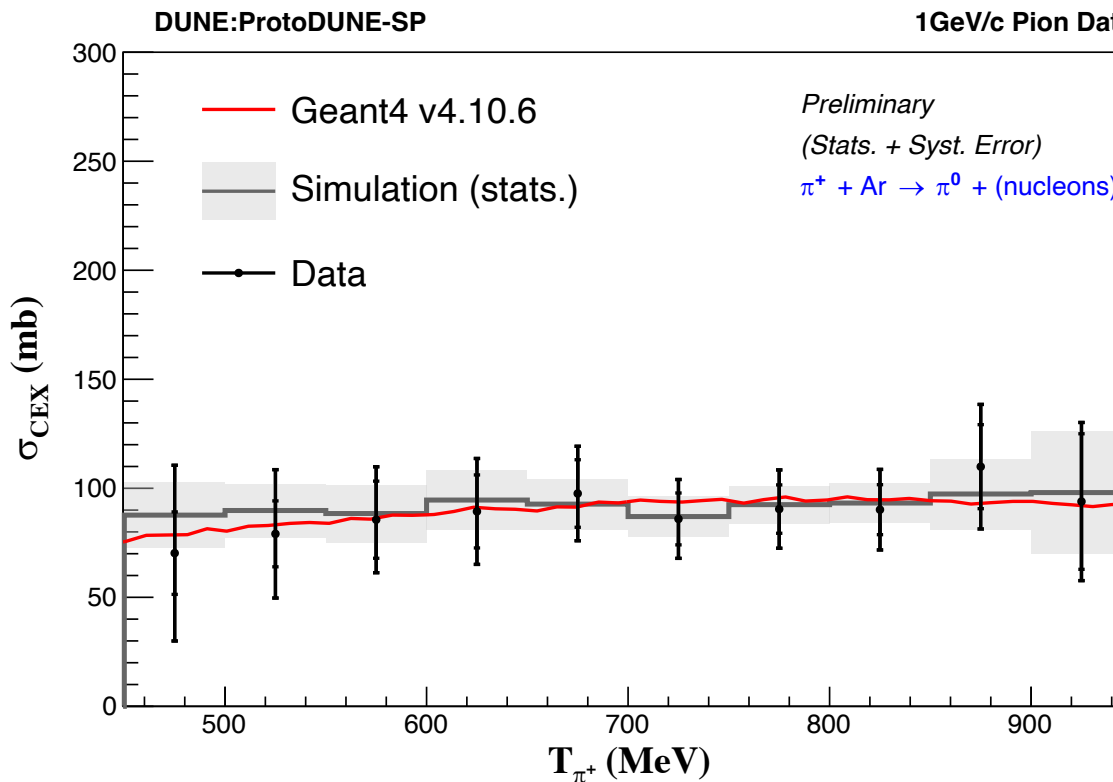


Fitted Parameters :

	$\alpha_{\pi^0 \geq 1}^{<700\text{MeV}}$	$\alpha_{\pi^0 \geq 1}^{>700\text{MeV}}$	$\alpha_{\pi^0 = 0}^{<700\text{MeV}}$	$\alpha_{\pi^0 = 0}^{>700\text{MeV}}$
MC	2.20	0.71	1.02	0.97

- We can now subtract the estimated background from the MC and do the unfolding.

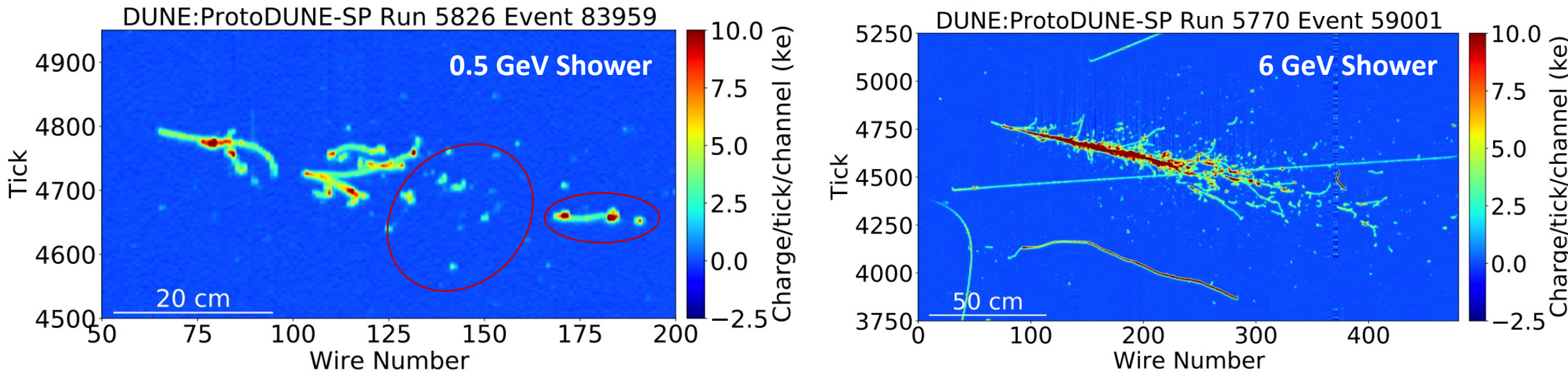
# Total Charge Exchange Cross Section



- Simulation refers as the reconstructed Monte-Carlo events.
- The four major sources of the systematic uncertainties are shown.

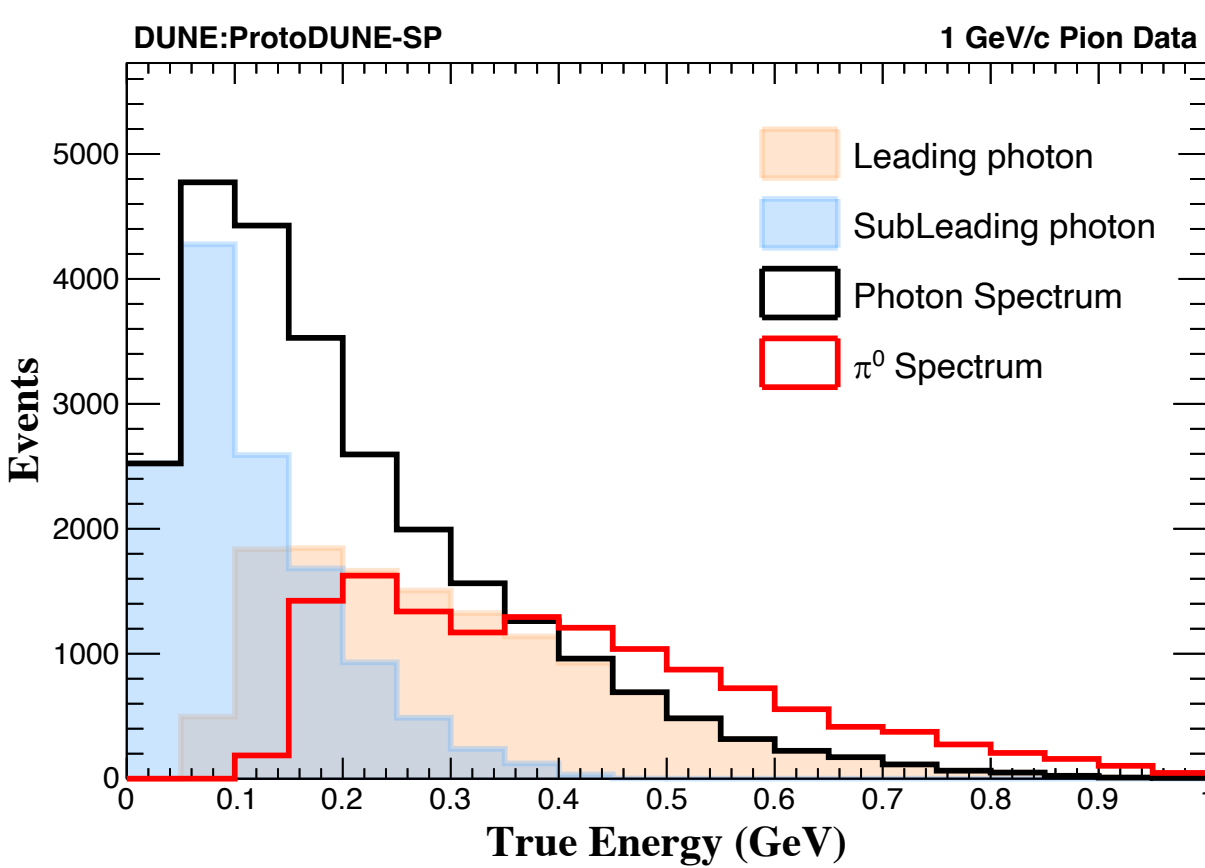
# Pion CEX Differential Cross-section

# Showers in TPC



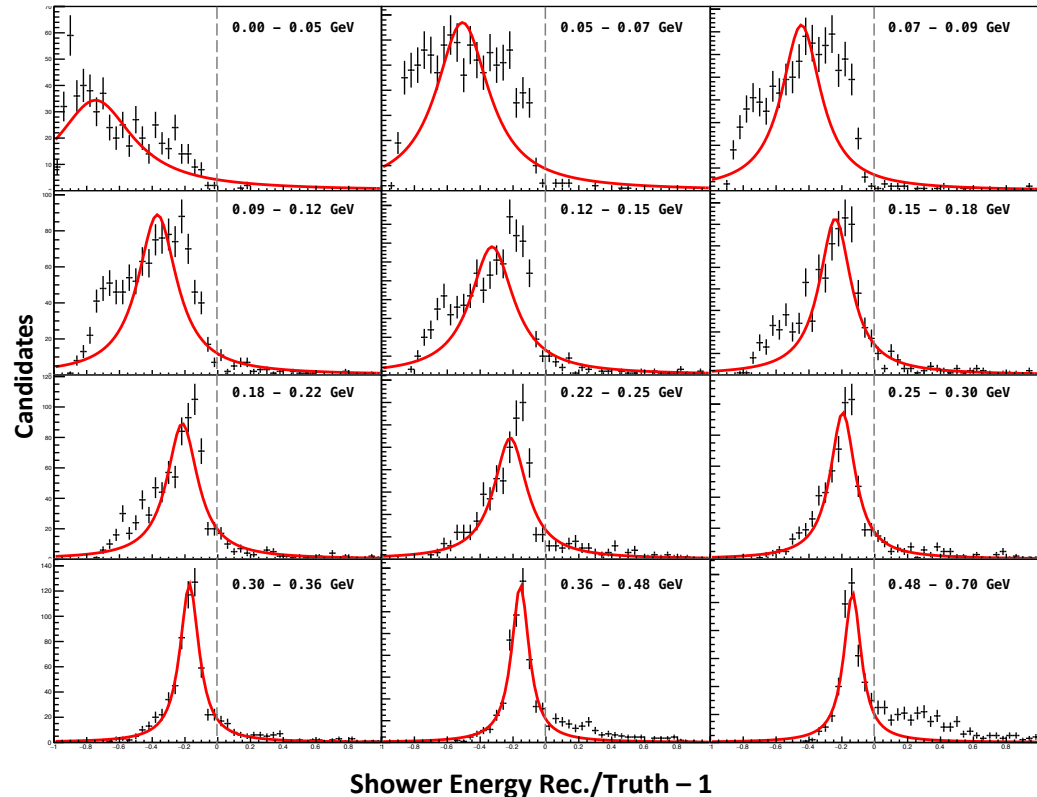
- Showers with different energy look quite different in the detector.
- Low energy showers are more stochastic and segmented:
  - ❖ Difficult to reconstruct  $\Rightarrow$  energy reconstruction bias

# Neutral Pion Energy

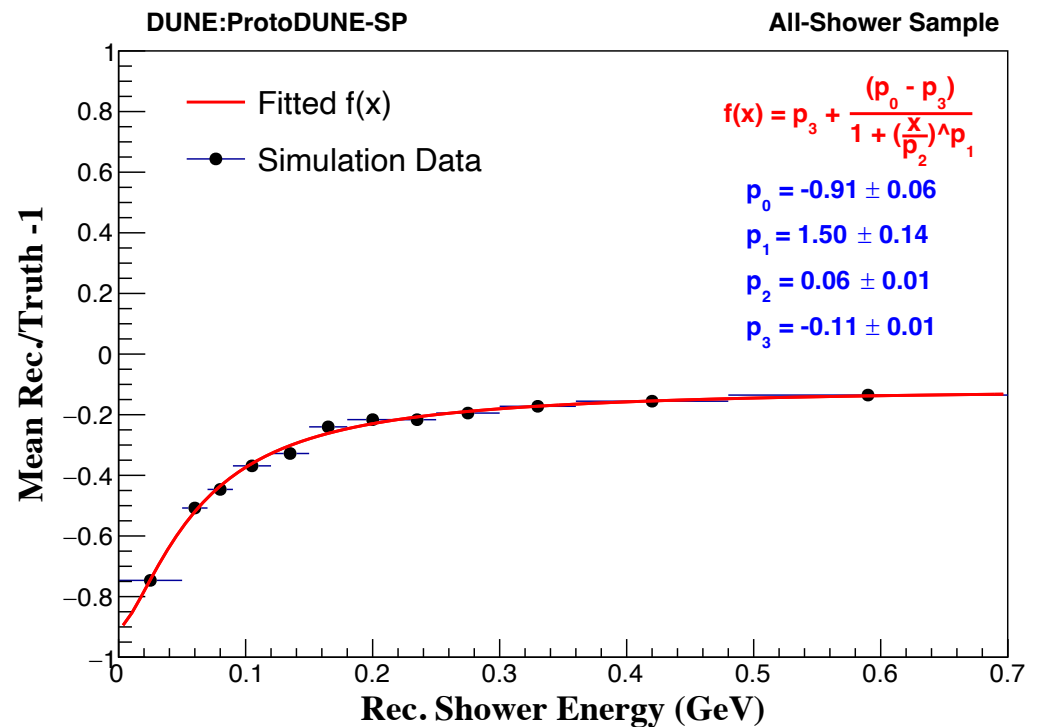


- The majority of  $\pi^0$  have energies ranging from 200 to 500 MeV
- Low energy sub-leading shower:
  - ❖ Less than 100 MeV (!)
  - ❖ Specific shower selections have been developed
- Need two reconstructed showers to get a neutral pion
  - ❖ This really reduces the selection efficiency for pion charge exchange events.

# Energy Correction

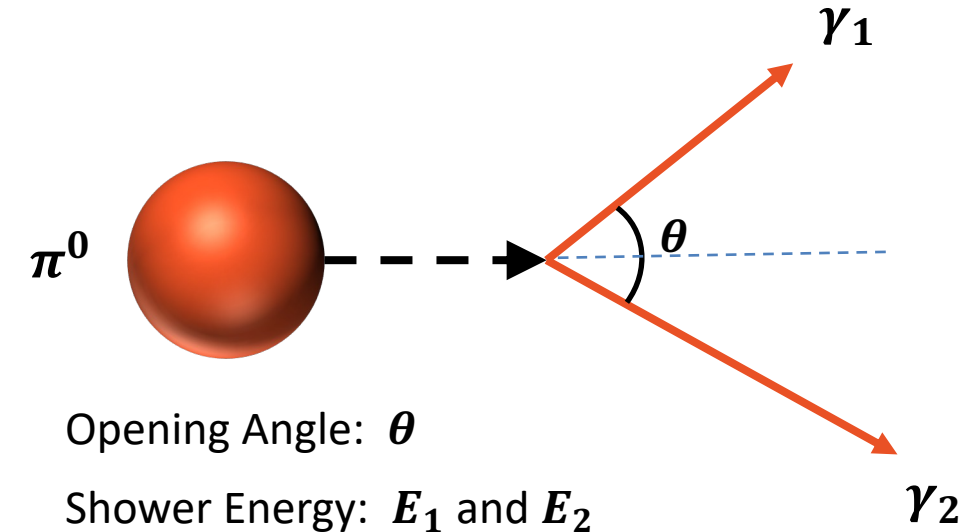
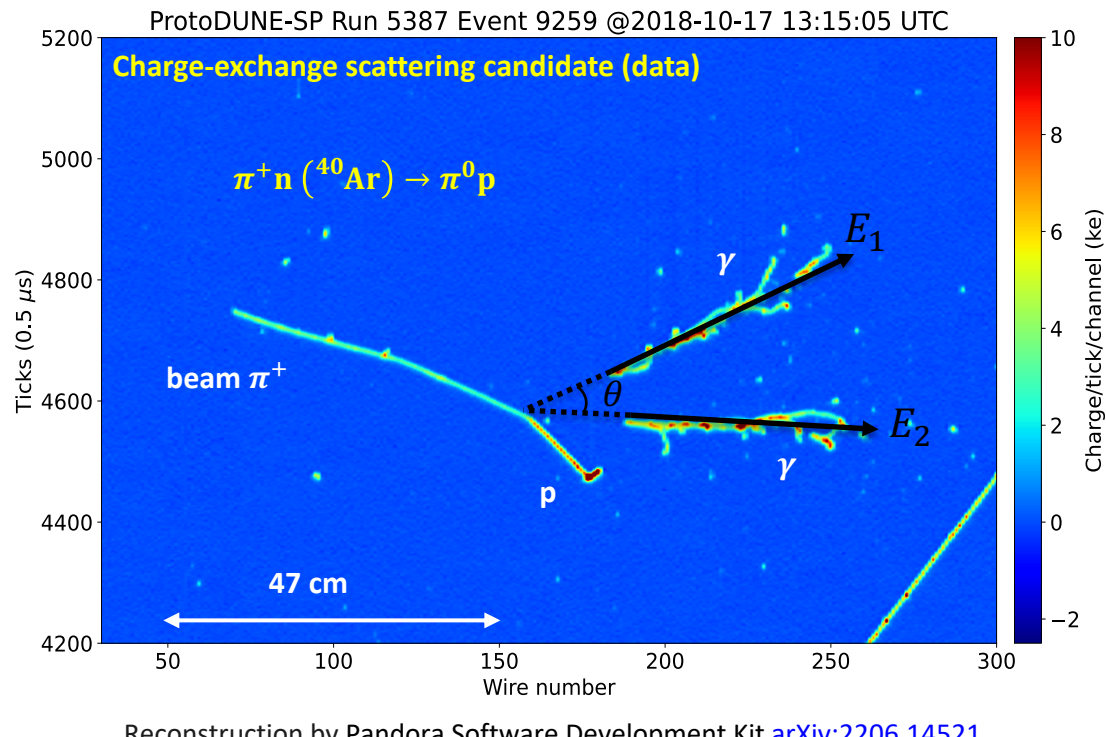


- A large shower energy bias is found in the whole energy range.
- Need MC-driven energy correction to improve the shower energy.



- Each date point is the mean fractional bias in that rec. energy bin
  - ❖ **Input:** raw shower energy
  - ❖ **Output:** correction factor (**event by event**)

# Kinematic Fitting



Invariant mass of two photons:

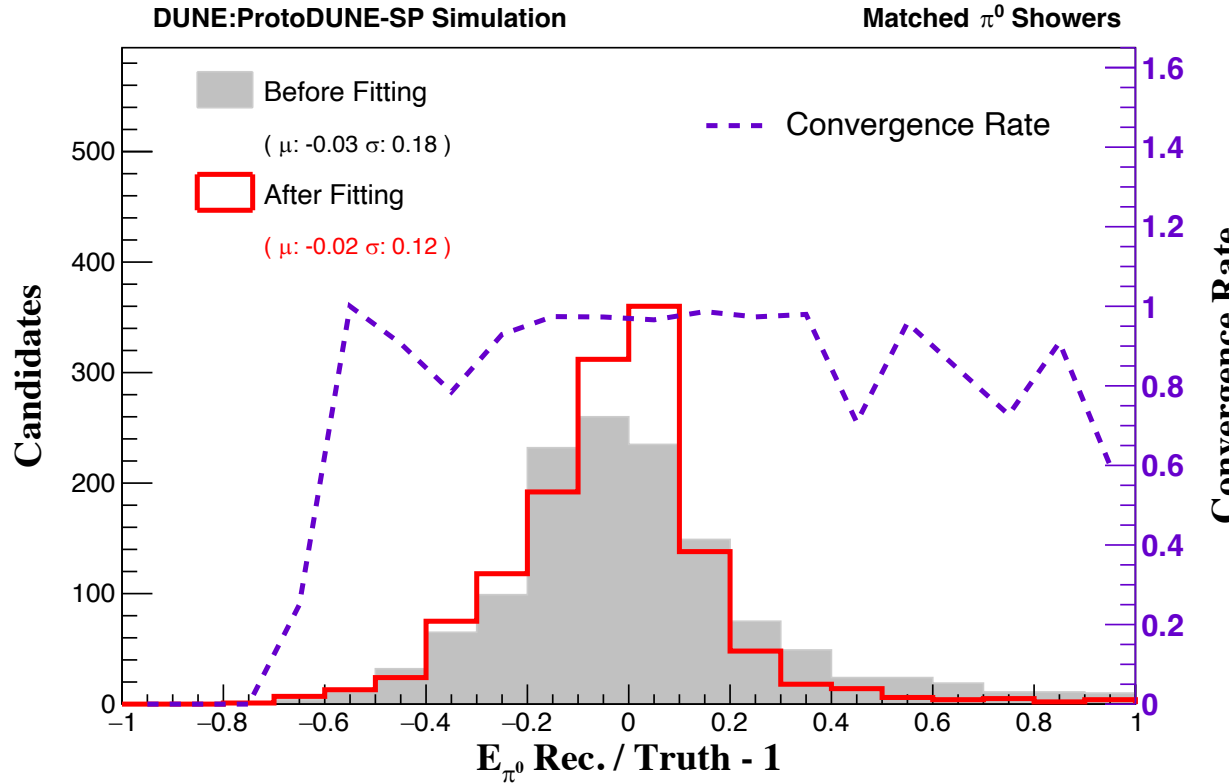
$$\diamond m_{\gamma\gamma}^2 = 2E_1E_2(1 - \cos(\theta))$$

- Use the invariant mass of two photons as a constraint.
- Vary both reconstructed **shower energy** and the **opening angle**, subjected to the **measurement uncertainty**.

# Kinematic Fitting

[1] MINERvA Collaboration, *Phys.Rev.D* 102 (2020) 7, 072007

[2] MicroBooNE Collaboration, *JINST* 15 (2020) 02, P02007

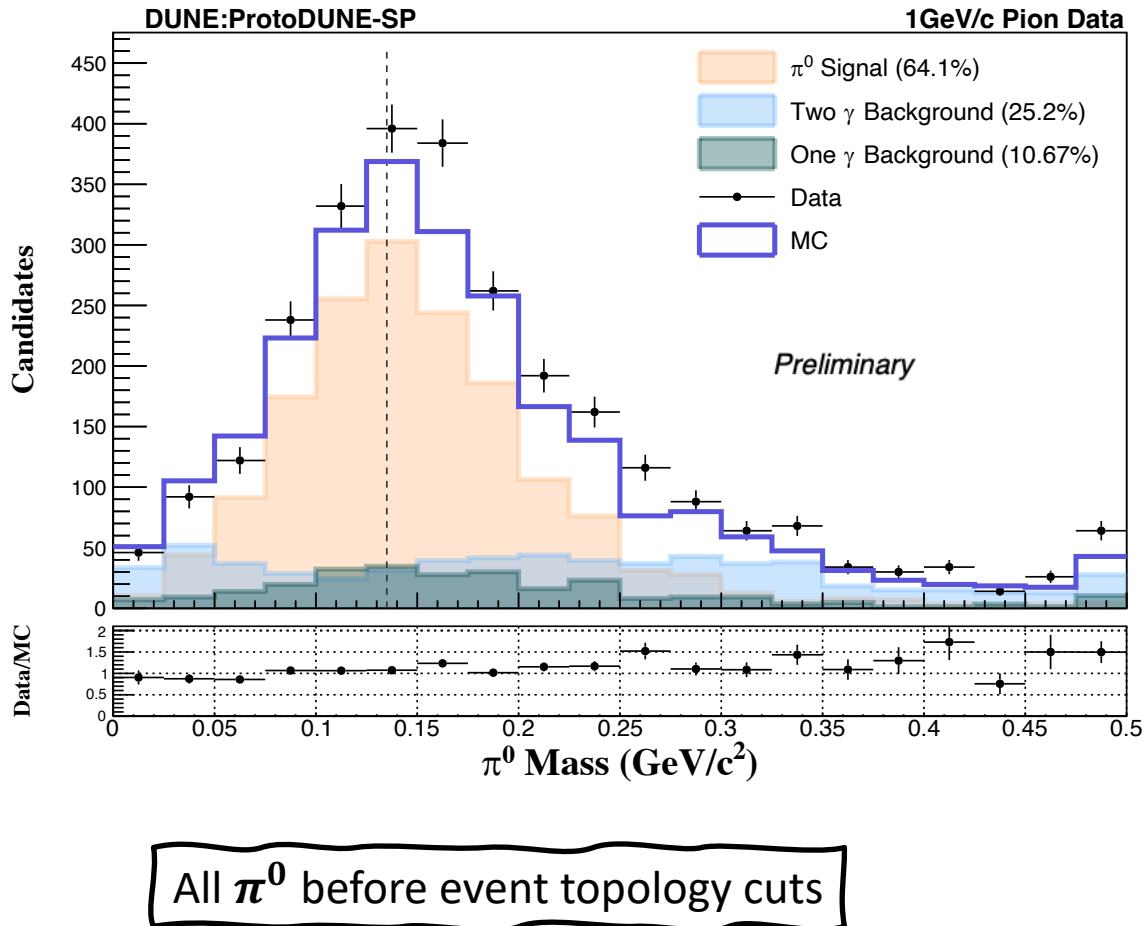


- The  $\pi^0$  energy resolution is **improved** from 18% to 12% (see in legend).
- KF has a larger impact on events where the  $\pi^0$  energy is overestimated.

$\pi^0$  energy resolution :

MINERvA [1]	MicroBooNE [2]	ProtoDUNE-SP
19%	10%	12%

# Reconstructed $\pi^0$ Mass

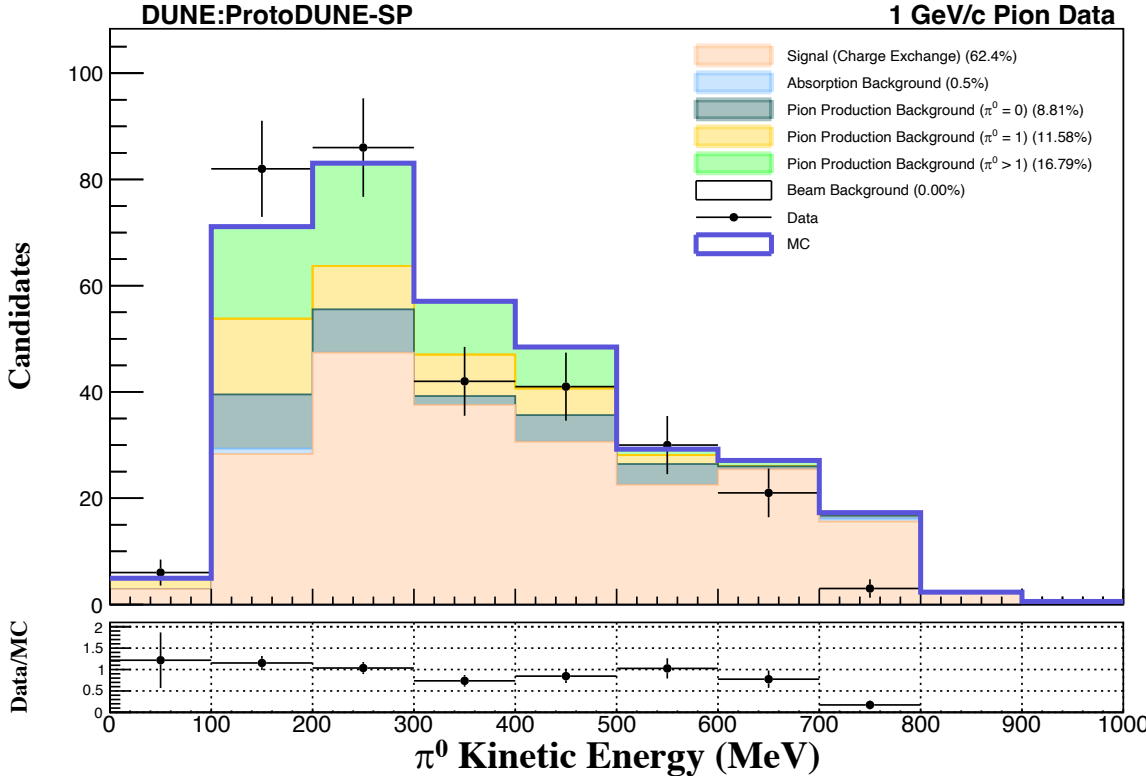


- The reconstructed  $m_{\gamma\gamma}$  invariant mass of all selected neutral pions.
- A mass window [50, 250] MeV is used to reduce background.

$m_{\gamma\gamma}$  Gaussian Fit:

MC	Data
$m_{\gamma\gamma}$	(139.4±3.56) MeV

# Reconstructed $T_{\pi^0}$



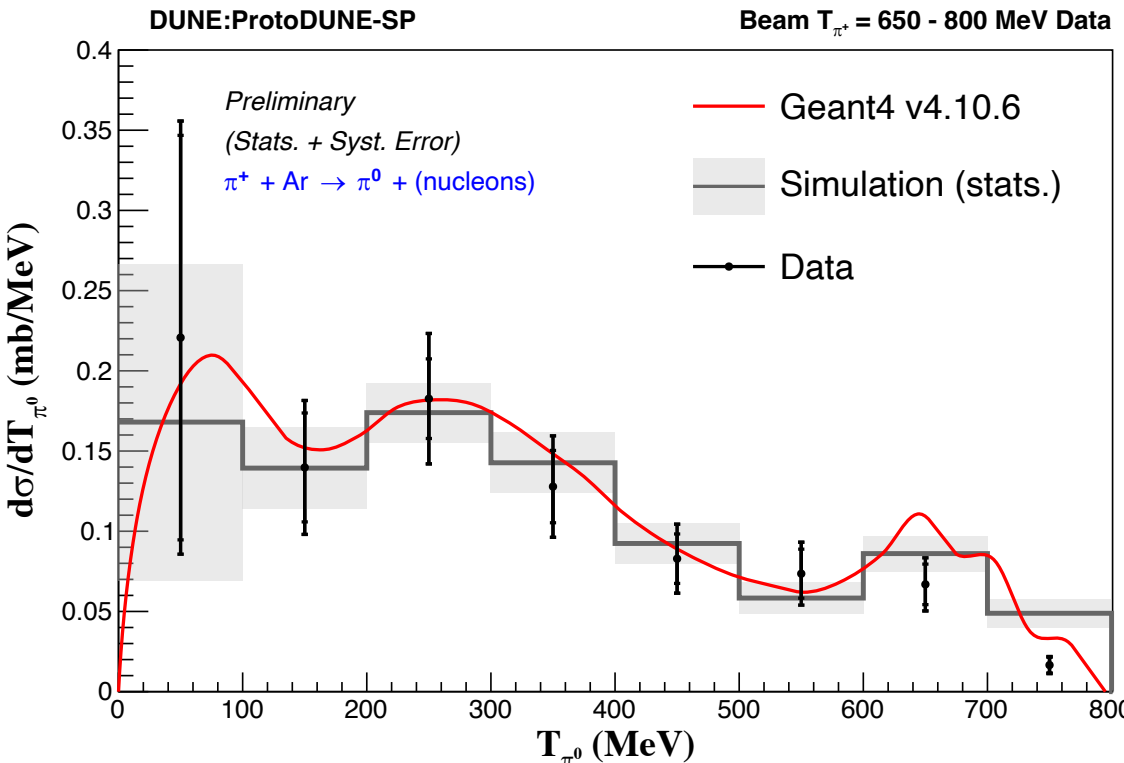
The reconstructed  $T_{\pi^0}$  kinetic energy of selected charge exchange events.

Pion production with  $\pi^0$  is the largest background.

$T_{\pi^0}$  is peaked around 250 MeV.

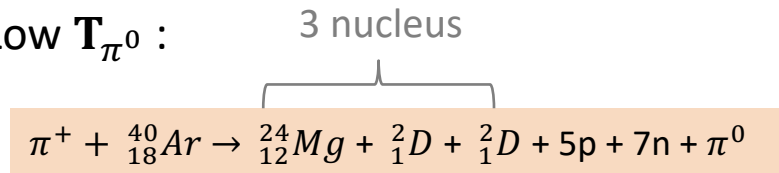
Selected  $\pi^0$  after event topology cuts and kinematic fitting

# Differential Cross-section $T_{\pi^0}$

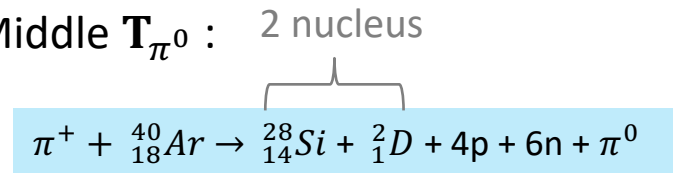


- The differential cross-section as a function of daughter  $\pi^0$  kinetic energy (beam  $\pi^+$  interacts with kinetic energy 650 - 800 MeV).
- Consider the following three regions:
  - Low  $T_{\pi^0}$  :  $T_{\pi^0} < 150$  MeV
  - Middle  $T_{\pi^0}$  :  $200 < T_{\pi^0} < 400$  MeV
  - High  $T_{\pi^0}$  :  $T_{\pi^0} > 650$  MeV
- Corresponds to different  $\pi^0$  kinematics.

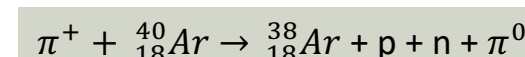
Low  $T_{\pi^0}$  :



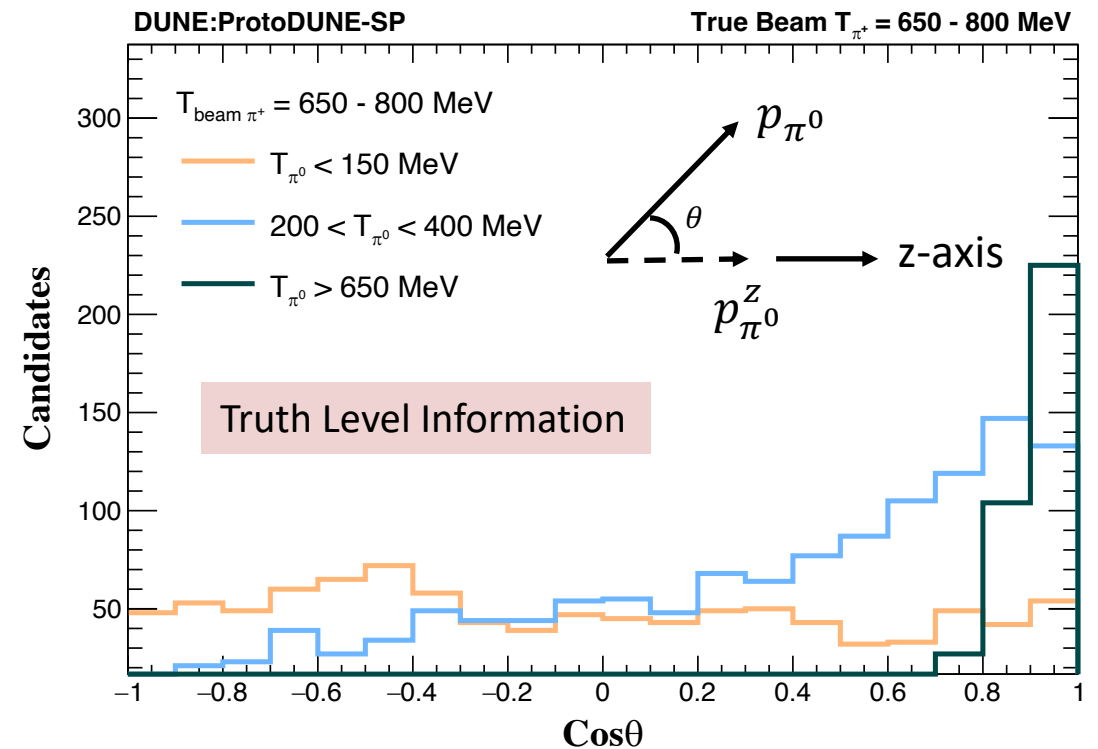
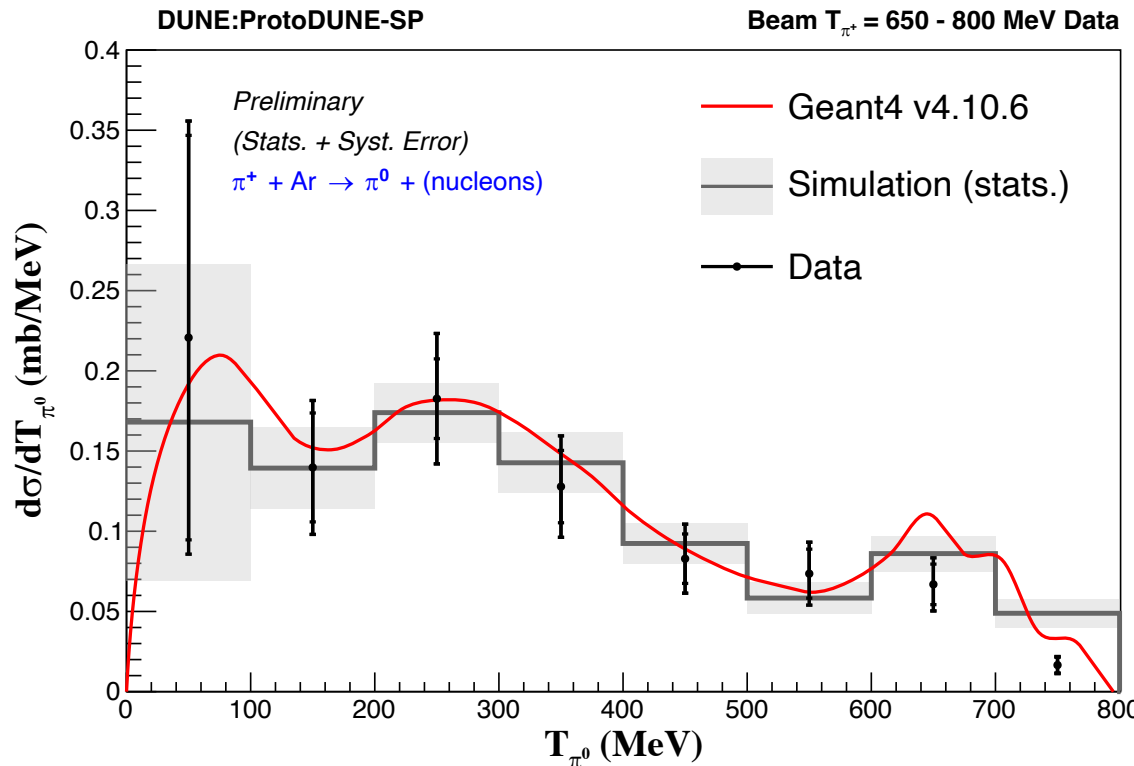
Middle  $T_{\pi^0}$  :



High  $T_{\pi^0}$  :

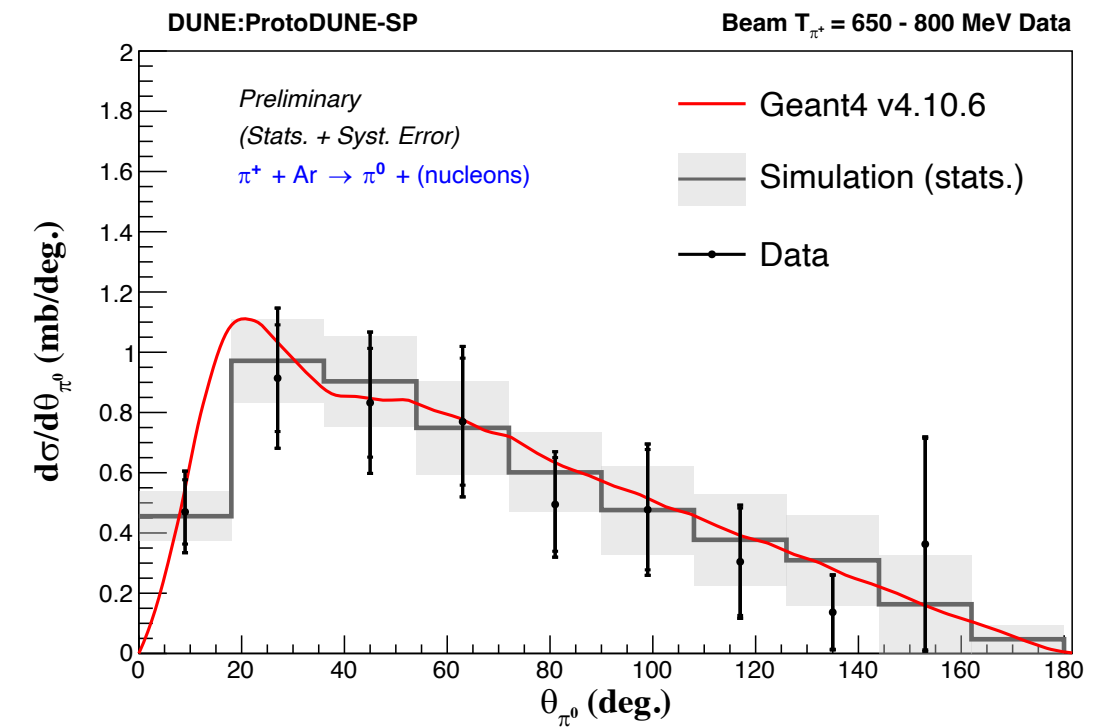
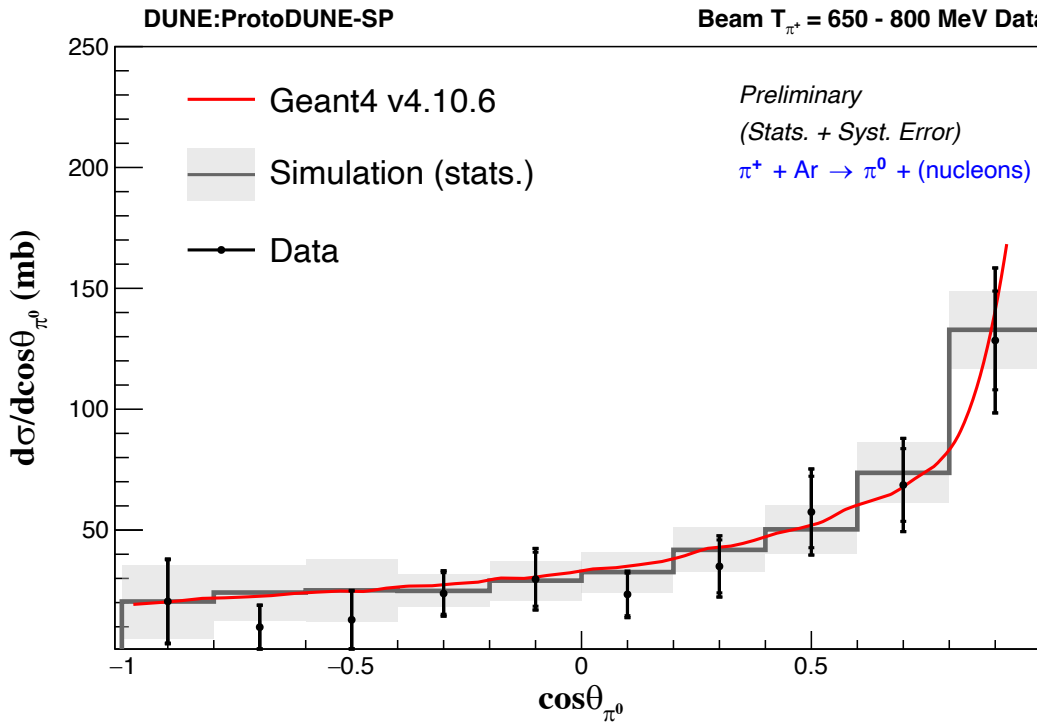


# Differential Cross-section $T_{\pi^0}$



- Low  $T_{\pi^0}$  :  $\pi^0$  was produced with no prefer direction.
- Middle  $T_{\pi^0}$  :  $\pi^0$  was produced with a forward direction.
- High  $T_{\pi^0}$  : Most of the  $\pi^0$  was produced along the beam direction.

# Differential Cross-section $\theta_{\pi^0}$



- Daughter  $\pi^0$  prefers to be produced in the forward direction.
- Current results are limited by the statistical errors.
- Consistent with the GEANT4 prediction.

# Summary

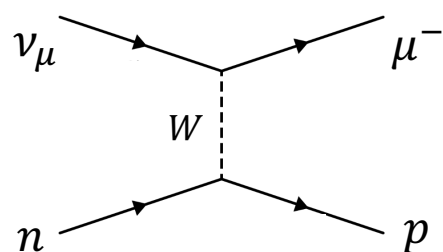
- The ProtoDUNE-SP has produced not only technical tests and calibrations, but also provided physics results.
  - ❖ First results on ProtoDUNE-SP detector performance: [DUNE Collaboration, JINST 15 \(2020\) 12, P12004](#)
  - ❖ Design, construction and operation of the ProtoDUNE-SP LArTPC: [DUNE Collaboration, JINST 17 \(2022\) 01, P01005](#)
  - ❖ Identification and reconstruction of low-energy electrons in the ProtoDUNE-SP detector: [Phys. Rev. D 107, 092012 \(2023\)](#)
  - ❖ Reconstruction of interactions in the ProtoDUNE-SP detector with Pandora: [Eur. Phys. J. C 83, 618 \(2023\)](#)
- Several cross-section measurements using  $\pi^+$ ,  $K^+$ , and proton beams with an argon target will be coming up soon.
- Stay tuned!

# Back-Up

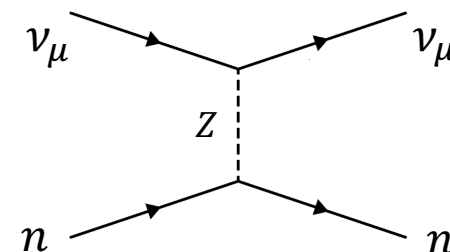
# Neutrino Detection

- Can only detect the presence of a neutrino if it interacts:
  - ❖ **Charged-current interactions**, where the neutrino converts into the corresponding charged lepton.
  - ❖ **Neutral-current interactions**, where the neutrino remains a neutrino, but transfers energy. (target recoils or breaks up)

**Charged-current**



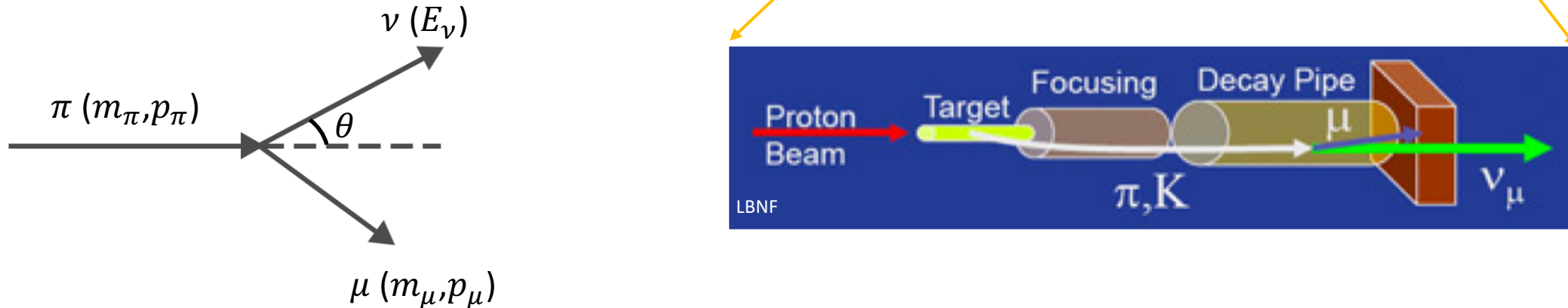
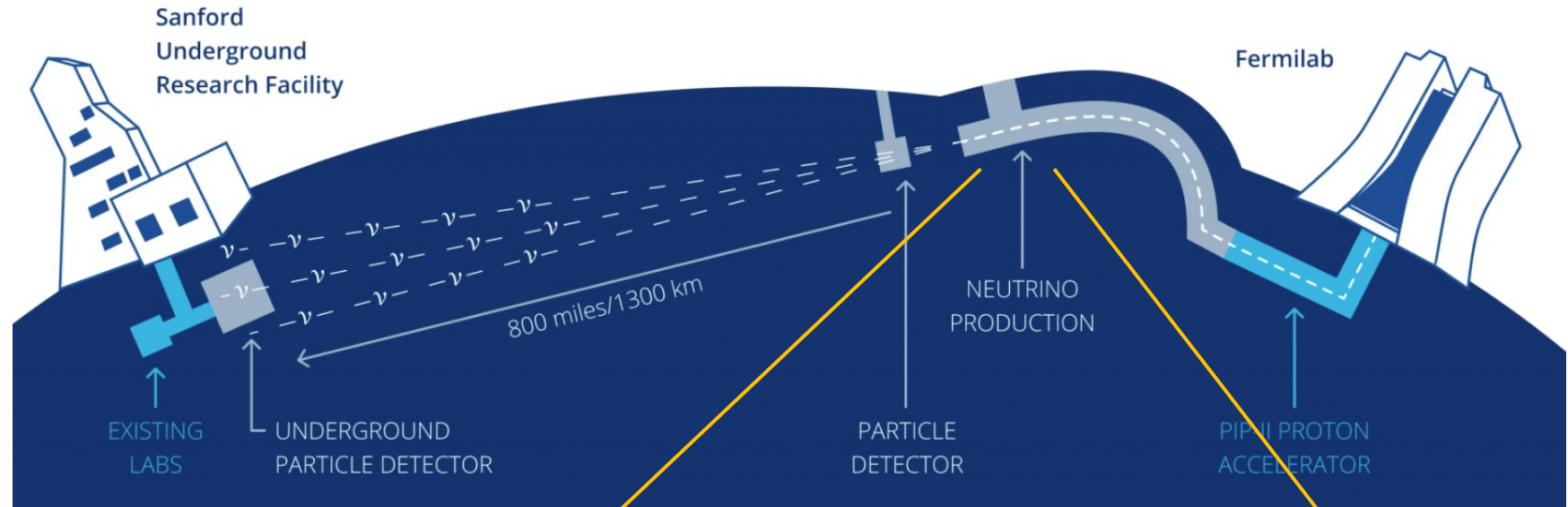
**Neutral-current**



- **Radiochemical experiments**
  - ❖ Homestake, SAGE
- **Liquid scintillator experiments**
  - ❖ KamLAND, MiniBooNE
- **Tracking experiments**
  - ❖ MINERvA, MicroBooNE, DUNE
- **Cherenkov experiments**
  - ❖ T2K, SNO

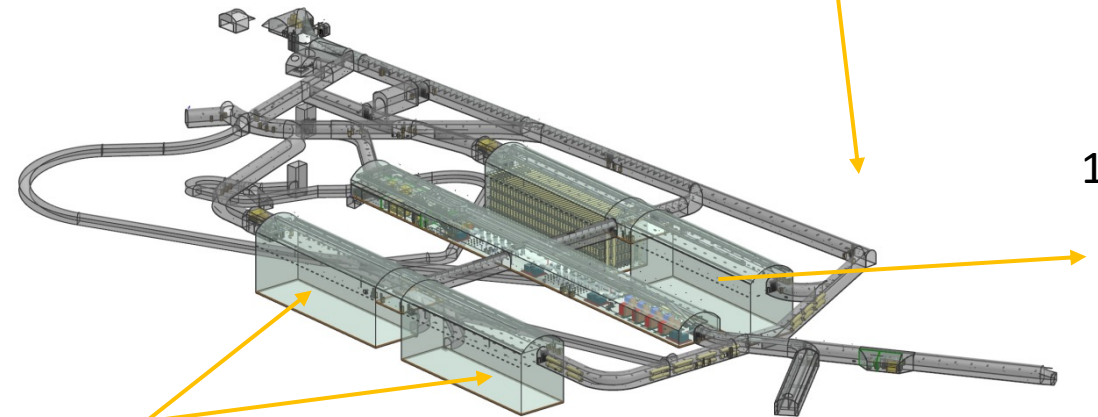
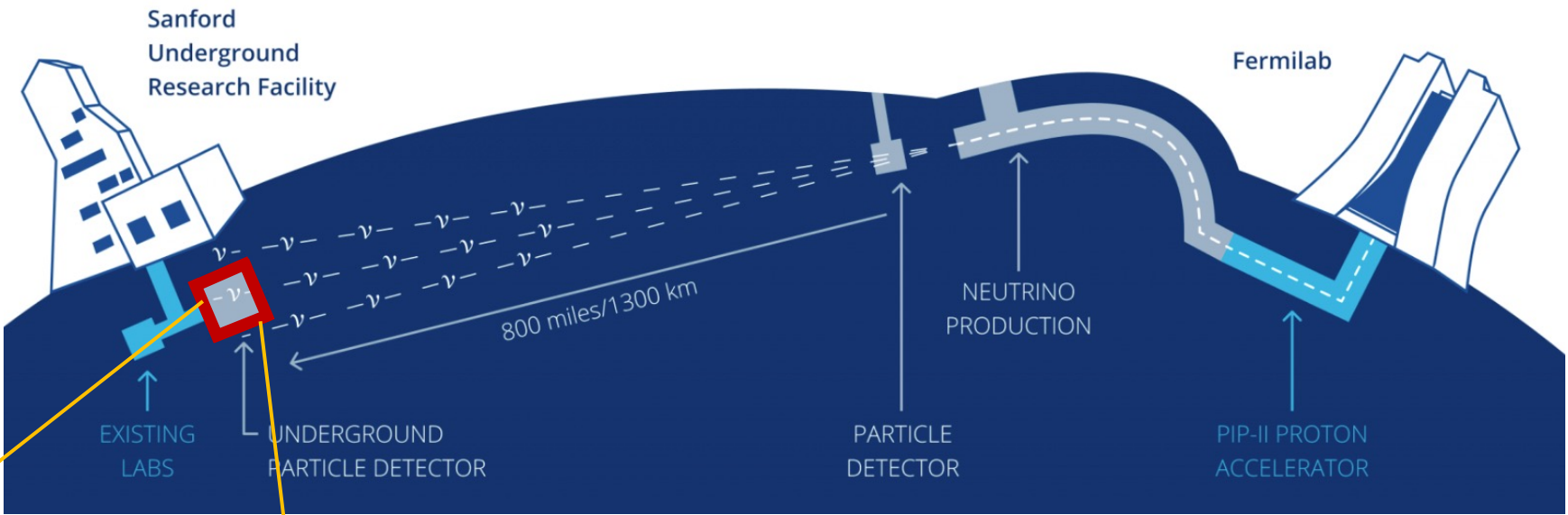
# DUNE Beam

- 1000+ scientists
- 170+ laboratories and universities
- 30+ countries

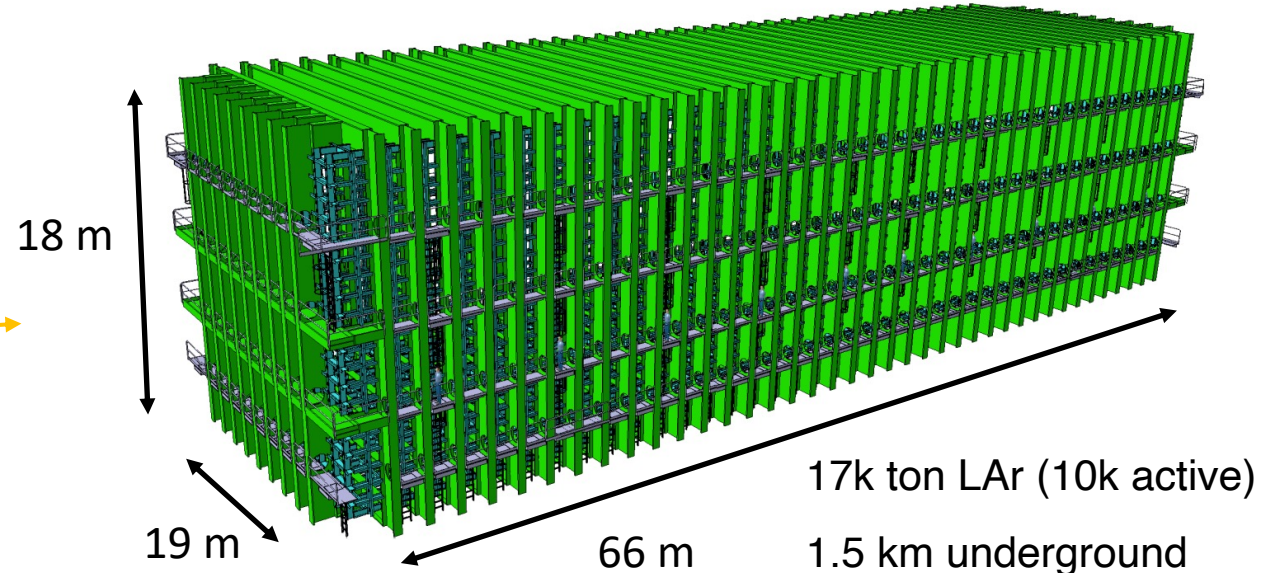


# DUNE FD

- 1000+ scientists
- 170+ laboratories and universities
- 30+ countries

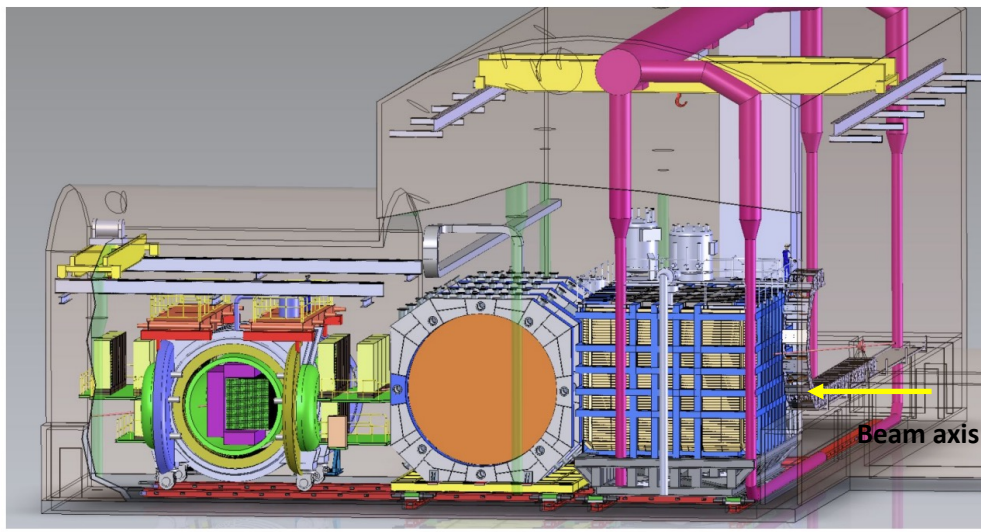
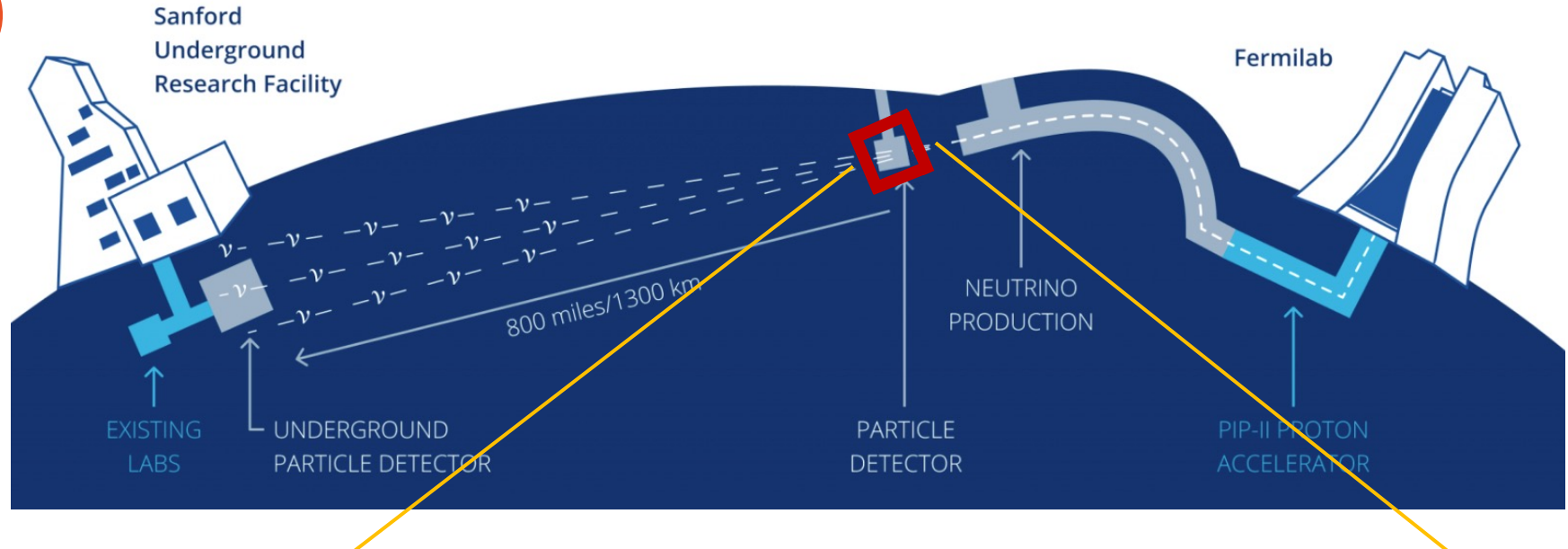


4 independent modules



# DUNE ND

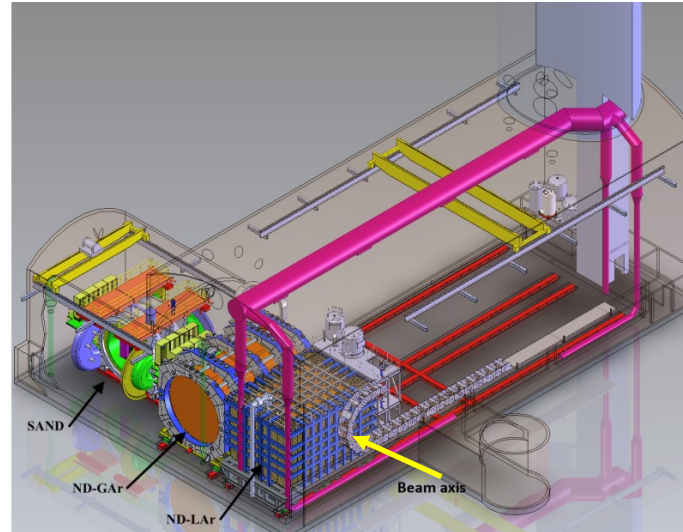
- 1000+ scientists
- 170+ laboratories and universities
- 30+ countries



SAND

ND-GAr

ND-LAr

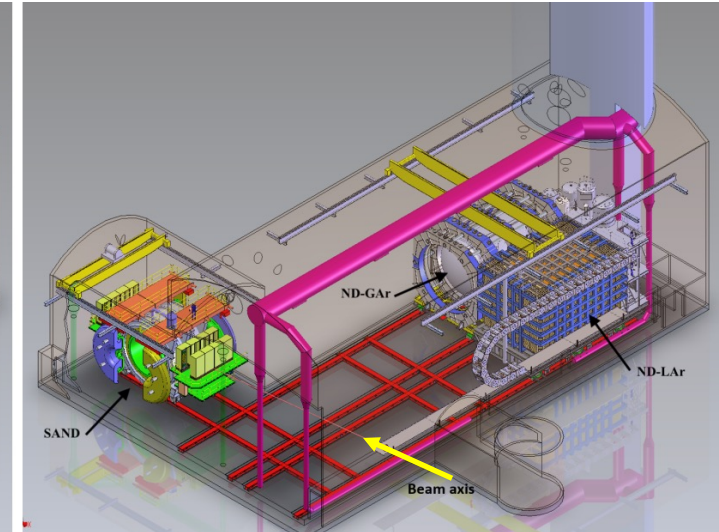


SAND

ND-GAr

ND-LAr

Beam axis



SAND

ND-GAr

ND-LAr

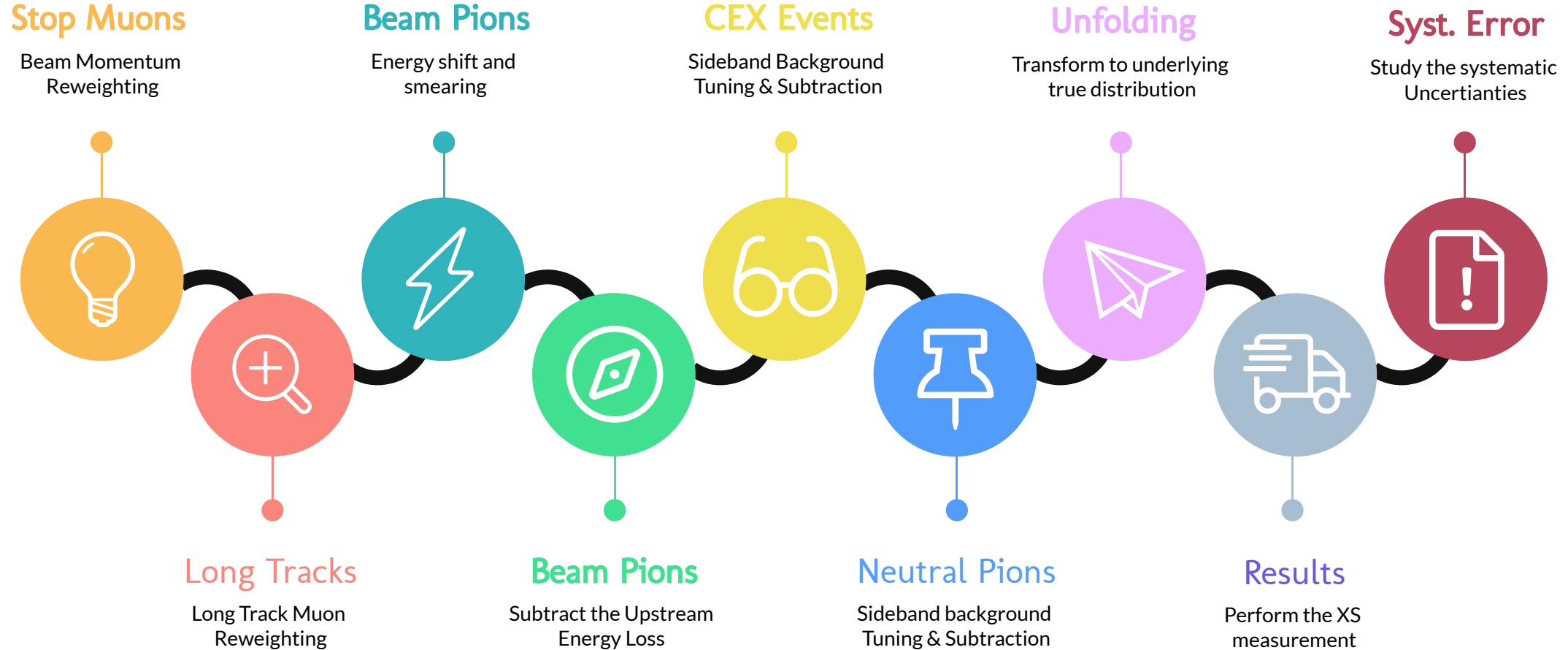
Beam axis

# DUNE Physics Program

- The primary goals are to:
  - ❖ Measure the neutrino oscillation by looking for the appearance of  $\nu_e(\bar{\nu}_e)$  from a pure  $\nu_\mu(\bar{\nu}_\mu)$  beam, including measurements of charge-parity (CP) phase and the determination of neutrino mass hierarchy.
  - ❖ Search for proton decay.
  - ❖ Observe the core-collapse supernova  $\nu_e$  neutrinos.



# Cross-section Measurement Roadmap



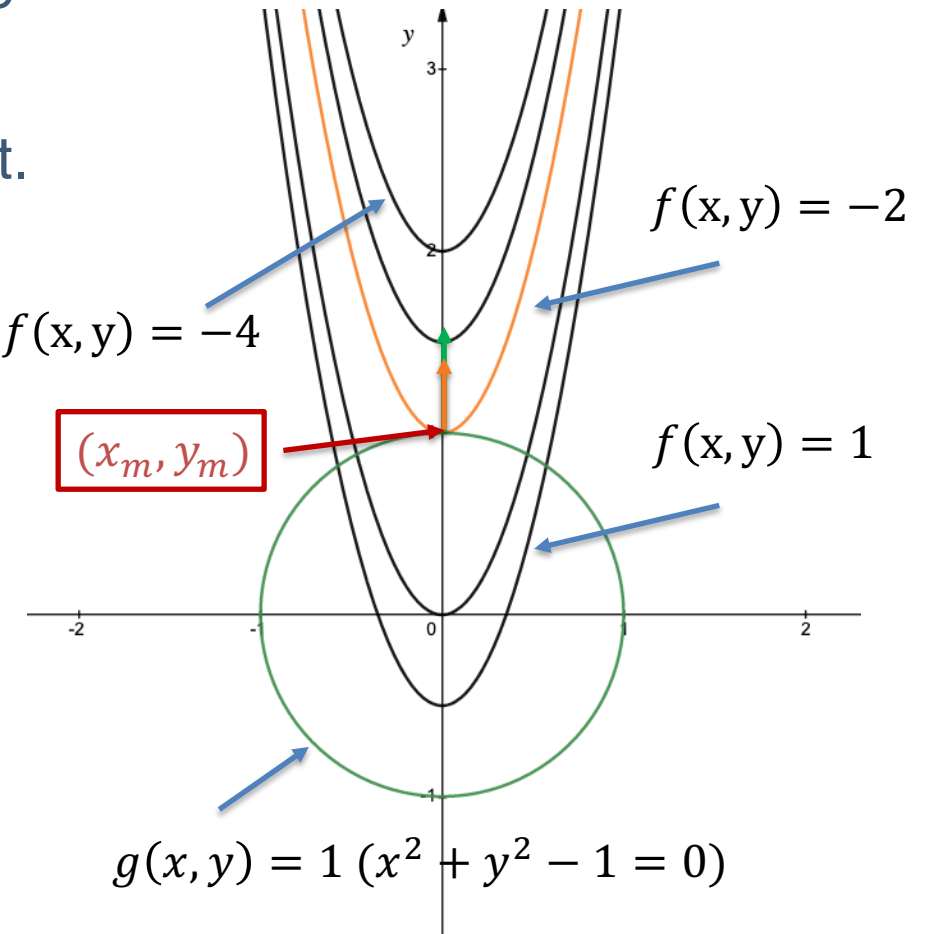
# Lagrange Multiplier Method

- Minimize the function  $f(x, y) = 8x^2 - 2y$  subject to the constraint  $g(x, y) = x^2 + y^2 - 1 = 0$ .
- Need to find a point where the two graphs are tangent.
  - Mathematically we represent it as:

$$\nabla f(x_m, y_m) = \lambda \nabla g(x_m, y_m)$$

- This scalar  $\lambda$  is the Lagrange Multiplier.
- Construct the function  $L(x, y, \lambda) = f(x, y) - \lambda g(x, y)$
- Set all partial derivatives to zero.
- Solve a set of linear equations to obtain  $(x_m, y_m)$ .

## Visualization



# $\chi^2$ Calculation

- Let  $\alpha$  be a column vector representing a set of **true values** and  $\alpha_0$  representing the **measured parameters** without any constraint.

$$\alpha = \begin{pmatrix} \alpha_1 \\ \alpha_2 \\ \vdots \\ \alpha_n \end{pmatrix}$$

$$\alpha_0 = \begin{pmatrix} \alpha_1^0 \\ \alpha_2^0 \\ \vdots \\ \alpha_n^0 \end{pmatrix}$$

- How well we measured parameters  $\alpha_0$ , which are subjected to an experimental resolution  $\sigma$ , match the true values  $\alpha$  can be quantified by computing the value of  $\chi^2$ ,

$$\chi^2 = (\alpha - \alpha_0) V_{\alpha_0}^{-1} (\alpha - \alpha_0)$$

- $V_{\alpha_0}^{-1}$  is the inverse of the covariance matrices ( $V_{\alpha_0} = \text{diag}(\sigma_i^2)$  for independent values)

# Toy Example

- Measuring the energies of three particles ( $E_1, E_2, E_3$ ) in unit of MeV and their true values are (4,9,16) MeV. These measured energies have an uncertainty  $(\sigma_1, \sigma_2, \sigma_3) = (0.5, 1, 1)$  MeV.
- One constraint equation can be used to improve the resolution,

$$E_1 + E_2 + E_3 = E_{sum} = 29 \quad \longrightarrow \quad H_1 = E_1 + E_2 + E_3 - 29$$

- The covariance matrix  $V_{\alpha_0}$  are computed to be,

$$V_{\alpha_0} = \begin{pmatrix} \sigma_1^2 & 0 & 0 \\ 0 & \sigma_2^2 & 0 \\ 0 & 0 & \sigma_3^2 \end{pmatrix}$$

$$\sigma = \sqrt{\frac{\sum(x_i - \mu)^2}{N}}$$

Variables in red are optimized in the end

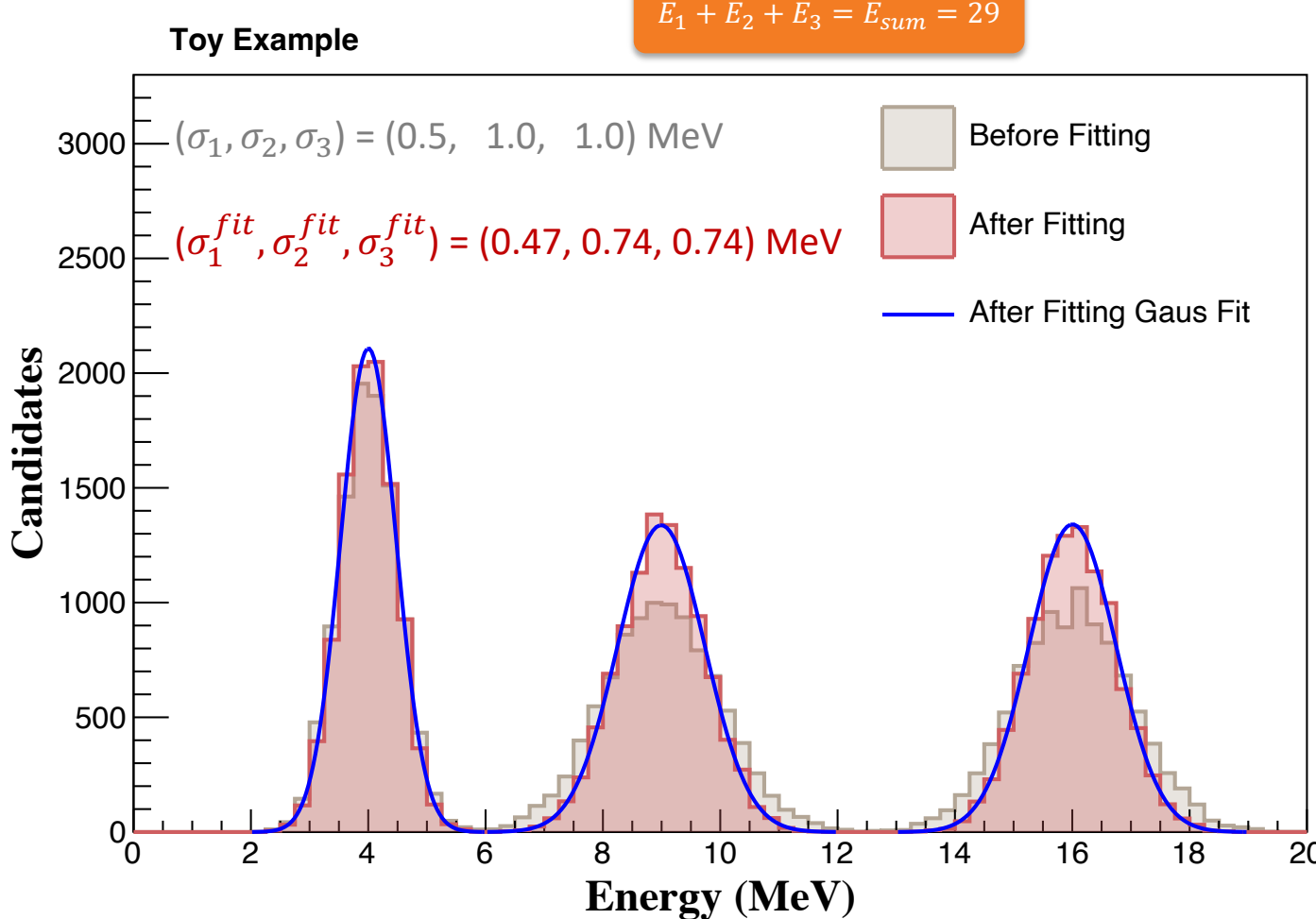
$$\chi^2 = \lambda * H_1 + (\alpha - \alpha_0) V_{\alpha_0}^{-1} (\alpha - \alpha_0)$$

Constraint equation

$\chi^2$  without any constraint

# Toy Example Results

$$\chi^2 = \lambda * H_1 + (\alpha - \alpha_0) V_{\alpha_0}^{-1} (\alpha - \alpha_0)$$



- Generated 10k random Gaussian numbers:
  - ❖ Mean values (4, 9, 16) MeV
  - ❖ Sigma (0.5, 1, 1) MeV
- Use the energy conservation law as constraint.
- Improvement is found in **energy resolution** for all three particles.

# Extract Cross-section

- Total CEX XS for bin  $i$  (beam  $T_{\pi^+}$  bin) is,

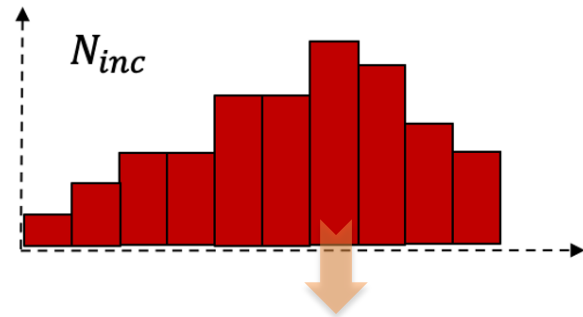
$$\sigma_i = \frac{m_{Ar}}{\rho N_A \delta E}$$

$$\left. \frac{dE}{dx} \right|_{E_i} \ln \left( \frac{N_{inc}}{N_{inc} - N_{int}} \right)_i$$

We perform the total CEX cross-section at **each bin  $i$**  of the measured beam  $\pi^+$  kinetic energy.

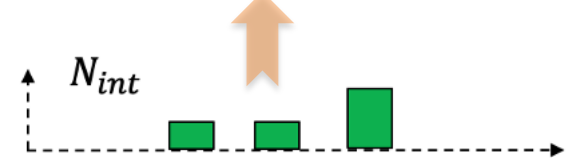
$\pi^+$  energy loss per unit length evaluated at each bin  $i$  centre using Bethe-Block formula.

Incident histogram



The number of **incident**  $\pi^+$  at each bin  $i$  the measured beam  $\pi^+$  kinetic energy.

Interacting histogram

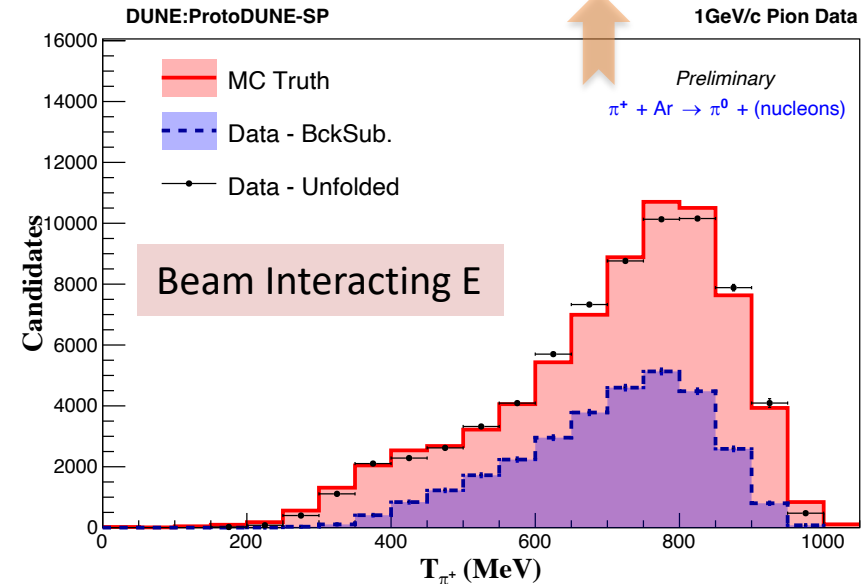
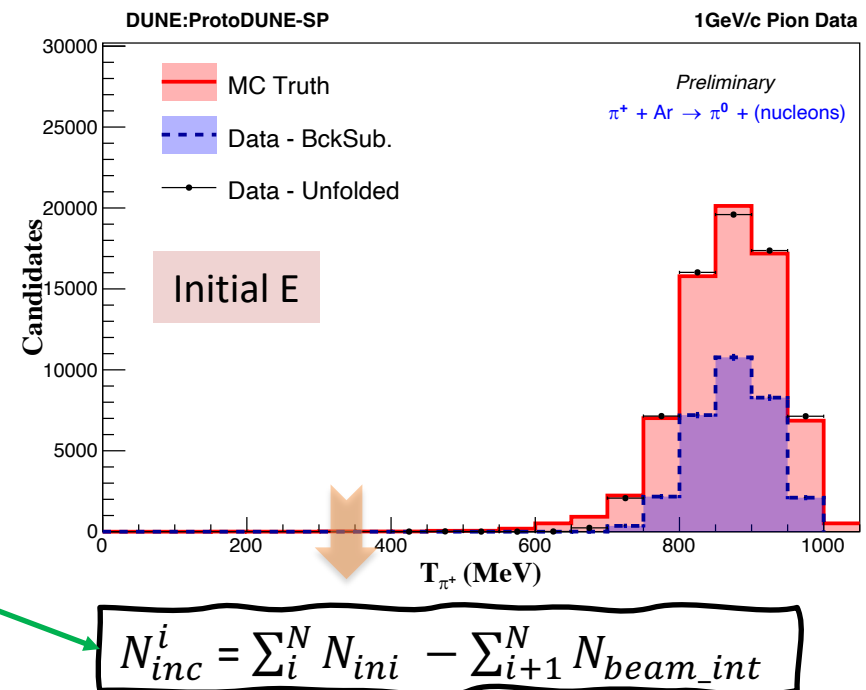
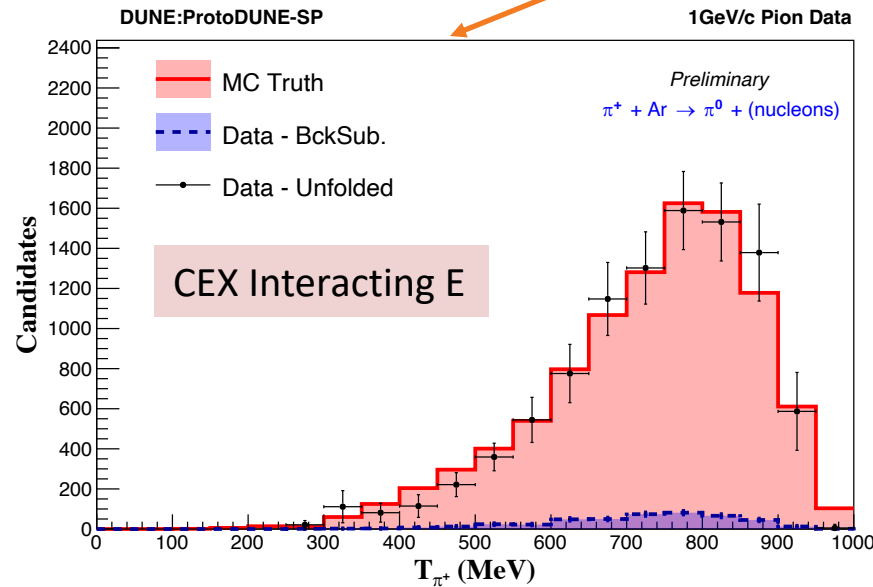


The number of **interacting**  $\pi^+$  via the charge exchange interactions at each bin  $i$  of the measured CEX interacting E histogram.

# Extract Cross-section

- Total CEX XS for bin  $i$  (beam  $T_{\pi^+}$  bin) is,

$$\sigma_i = \frac{m_{Ar}}{\rho N_A \delta E} \left. \frac{dE}{dx} \right|_{E_i} \ln \left( \frac{N_{inc}}{N_{inc} - N_{int}} \right)_i$$



# Differential Cross Section Formula

- Calculate the differential cross section as,

$$\left( \frac{d\sigma}{dT_{\pi^0}} \right)_{ij} = \frac{m_{Ar}}{\rho N_A \delta E} \frac{dE}{dx} \Big|_{E_i} \frac{1}{(\Delta T_{\pi^0})} \frac{N_{int}^{ij}}{N_{inc}^i} \quad (\text{Eq. 1})$$

- Thin slice total CEX cross section is,

$$\sigma_i = \frac{m_{Ar}}{\rho N_A \delta E} \frac{dE}{dx} \Big|_{E_i} \frac{N_{int}^i}{N_{inc}^i} \quad (\text{Eq. 2})$$

- Then the differential cross section formula is (Sub. Eq. 2 into Eq. 1),

$$\left( \frac{d\sigma}{dT_{\pi^0}} \right)_{ij} = \frac{1}{(\Delta T_{\pi^0})} \frac{N_{int}^{ij}}{N_{int}^i} \sigma_i$$

Measured total  
CEX cross-section

$$\sigma_i \approx \frac{m_{Ar}}{\rho N_A \delta E} \frac{dE}{dx} \Big|_{E_i} \frac{N_{int}^i}{N_{inc}^i}$$

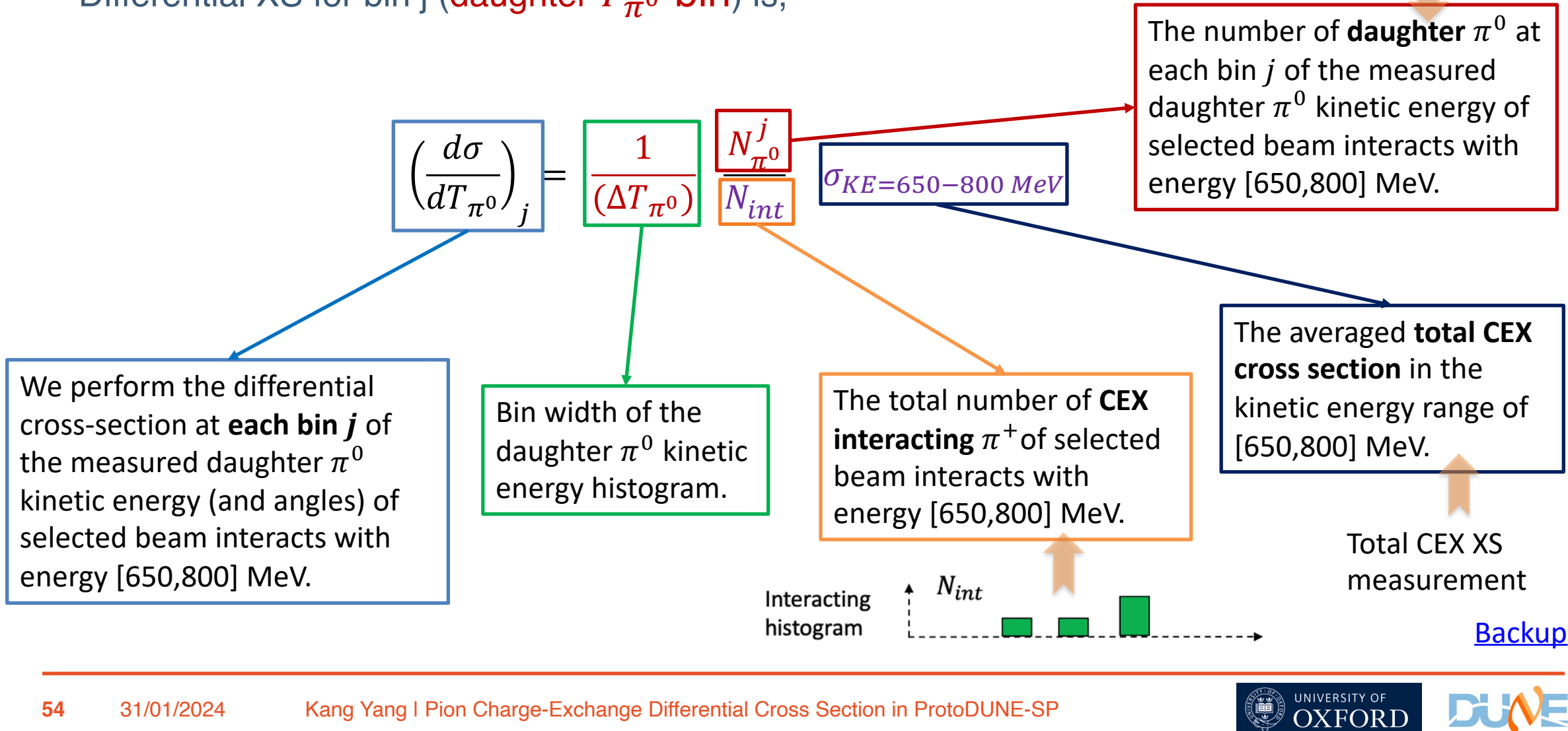
$\Delta T_{\pi^0}$  is the bin width of  $\pi^0$  KE

Index  $i$  : beam  $T_{\pi^+}$  bin,

Index  $j$  : daughter  $T_{\pi^0}$  bin

# Extract Differential Cross-Section

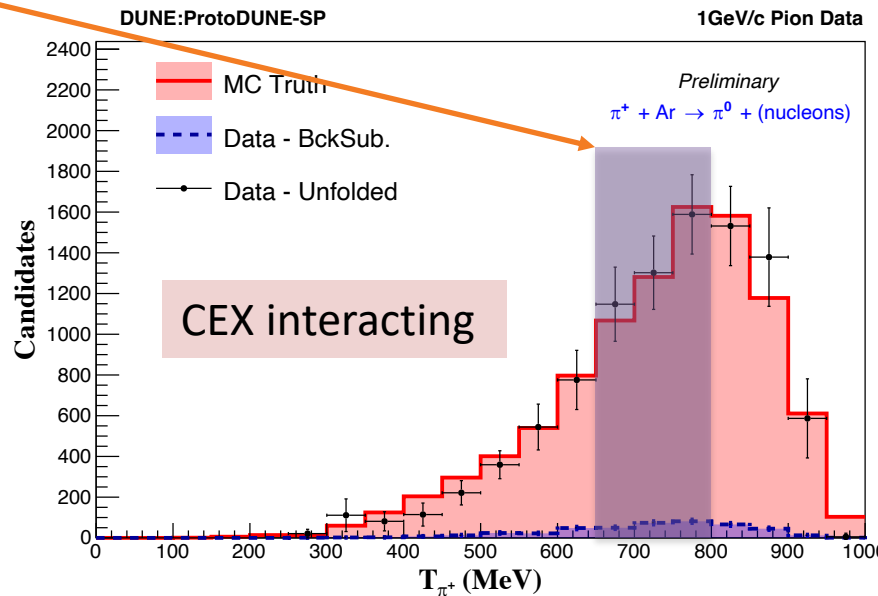
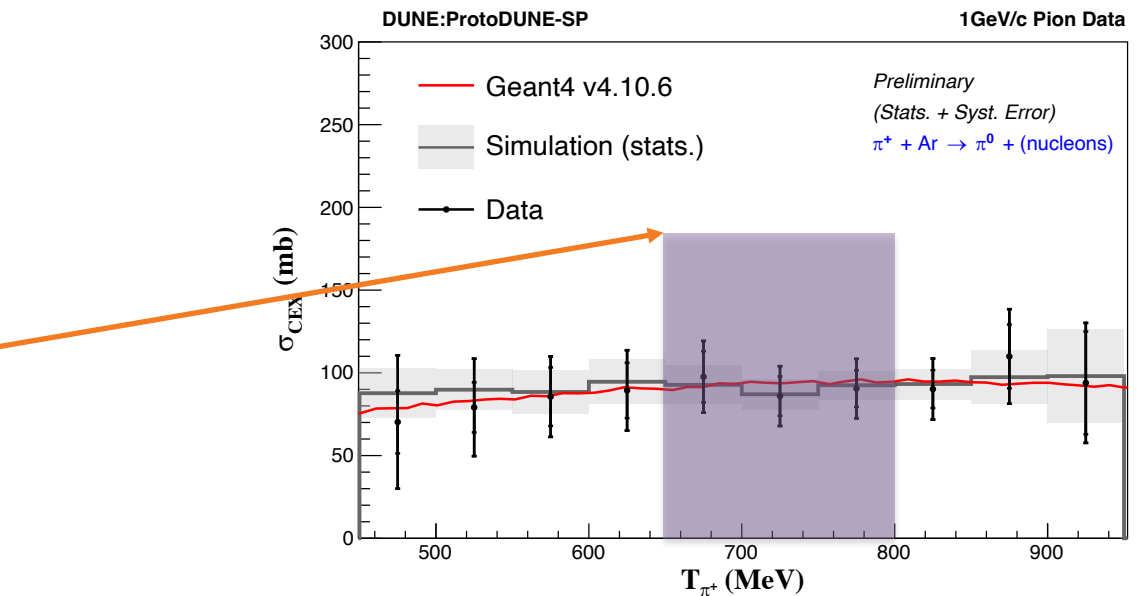
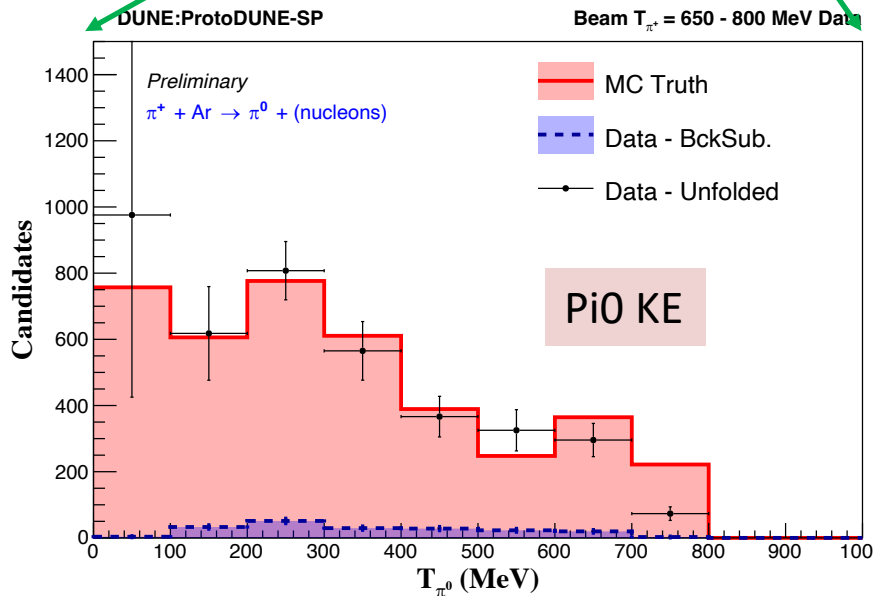
- Differential XS for bin  $j$  (daughter  $T_{\pi^0}$  bin) is,



# Extract $d\sigma$

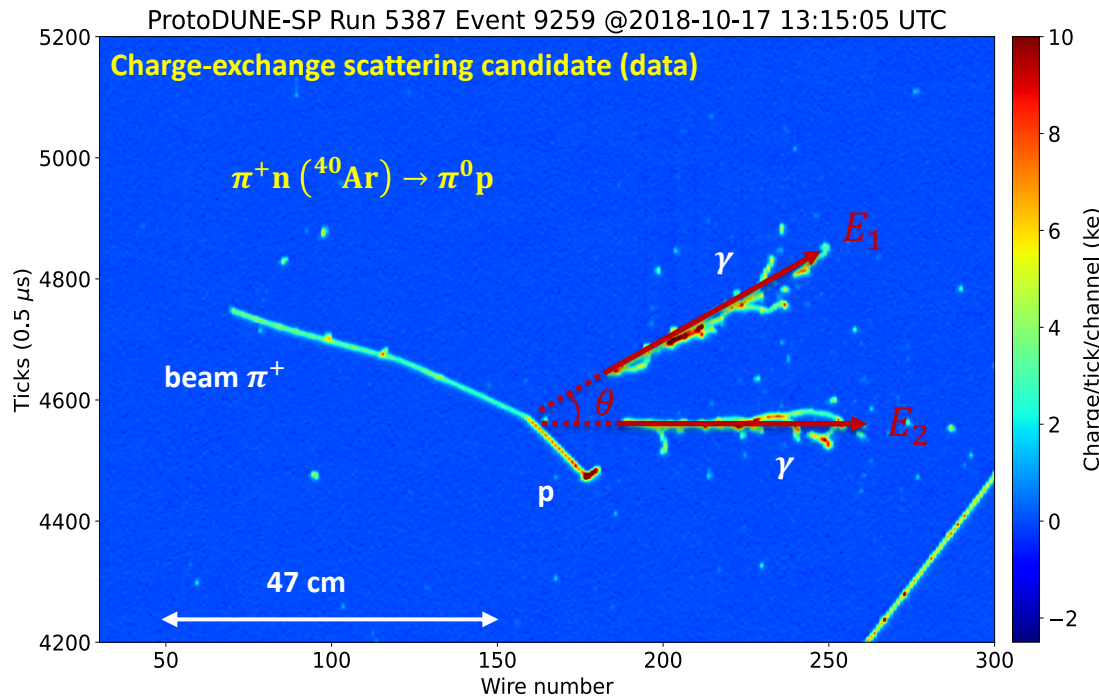
- Differential XS for bin  $j$  (daughter  $T_{\pi^0}$  bin) is,

$$\left(\frac{d\sigma}{dT_{\pi^0}}\right)_j = \frac{1}{(\Delta T_{\pi^0})} \frac{N_{int}^j}{N_{int}} \quad \sigma_{KE} = 650 - 800 \text{ MeV}$$

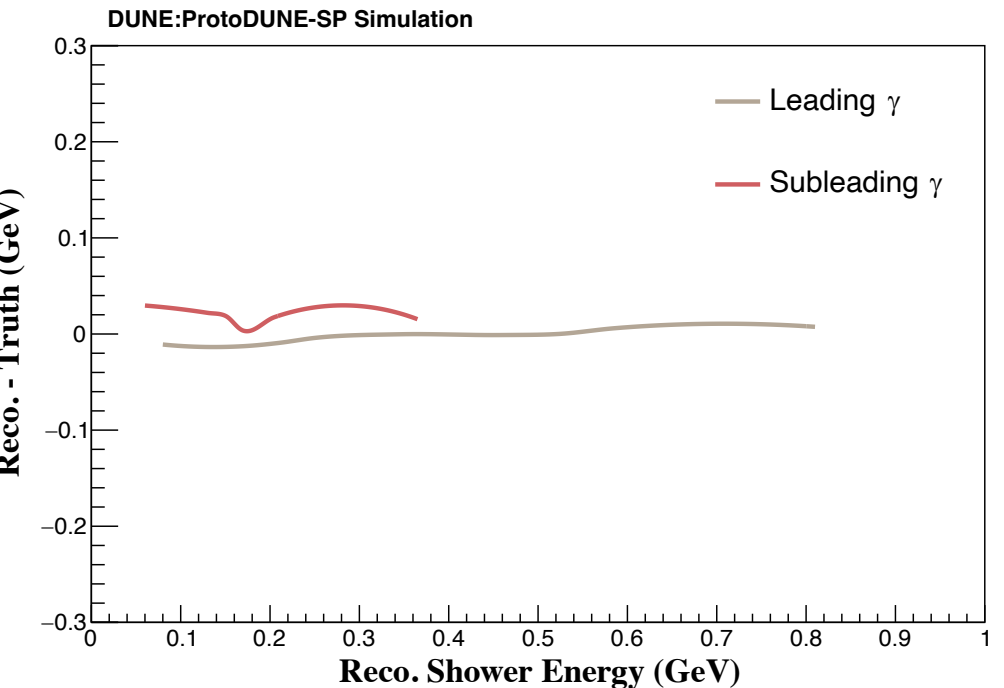


Backup

# Kinematic Fitting



- Minimizing:
  - ❖  $\chi^2 = \lambda * \{2 * E_1 E_2 [1 - \cos(\theta)] - m_{\pi^0}^2\} + (\alpha - \alpha_0) V_{\alpha_0}^{-1} (\alpha - \alpha_0)$
  - ❖ where  $\alpha = (E_1 \quad E_2 \quad \theta)$
  - ❖  $V_{\alpha_0}^{-1}$  is the inverse of the covariance matrix

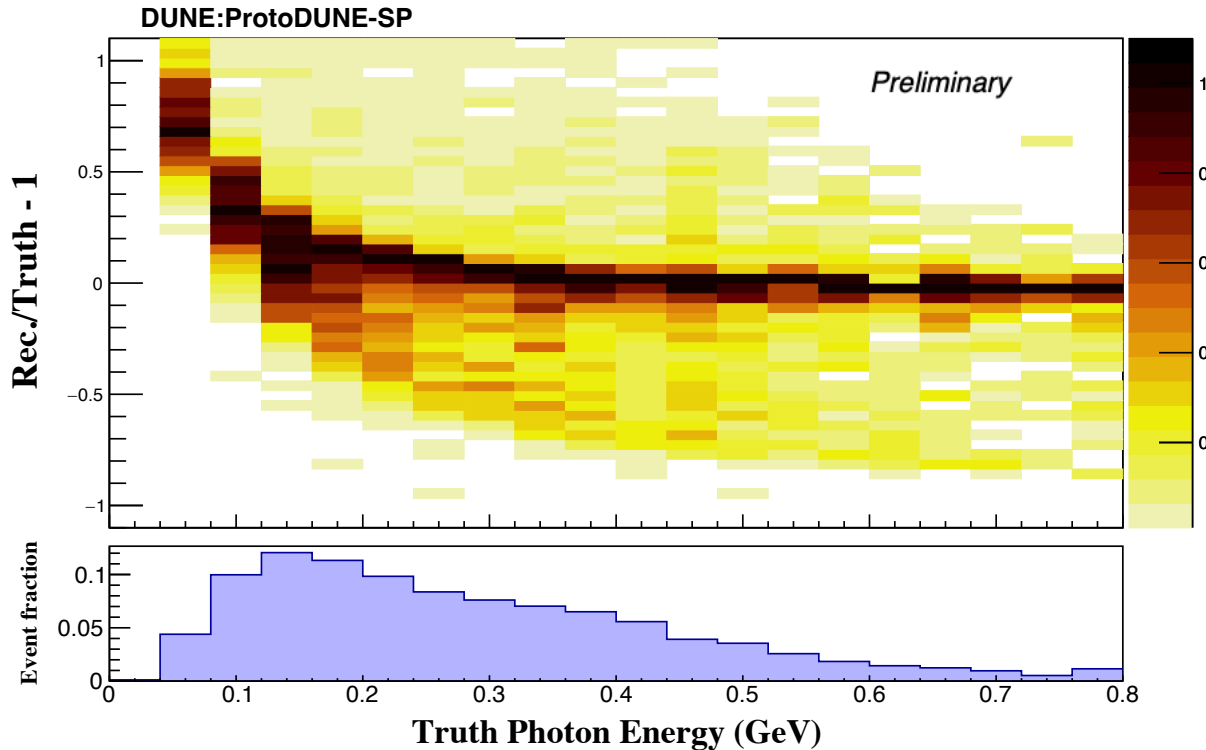


- No obvious energy dependence is found on the absolute difference of rec. and truth shower energy.
- Use the shower-energy independent covariance matrix.

# Pion Charge Exchange Statistics

	Total Events(MC)	Selected Events(MC)	Total Events(Data)	Selected Events(Data)
Beam PDG Cut	298,194	170,238	1,215,251	119,545
Pandora Track Cut	170,238	142,362	119,545	100,150
Beam Quality Cut	142,362	100,824	100,150	70,441
APA3 EndZ Cut	100,824	82,212	70,441	54,128
Michel score Cut	82,212	80,616	54,128	52,872
Chi2/DOF Cut	80,616	76,583	52,872	49,712
Beam Scraper Cut	76,583	60,174	49,712	34,783
Two $\pi^0$ Showers	60,174	2,155	34,783	1,382
No Daughter $\pi^+$	2,155	1,708	1,382	1,088
No Michel $e$	1,708	1,614	1,088	1,014
One Daughter $\pi^0$	1,614	1,146	1,014	665
		1,146(840)		665

# Shower Energy (After Correction)



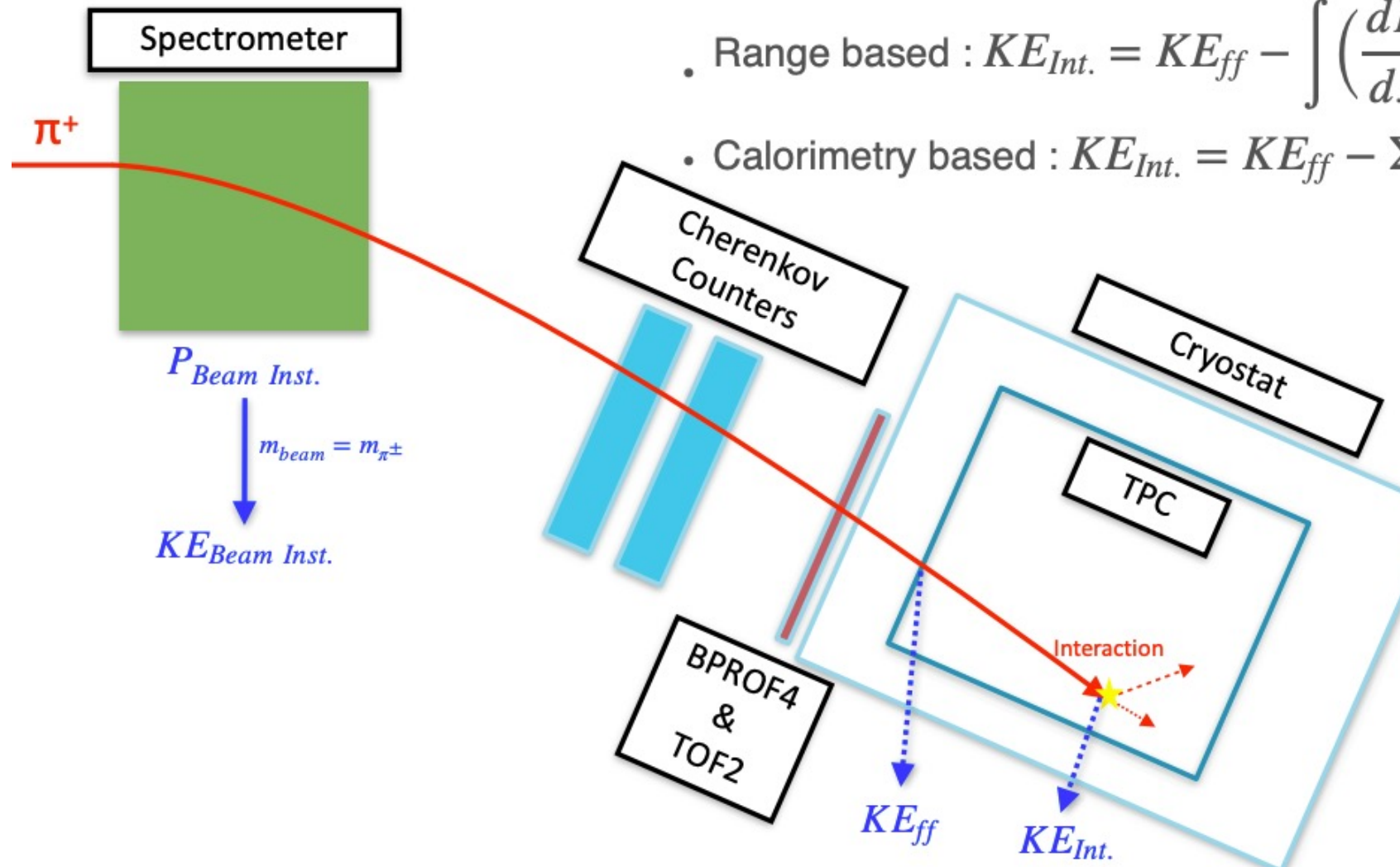
Shower Energy Correction Function Parameters :

	$p_0$	$p_1$	$p_2$	$p_3$
MC/Data	-0.91	1.50	0.06	-0.11

$$E_{cor.} = p_3 + \frac{(p_0 - p_3)}{1 + \left(\frac{E_{raw}}{p_2}\right)^{p_1}}$$

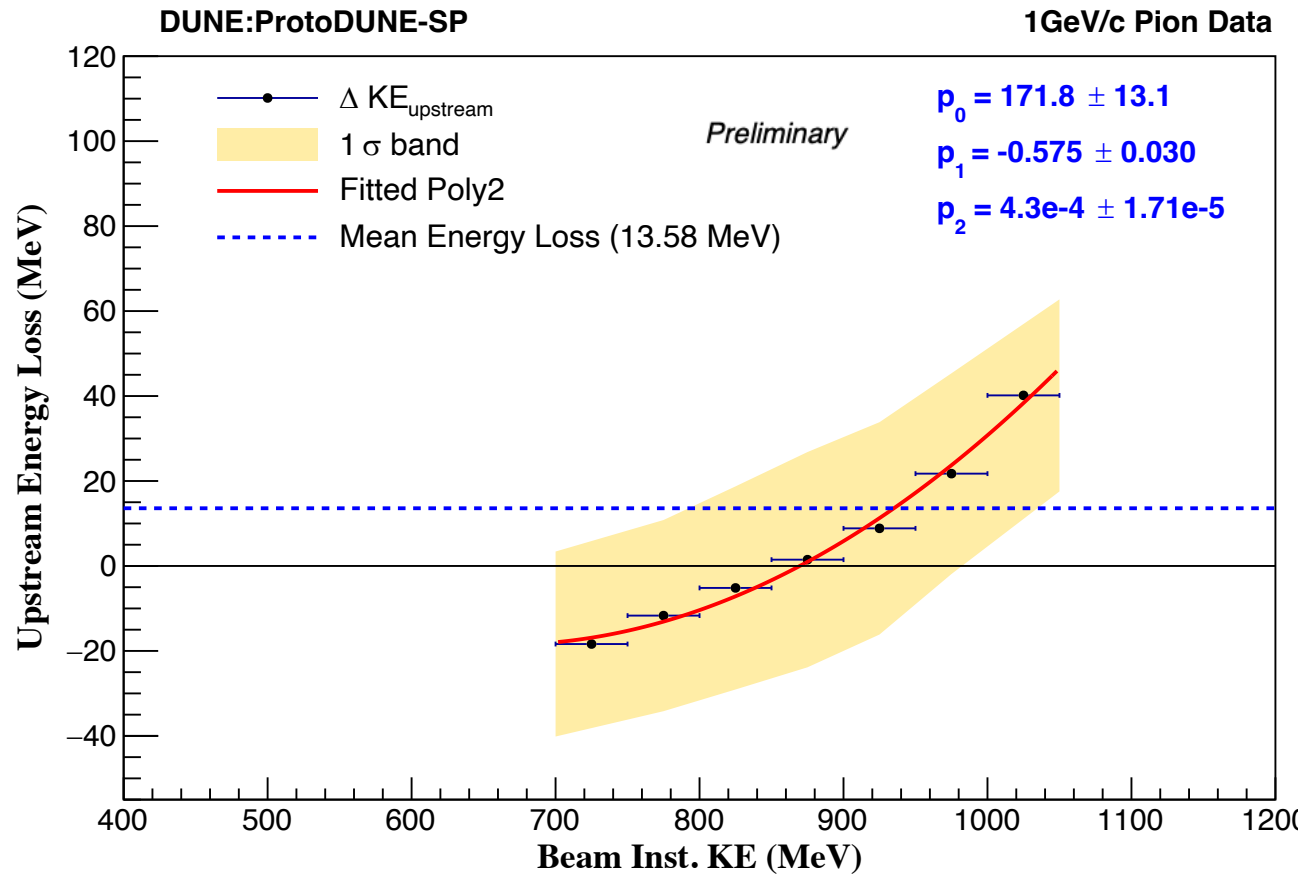
Particle Type	Energy/Mom. (frac. bias)	Theta* (deg.) (abs. difference)	Phi (deg.) (abs. difference)	Performance
Daughter Shower	$2.38\% \pm 0.19$	$2.56 \pm 5.78$	$0.18 \pm 8.10$	Good

# Upstream Energy Loss



Credit: Sungbin Oh

# Upstream Energy Loss



- The upstream energy loss is plotted as a function of the beam inst. kinetic energy.
- The upstream energy loss is energy dependent.
- Color band shows the  $1\sigma$  region of the upstream energy loss distribution at a particular energy.

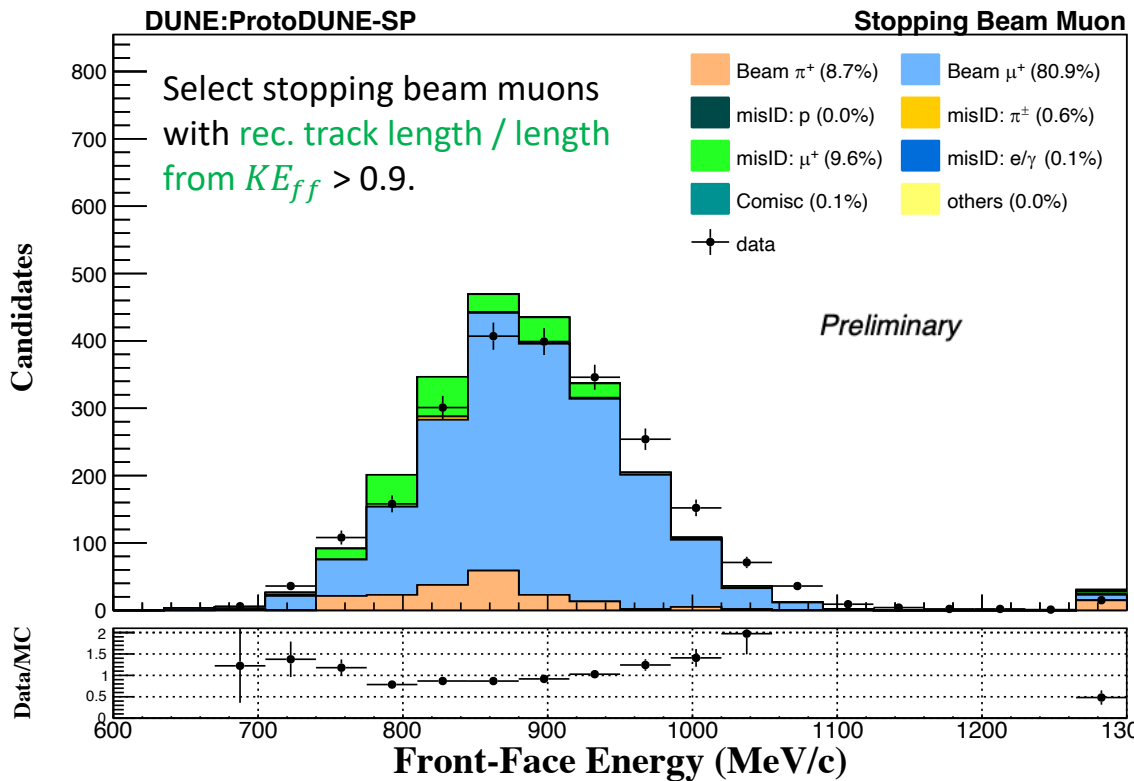
Fitted Poly2 Parameters :

	$p_0$	$p_1$	$p_2$
MC/Data	171.8	-0.575	4.3e-4

# Stopping Beam Muon

$$\frac{-(p - \mu_{fit})^2}{2\sigma_{fit}^2}$$

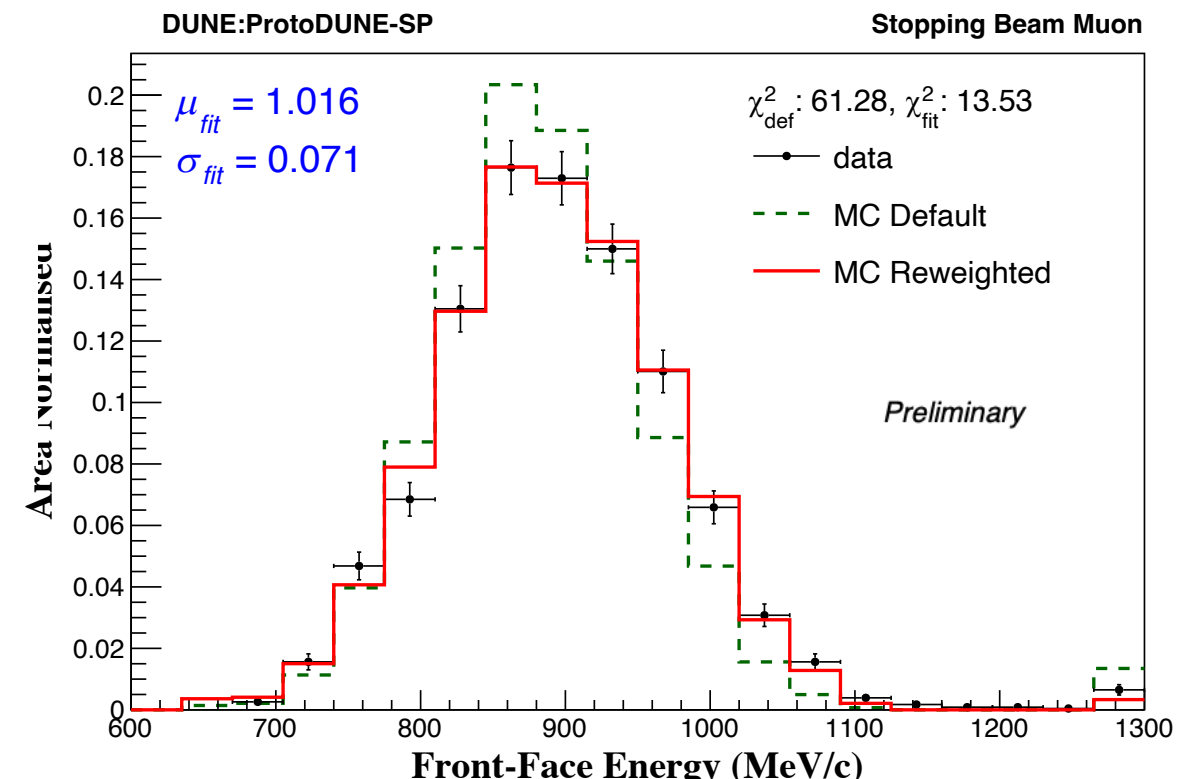
$$/ e^{\frac{-(p - \mu_{true})^2}{2\sigma_{true}^2}}$$



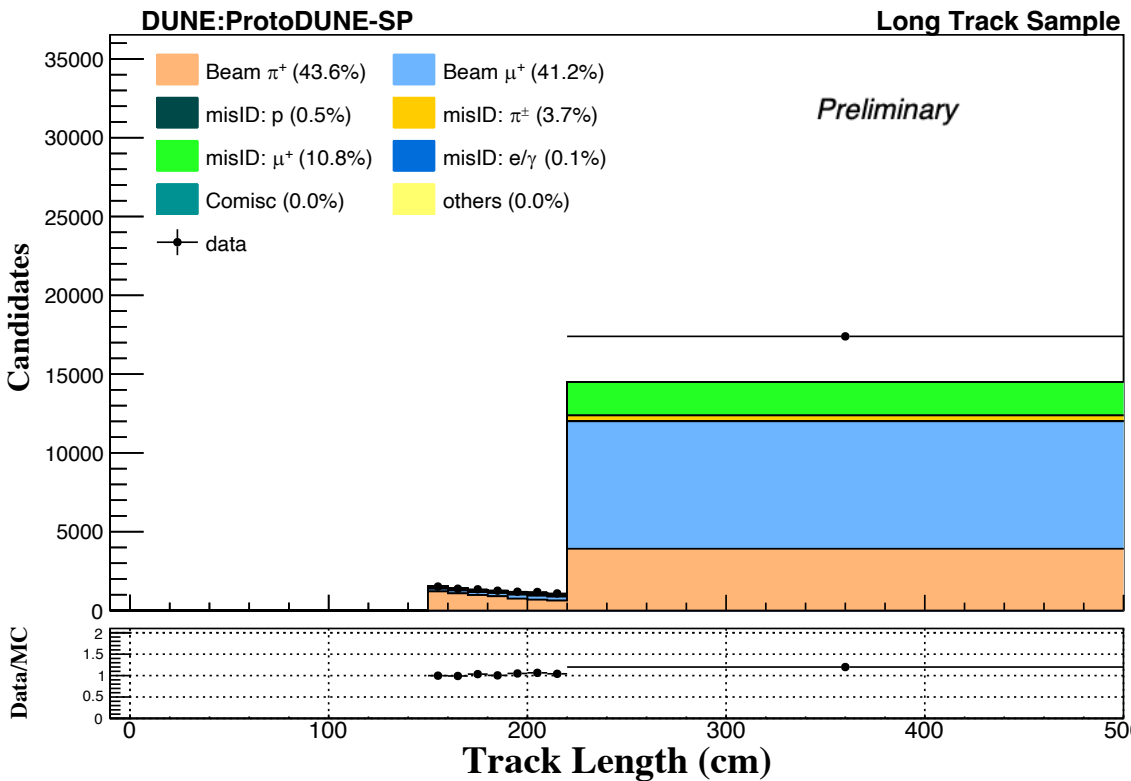
- A similar mismodeling is found in beam stopping muon sample.
- Apply a weight on a event by event basis to pion beam using fitted parameters from stopping muons.

Fitted Parameters :

	$\mu_{true}$	$\sigma_{true}$	$\mu_{fit}$	$\sigma_{fit}$	$p$
MC	1.0036	0.0595	1.0160	0.0708	Truth start P

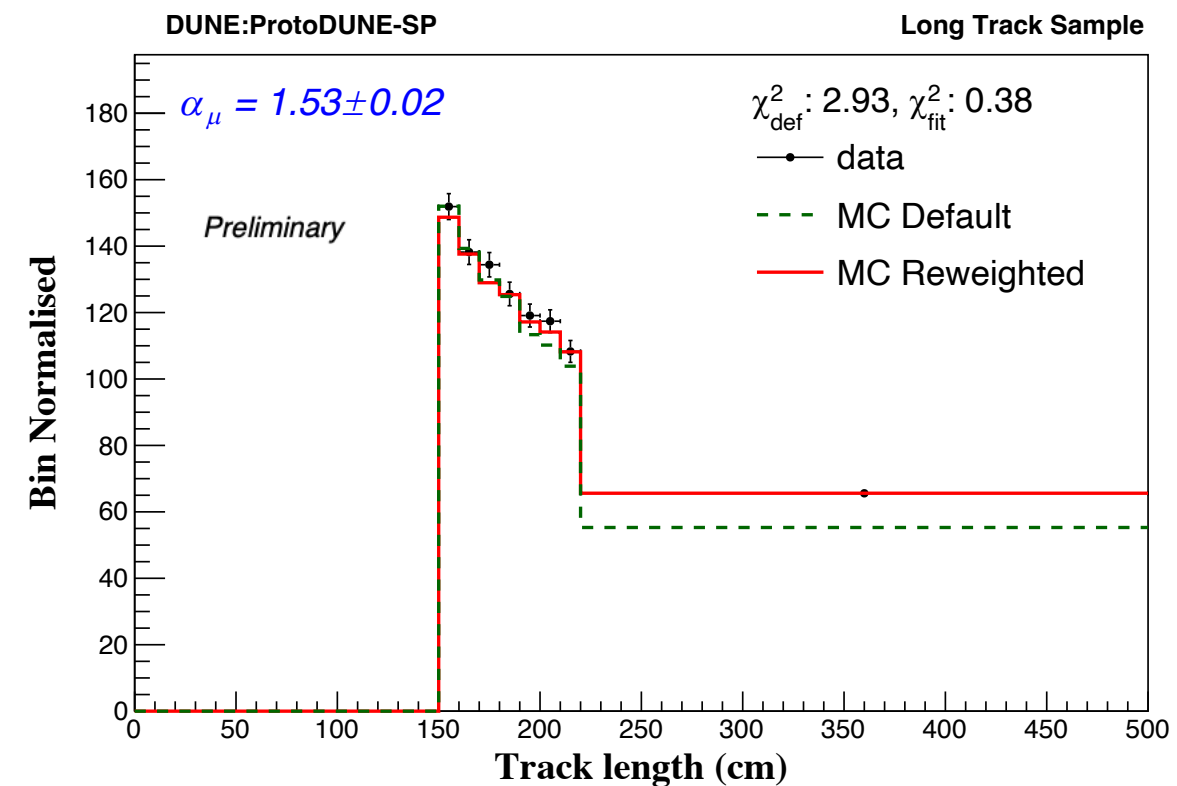


# Long Track Sample

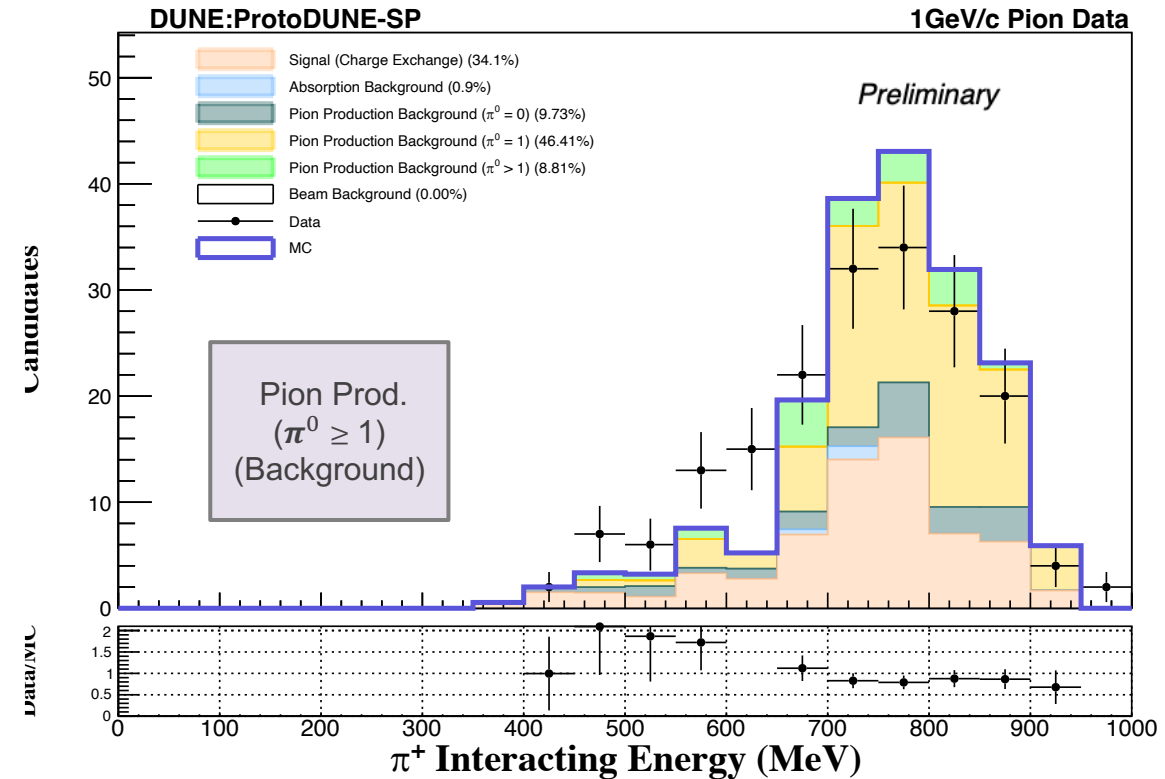
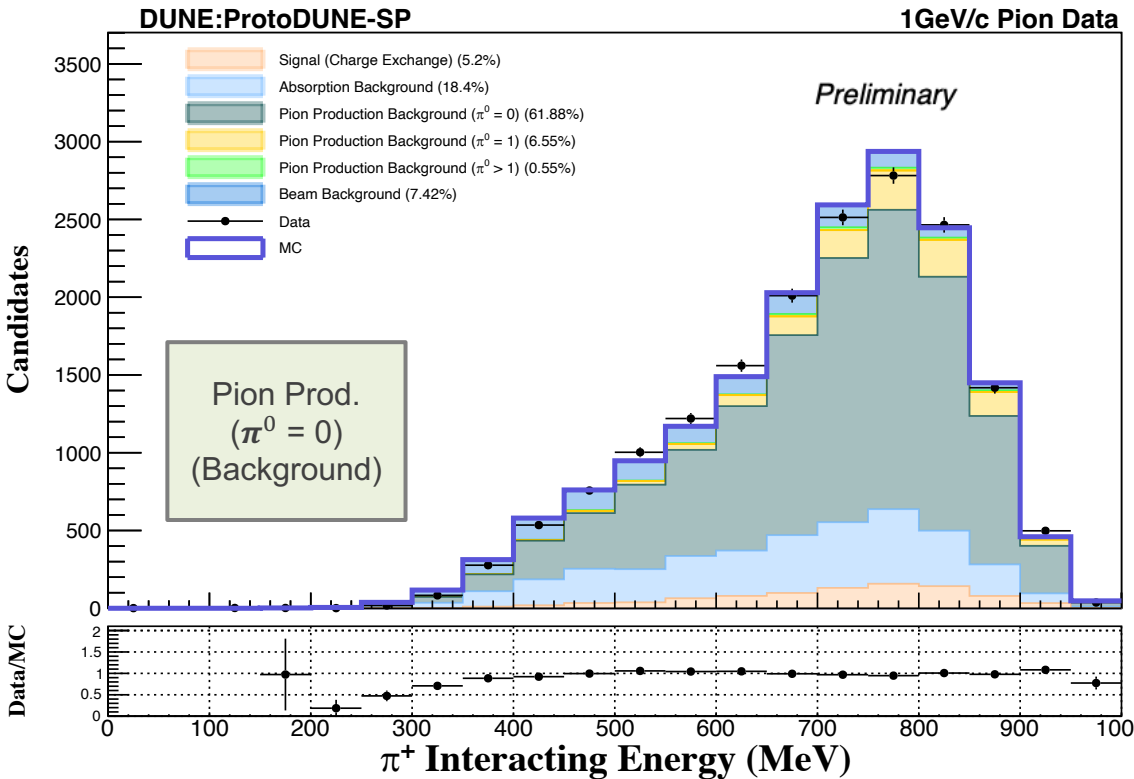


➤ Select long tracks with [rec. track length](#) > 150 cm.

- Need to scale up the muon components by a factor of  $1.53 \pm 0.02$ .

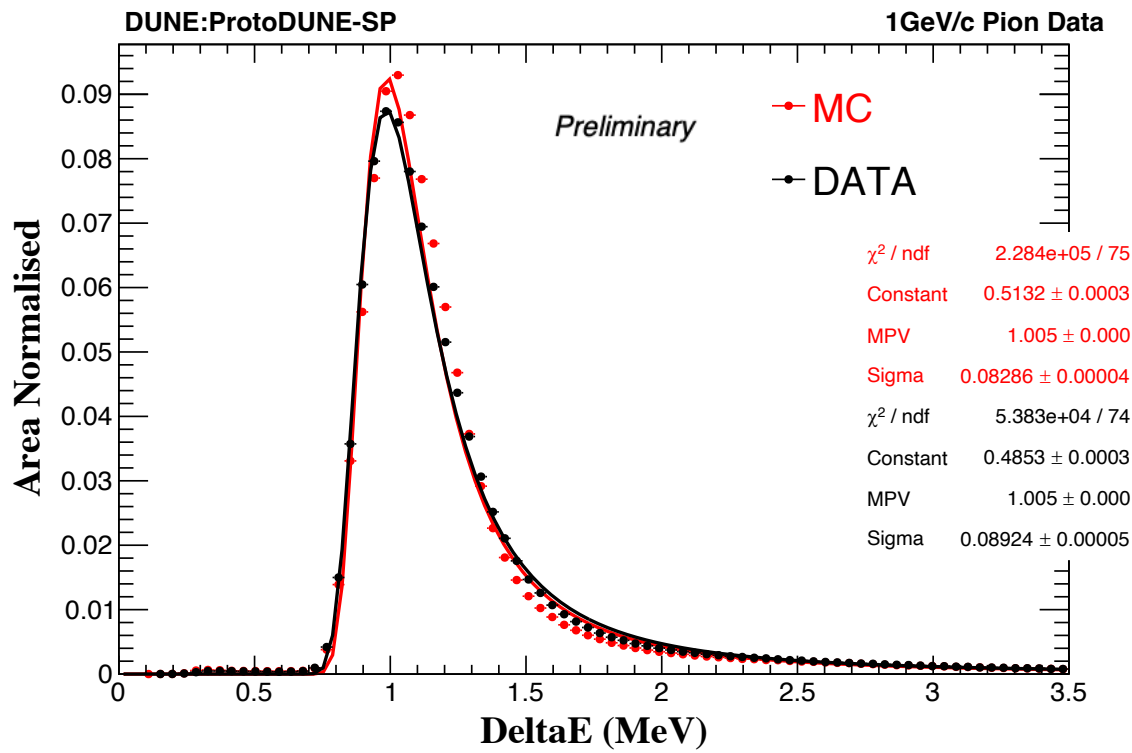


# Sideband Background Tuning



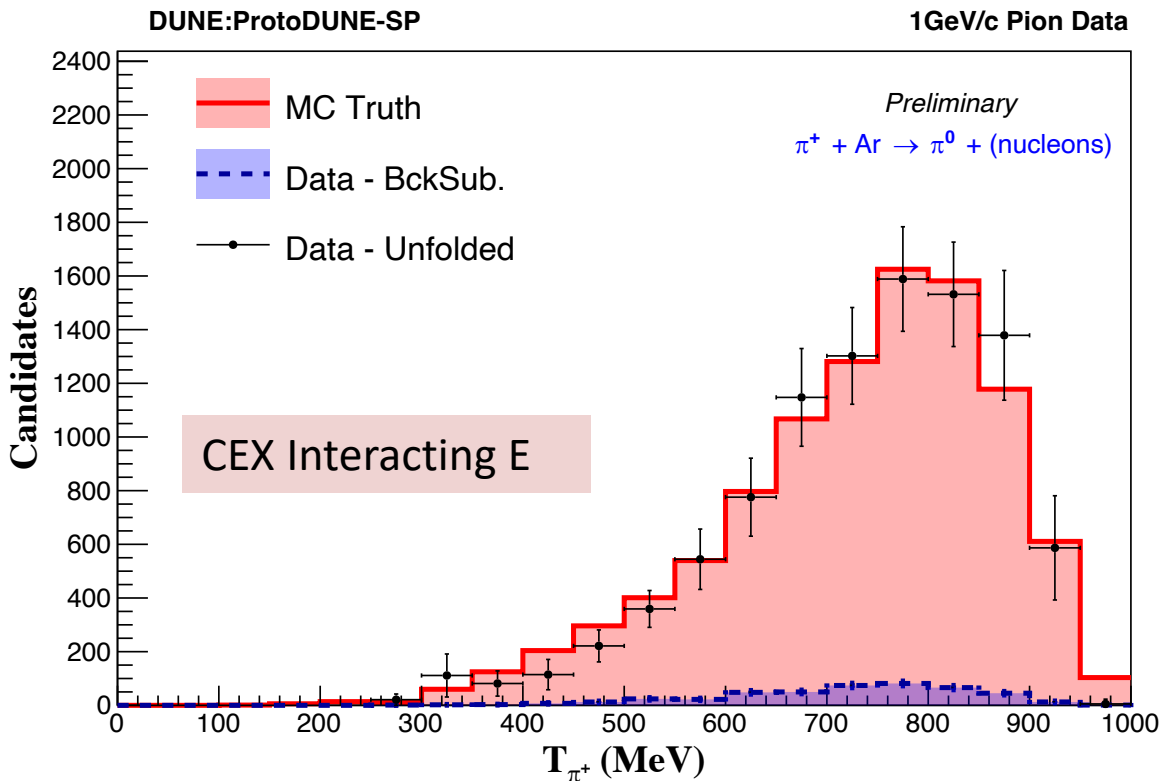
- Switching the cuts on the final state particles to select background dominated sideband channels.
- Keep the signal part unchanged, simultaneously vary the  $\pi^0 = 0$  (left hist.) and  $\pi^0 \geq 1$  (right hist.) pion production backgrounds to minimise the  $\chi^2$  of two histograms above.

# Energy Deposit from Calorimetry

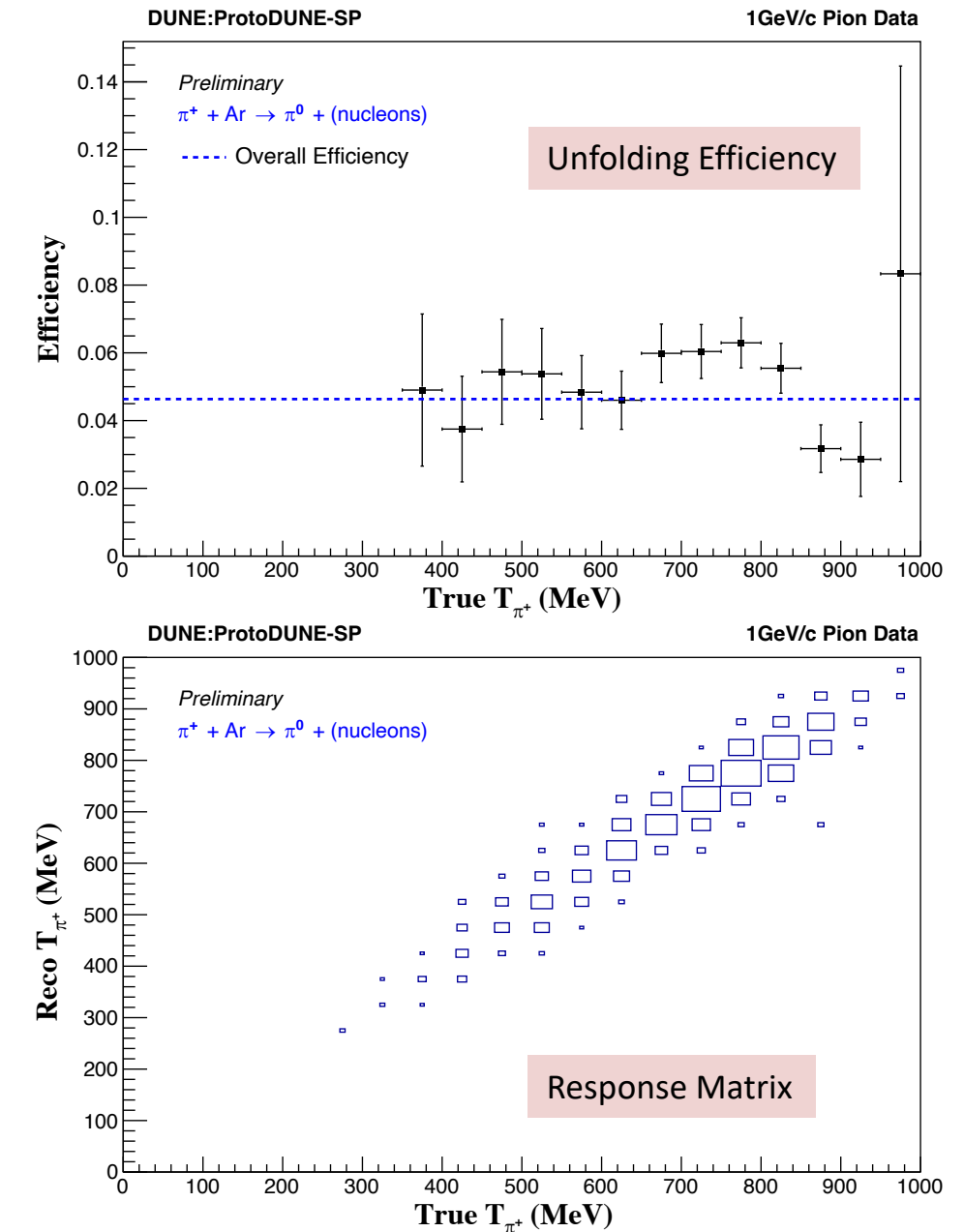


- The biggest advantage of a LArTPC detector is its granularity when measuring the particles.
- We are able to measure the energy deposit every one MeV (this is after the dEdx calibration)
- Choose 1MeV slice width and perform the XS measurement in a 50MeV binning is possible.

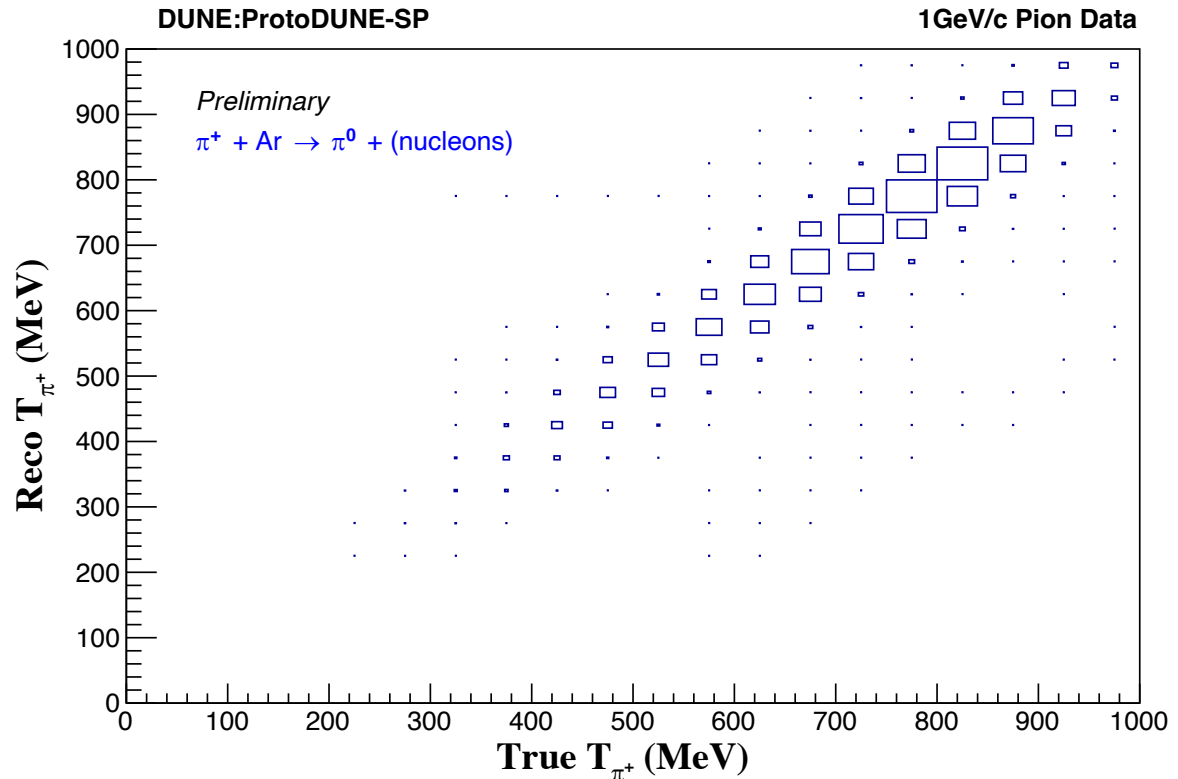
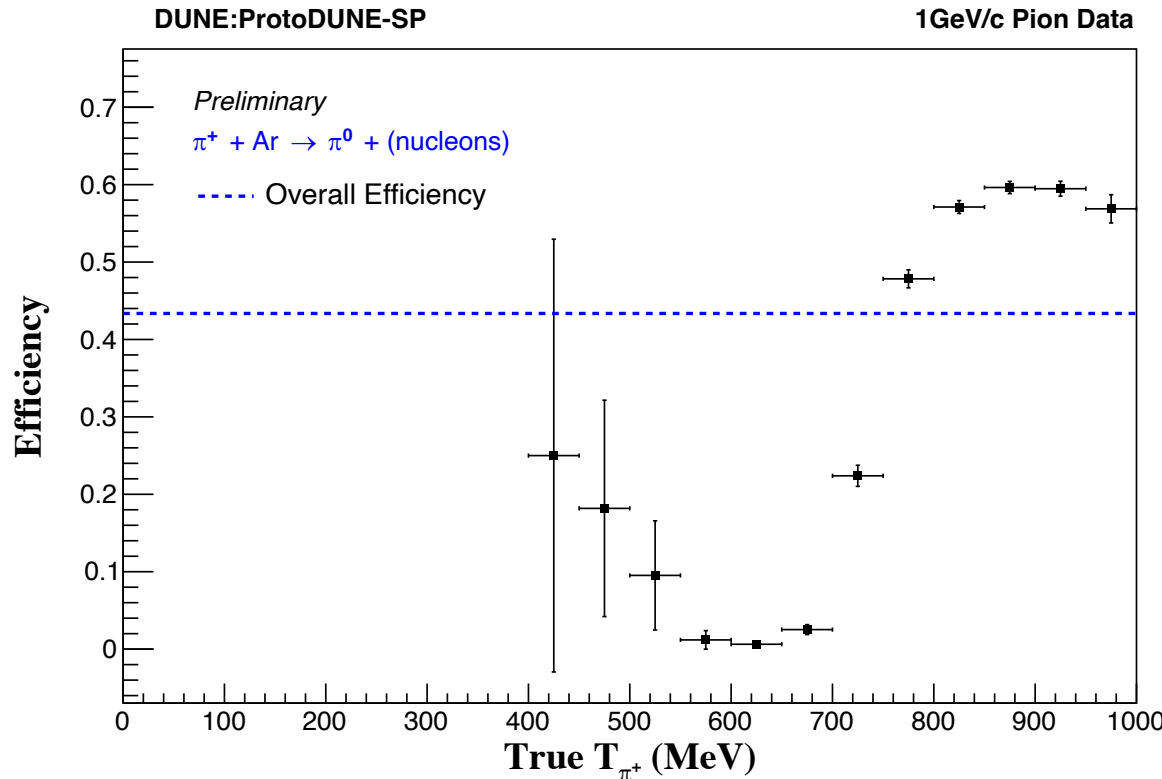
# Unfolding



- Iterative Bayesian unfolding ([RooUnfold package](#))
- Overall efficiency for CEX events is about 5% .

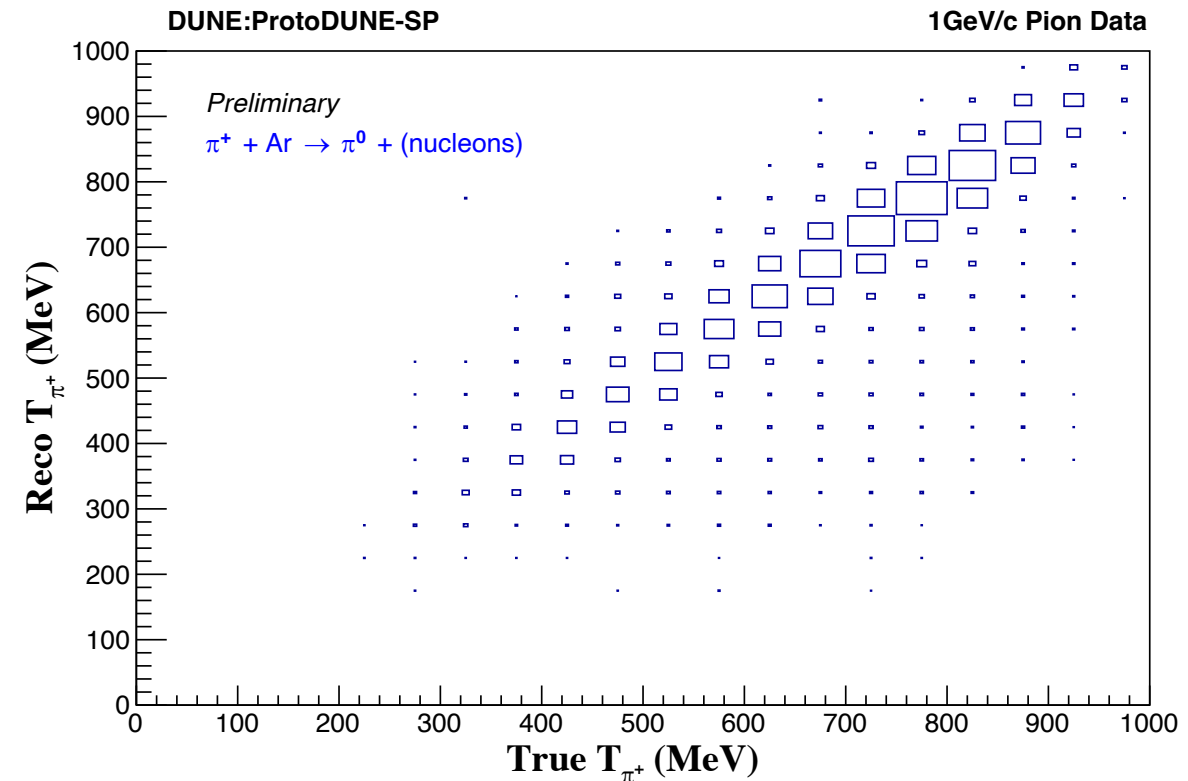
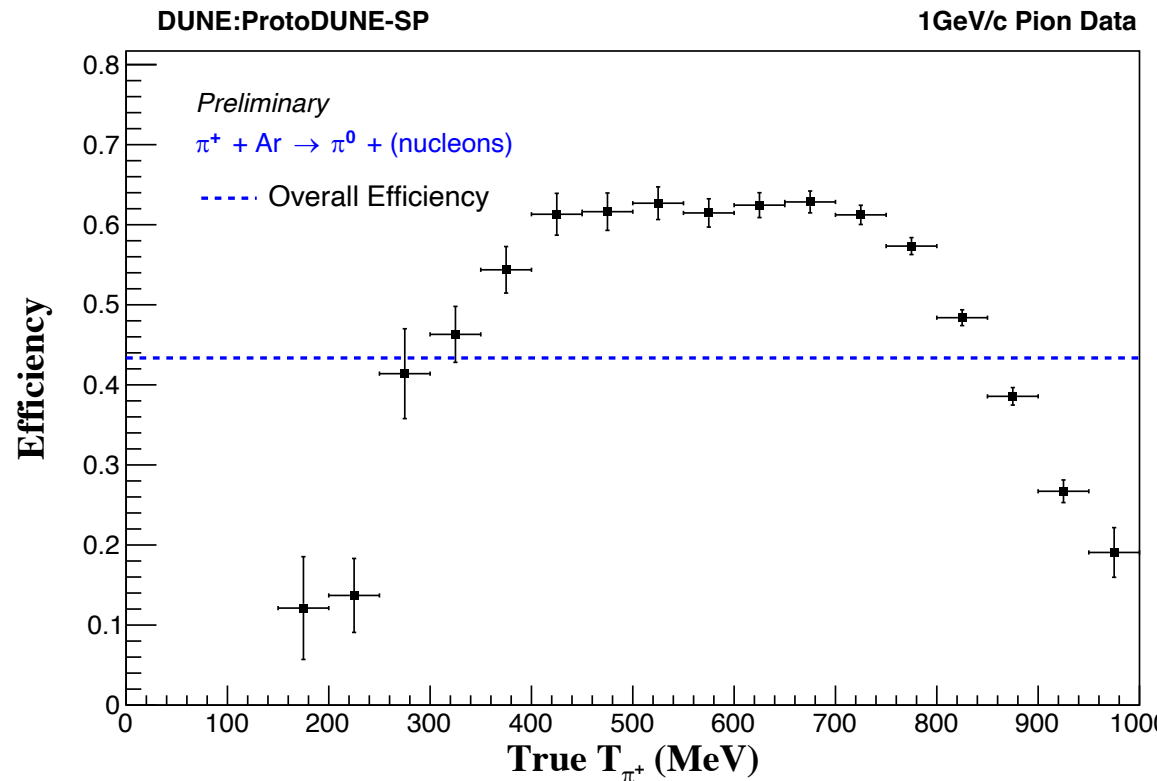


# Unfolding – Initial E



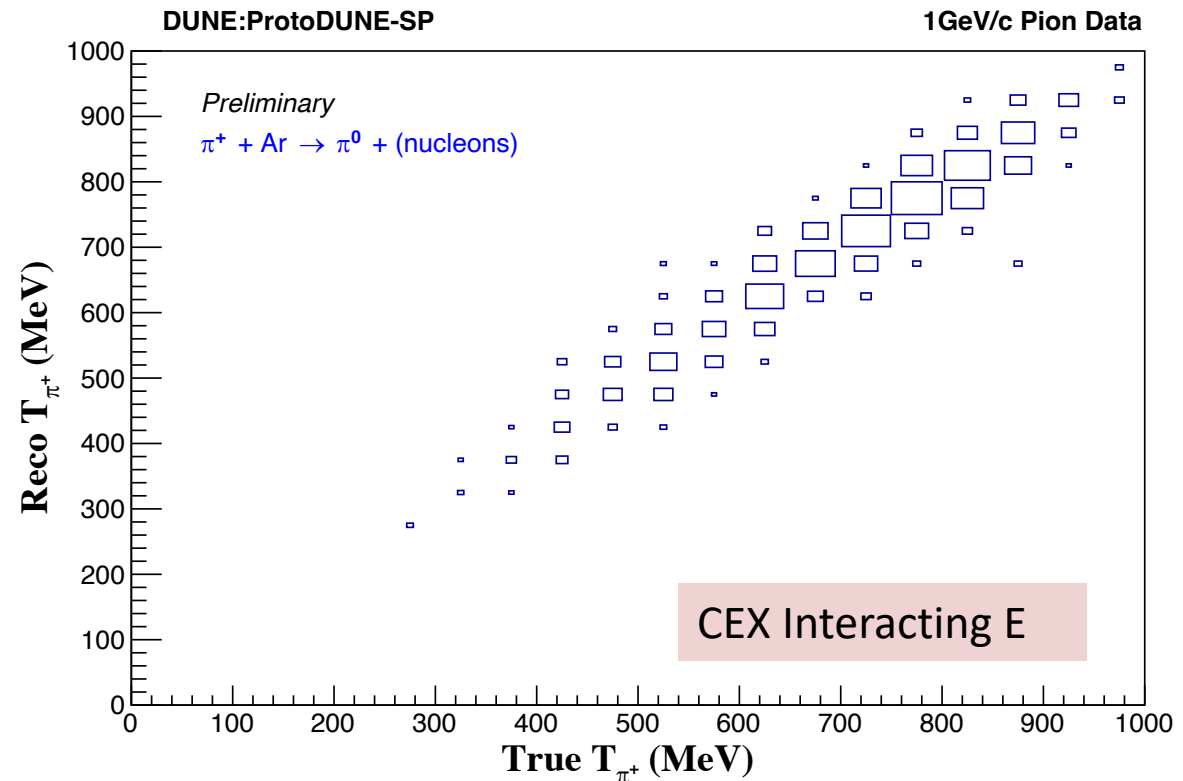
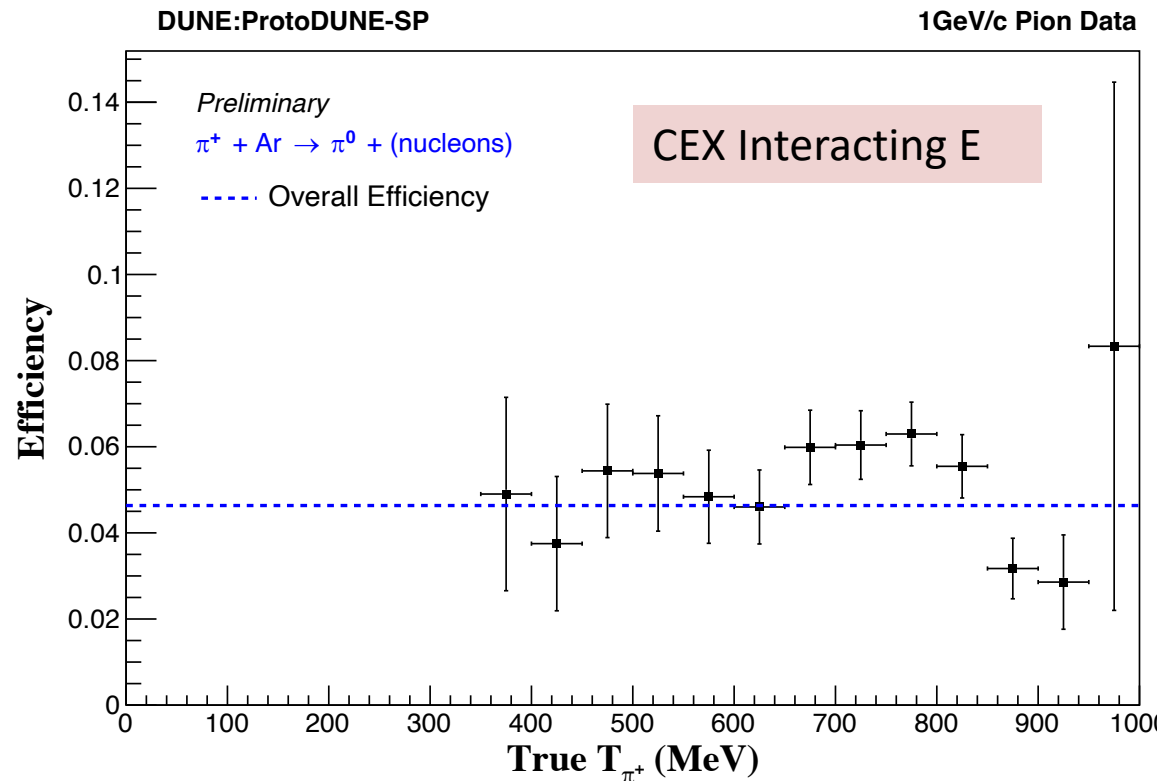
- Overall Efficiency is about 45%.

# Unfolding – Beam Interacting E



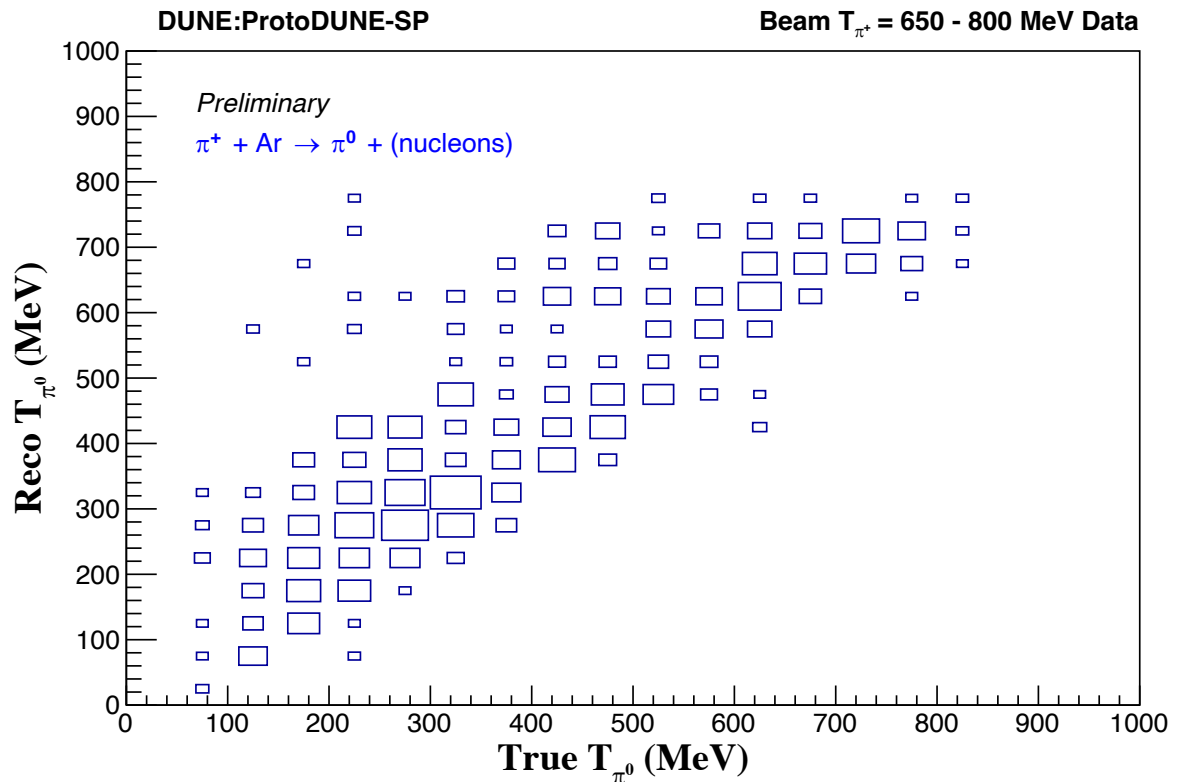
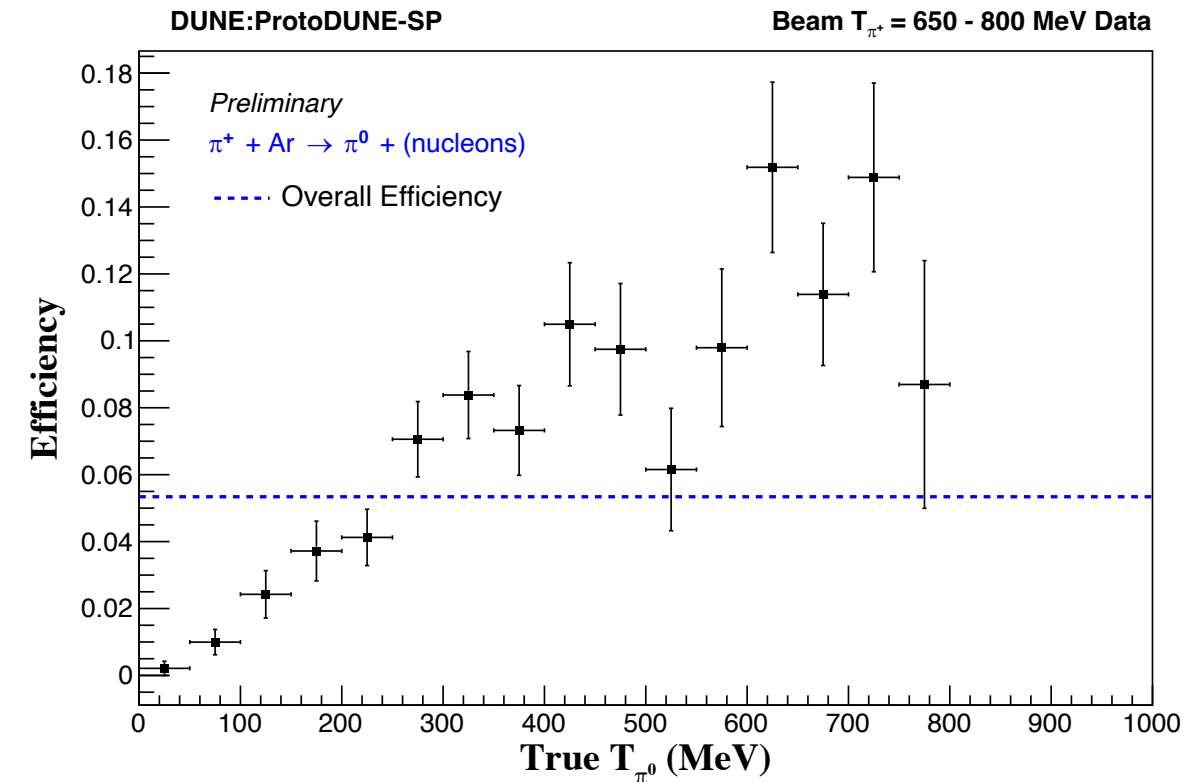
- Overall Efficiency is about 45%.

# Unfolding - CEX Interacting E



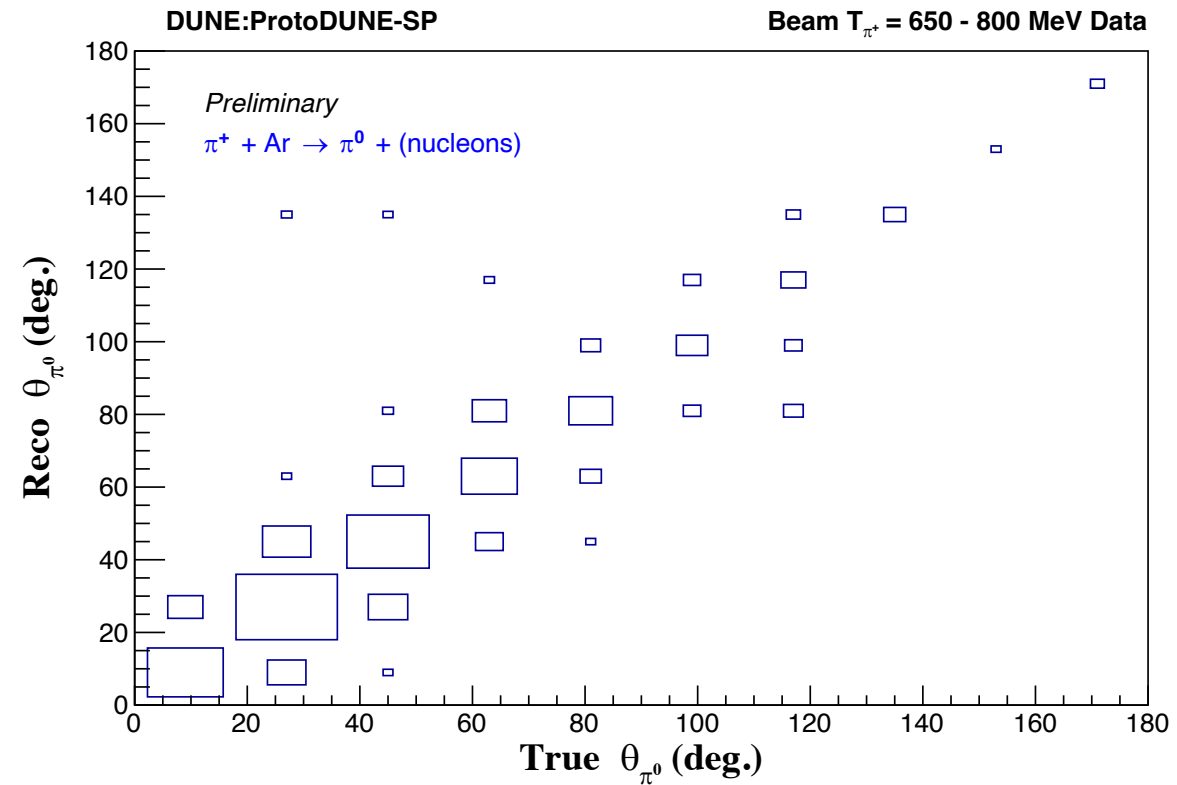
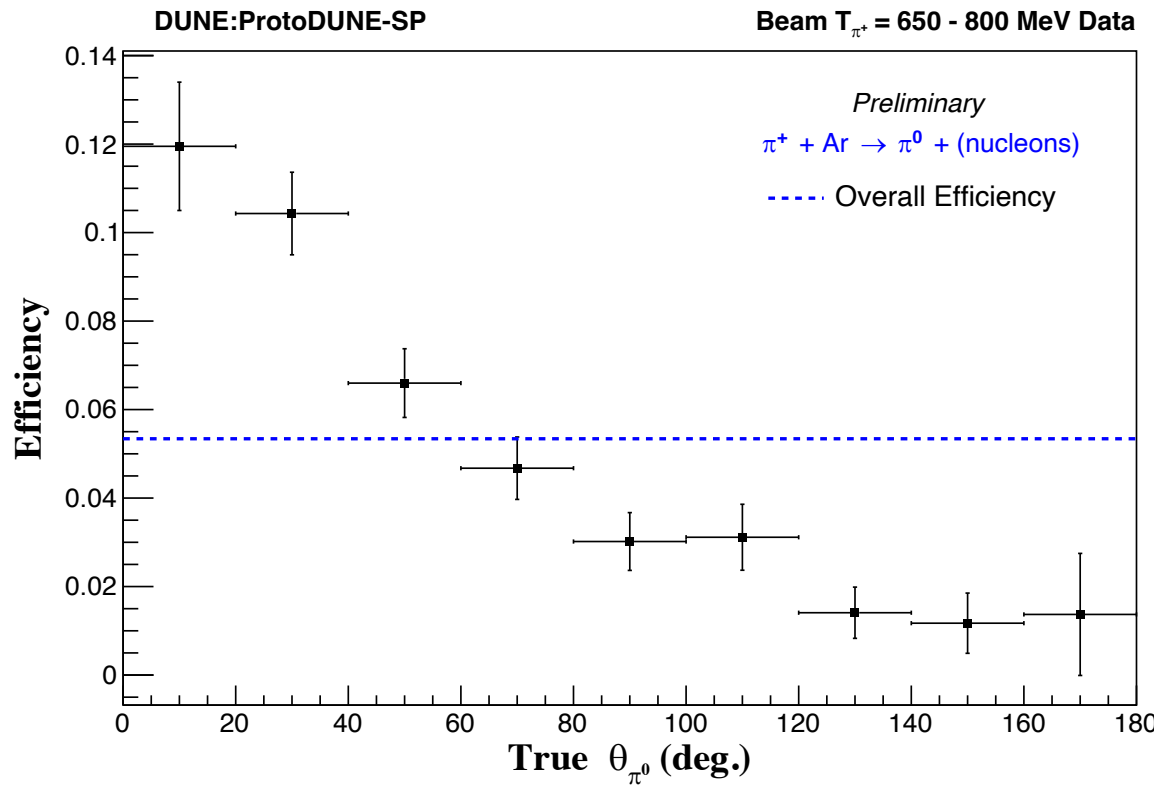
- The unfolding efficiency (left) and the response matrix for CEX Interacting E.
- Overall efficiency is about 5%.
- Unfolding of Initial E and beam interacting E are in the back up slides.

# Unfolding – Pi0 KE



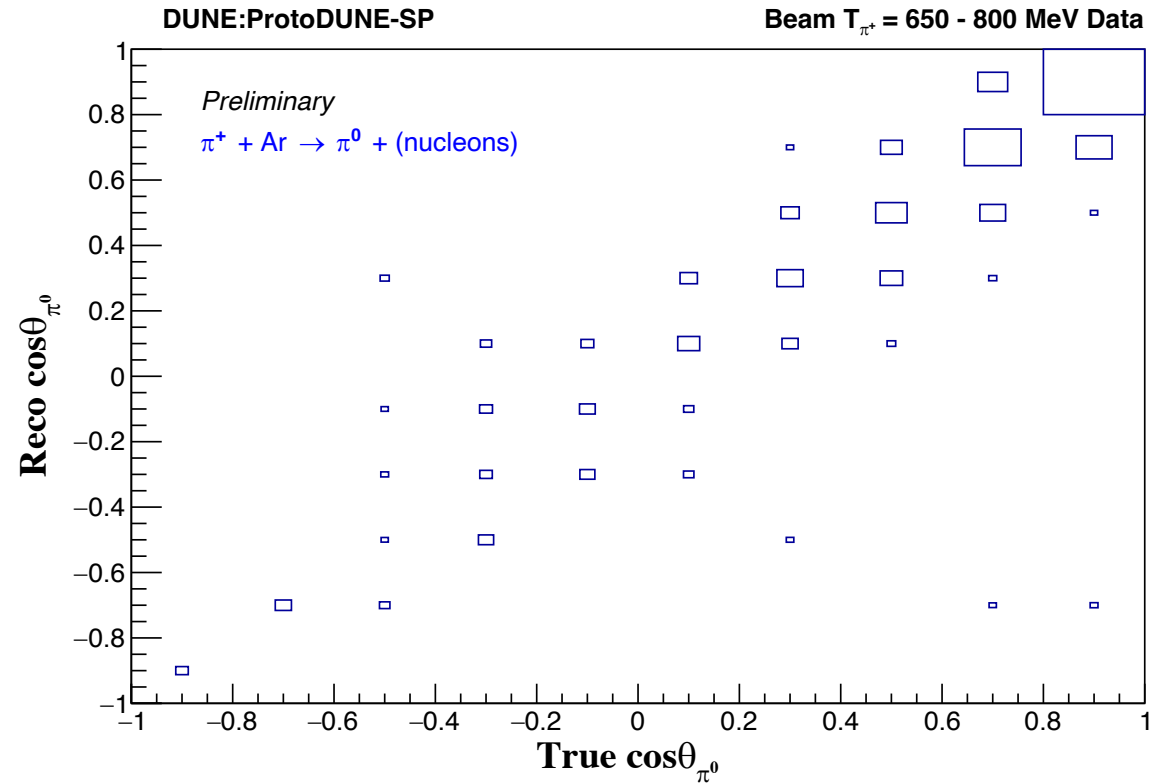
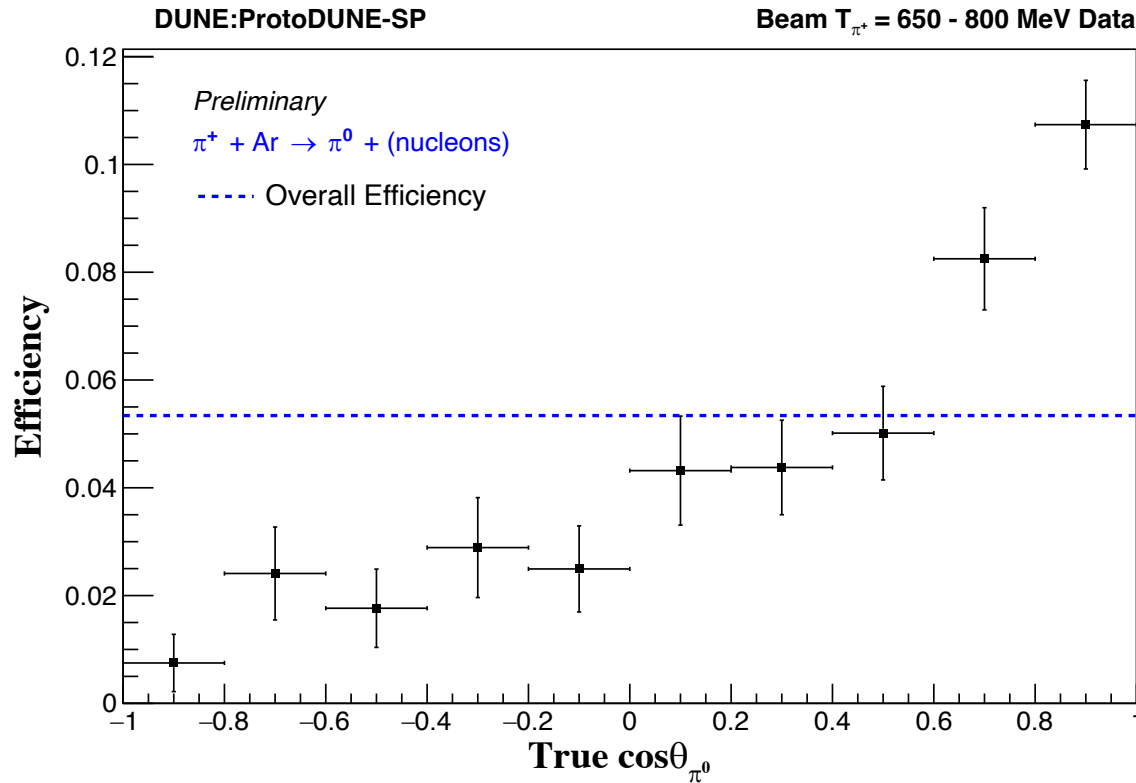
- The efficiency increases as the energy increases.

# Unfolding – Pi0 Theta



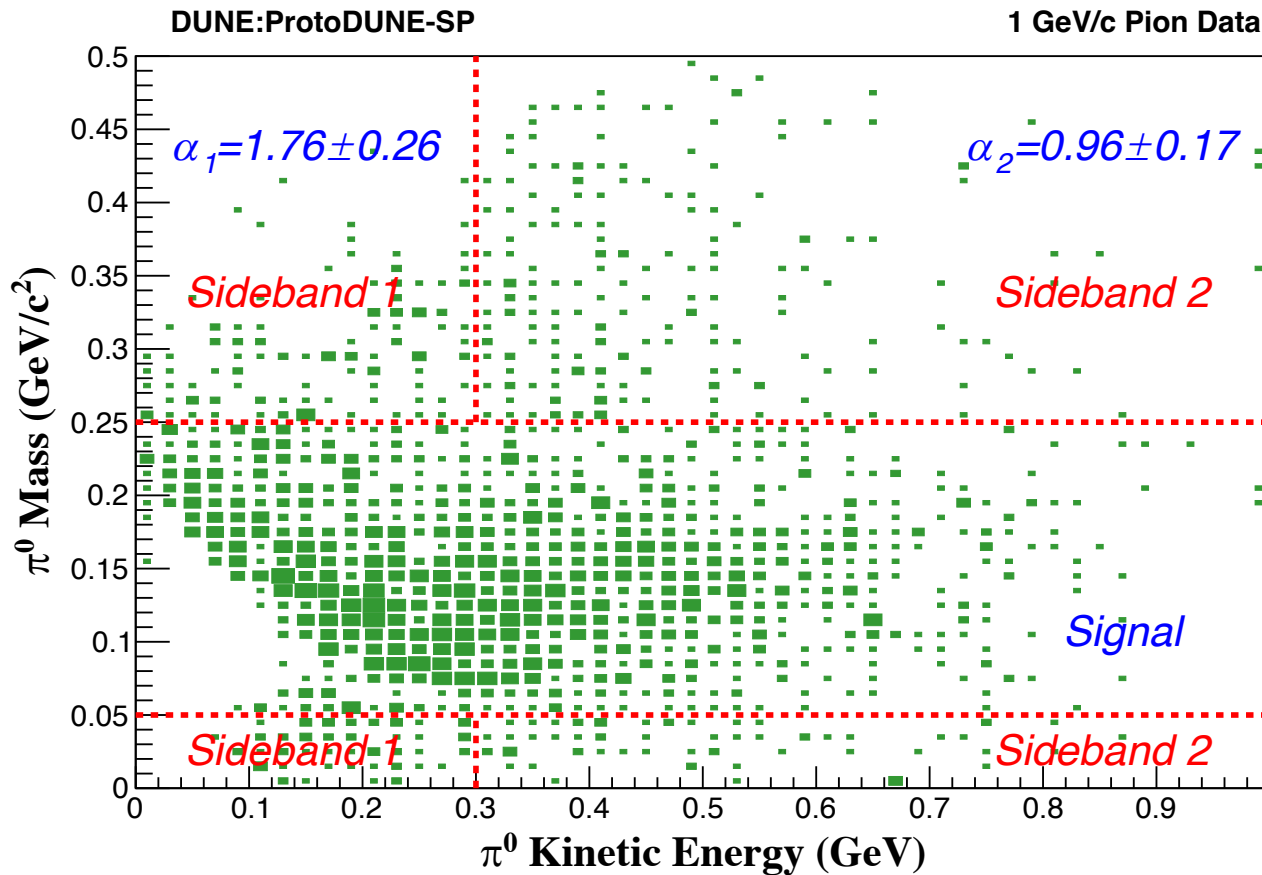
- Low efficiency for large theta angle (backward moving particles).

# Unfolding – Pi0 CosTheta



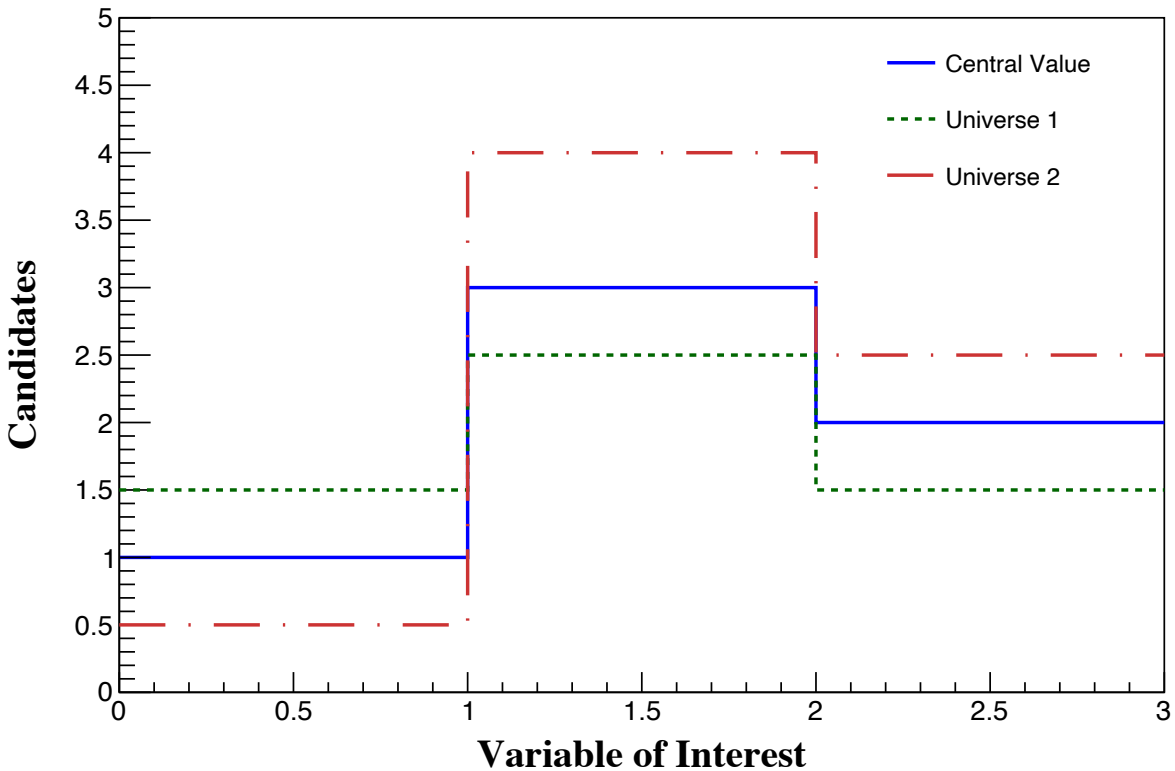
- Low efficiency for backward moving particles.

# Sideband Bck. Tuning



- Two sidebands defined outside the mass window:
  - ❖ Backgrounds are allowed to vary through  $\chi^2$  minimization in the  $\pi^0$  mass distribution for each sideband
- The fitted two scaling factors in each sideband region are shown in blue.
- An underestimation of low-energy  $\pi^0$  in the simulation

# Estimating systematics



- We shift one single parameter and run the simulation again to create an **“alternative universe”**.
- The difference between the distributions gives a **measure of the uncertainty** due to this shifted parameter.
- We make the variation and evaluate all systematic sources on the list.

# Covariance Matrix

- We need to consider that different bins may be correlated in our analysis.
- The covariance matrix is a  $N \times N$  matrix, where  $N$  is the number of bins of our variable of interest.
- For any two bins,  $i$  and  $j$ , the covariance matrix is defined as:

$$M_{ij} = M_{ji} = \frac{\sum_{k=1}^n (x_{i_k} - \bar{x}_i)(x_{j_k} - \bar{x}_j)w_k}{\sum_{k=1}^n w_k}$$

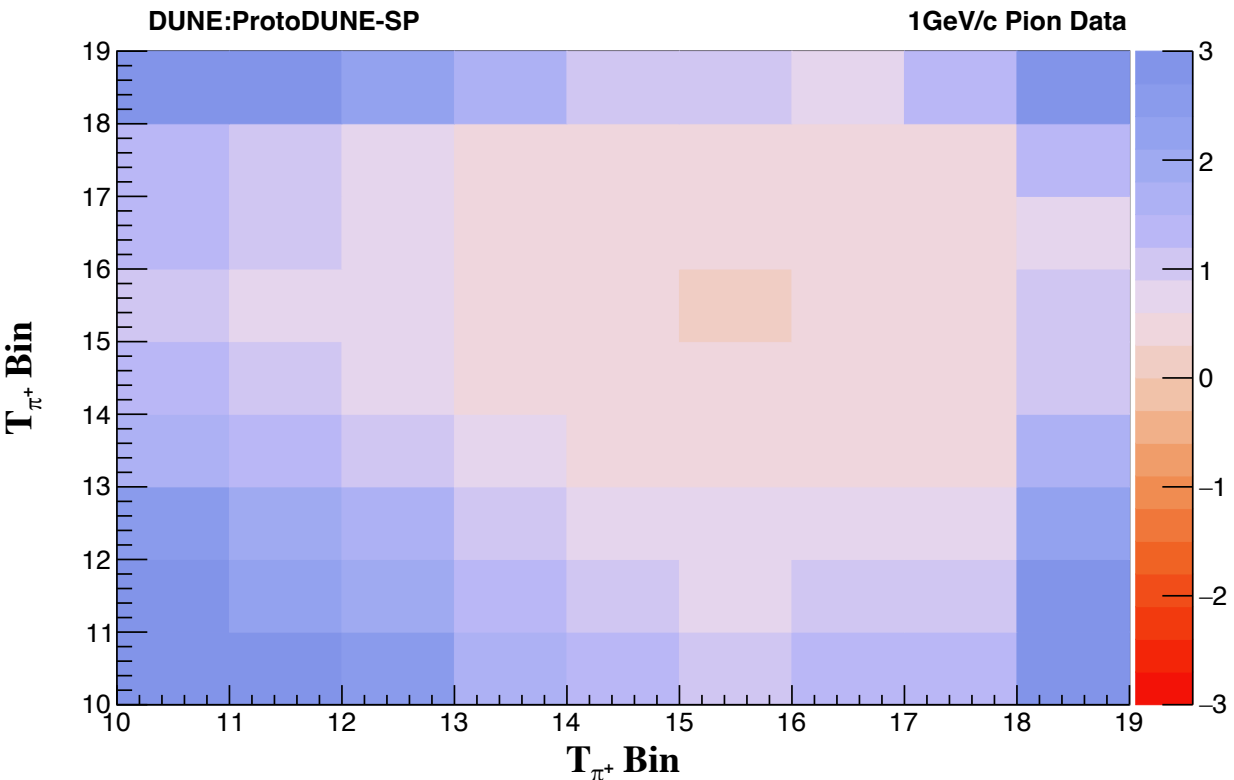
$$M_{ij} = M_{ji} = \frac{\sum_{k=1}^n (x_{i_k} - \bar{x}_i)(x_{j_k} - \bar{x}_j)w_k}{\sum_{k=1}^n w_k}$$

- $n$  is the total number of universes
- $w_k$  is the weight for a universe  $k$  (default value = 1)
- $x_{i_k}$  is the candidate count in bin  $i$  in a universe  $k$ .
- $\bar{x}_i$  is the mean candidate count in bin  $i$ , averaged over all universes.

# Covariance Matrix

- We need to consider that different bins may be correlated in our analysis.
- The covariance matrix is a  $N \times N$  matrix, where  $N$  is the number of bins of our variable of interest.
- For any two bins,  $i$  and  $j$ , the covariance matrix is defined as:

$$M_{ij} = M_{ji} = \frac{\sum_{k=1}^n (x_{ik} - \bar{x}_i)(x_{jk} - \bar{x}_j) w_k}{\sum_{k=1}^n w_k}$$



# Systematic Uncertainty

